CHAPTER

Properties of Engineering Materials

8

It is now clear from the discussion in Chapter 7 that the structural designer requires a knowledge of the behaviour of materials under different types of load before he/she can be reasonably sure of designing a safe and, at the same time, economic structure.

One of the most important properties of a material is its strength, by which we mean the value of stress at which it fractures. Equally important in many instances, particularly in elastic design, is the stress at which yielding begins. In addition, the designer must have a knowledge of the stiffness of a material so that he/she can prevent excessive deflections occurring that could cause damage to adjacent structural members. Other factors that must be taken into consideration in design include the character of the different loads. For example, it is common experience that a material, such as cast iron fractures readily under a sharp blow whereas mild steel merely bends.

In Chapter 1 we reviewed the materials that are in common use in structural engineering; we shall now examine their properties in detail.

8.1 Classification of engineering materials

Engineering materials may be grouped into two distinct categories, ductile materials and brittle materials, which exhibit very different properties under load. We shall define the properties of ductility and brittleness and also some additional properties which may depend upon the applied load or which are basic characteristics of the material.

Ductility

A material is said to be *ductile* if it is capable of withstanding large strains under load before fracture occurs. These large strains are accompanied by a visible change in cross-sectional dimensions and therefore give warning of impending failure. Materials in this category include mild steel, aluminium and some of its alloys, copper and polymers.

Brittleness

A brittle material exhibits little deformation before fracture, the strain normally being below 5%. Brittle materials therefore may fail suddenly without visible warning. Included in this group are concrete, cast iron, high-strength steel, timber and ceramics.

Elastic materials

A material is said to be *elastic* if deformations disappear completely on removal of the load. All known engineering materials are, in addition, *linearly elastic* within certain limits of stress so that strain, within these limits, is directly proportional to stress.

Plasticity

A material is perfectly *plastic* if no strain disappears after the removal of load. Ductile materials are *elastoplastic* and behave in an elastic manner until the *elastic limit* is reached after which they behave plastically. When the stress is relieved the elastic component of the strain is recovered but the plastic strain remains as a *permanent set.*

Isotropic materials

In many materials the elastic properties are the same in all directions at each point in the material although they may vary from point to point; such a material is known as *isotropic.* An isotropic material having the same properties at all points is known as *homogeneous*, e.g. mild steel.

Anisotropic materials

Materials having varying elastic properties in different directions are known as *anisotropic.*

Orthotropic materials

Although a structural material may possess different elastic properties in different directions, this variation may be limited, as in the case of timber which has just two values of Young's modulus, one in the direction of the grain and one perpendicular to the grain. A material whose elastic properties are limited to three different values in three mutually perpendicular directions is known as *orthotropic.*

8.2 Testing of engineering materials

The properties of engineering materials are determined mainly by the mechanical testing of specimens machined to prescribed sizes and shapes. The testing may be static or dynamic in nature depending on the particular property being investigated. Possibly the most common mechanical static tests are tensile and compressive tests which are carried out on a wide range of materials. Ferrous and non-ferrous metals are subjected to both forms of test, while compression tests are usually carried out on many non-metallic materials, such as concrete, timber and brick, which are normally used in compression. Other static tests include bending, shear and hardness tests, while the toughness of a material, in other words its ability to withstand shock loads, is determined by impact tests.

Tensile tests

Tensile tests are normally carried out on metallic materials and, in addition, timber. Test pieces are machined from a batch of material, their dimensions being specified by Codes of Practice. They are commonly circular in cross section, although flat test pieces having rectangular cross sections are used when the batch of material is in the form of a plate. A typical test piece would have the dimensions specified in Fig. 8.1. Usually the diameter of a central portion of the test piece is fractionally less than that of the remainder to ensure that the test piece fractures between the gauge points.

Before the test begins, the mean diameter of the test piece is obtained by taking measurements at several sections using a micrometer screw gauge. Gauge points are punched at the required gauge length, the test piece is placed in the testing machine and a suitable strain measuring device, usually an extensometer, is attached to the test piece at the gauge points so that the extension is measured over the given gauge length. Increments of load are applied and the corresponding extensions recorded. This procedure continues until yield (see Section 8.3) occurs, when the extensometer is removed as a precau-

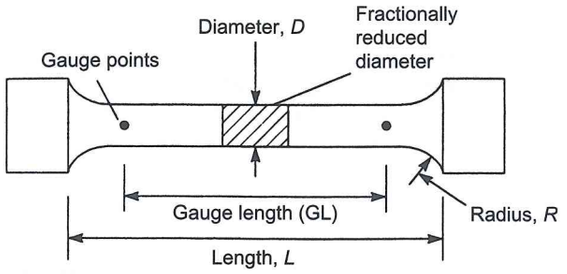

FIGURE 8.1
Standard cylindrical test piece.

extensions are measured by dividers placed in the gauge points until, ultimately, the test piece fractures. The final gauge length and the diameter of the test piece in the region of the fracture are measured so that the percentage elongation and percentage reduction in area may be calculated. The two parameters give a measure of the ductility of the material.

A stress–strain curve is drawn (see Figs 8.8 and 8.12), the stress normally being calculated on the basis of the original cross-sectional area of the test piece, i.e. a *nominal stress* as opposed to an *actual stress* (which is based on the actual area of cross section). For ductile materials there is a marked difference in the latter stages of the test as a considerable reduction in cross-sectional area occurs between yield and fracture. From the stress–strain curve the ultimate stress, the yield stress and Young's modulus, E, are obtained (see Section 7.7).

There are a number of variations on the basic tensile test described above. Some of these depend upon the amount of additional information required and some upon the choice of equipment. Thus there is a wide range of strain measuring devices to choose from, extending from different makes of mechanical extensometer, e.g. Huggenberger, Lindley, Cambridge, to the electrical resistance strain gauge. The last would normally be used on flat test pieces, one on each face to eliminate the effects of possible bending. At the same time a strain gauge could be attached in a direction perpendicular to the direction of loading so that lateral strains are measured. The ratio lateral strain/longitudinal strain is Poisson's ratio, ν, (Section 7.8).

Testing machines are usually driven hydraulically. More sophisticated versions employ load cells to record load and automatically plot load against extension or stress against strain on a pen recorder as the test proceeds, an advantage when investigating the distinctive behaviour of mild steel at yield.

Compression tests

A compression test is similar in operation to a tensile test, with the obvious difference that the load transmitted to the test piece is compressive rather than tensile. This is achieved by placing the test piece between the platens of the testing machine and reversing the direction of loading. Test pieces are normally cylindrical and are limited in length to eliminate the possibility of failure being caused by instability (Chapter 21). Again contractions are measured over a given gauge length by a suitable strain measuring device.

Variations in test pieces occur when only the ultimate strength of the material in compression is required. For this purpose concrete test pieces may take the form of cubes having edges approximately 10 cm long, while mild steel test pieces are still cylindrical in section but are of the order of 1 cm long.

Bending tests

Many structural members are subjected primarily to bending moments. Bending tests are therefore carried out on simple beams constructed from the different materials to determine their behaviour under this type of load.

Two forms of loading are employed the choice depending upon the type specified in Codes of

loading system as shown in Fig. 8.2(a). Two concentrated loads are applied symmetrically to the beam, producing zero shear force and constant bending moment in the central span of the beam (Fig. 8.2(b) and (c)). The condition of pure bending is therefore achieved in the central span (see Section 9.1).

The second form of loading system consists of a single concentrated load at mid-span (Fig. 8.3(a)) which produces the shear force and bending moment diagrams shown in Fig. 8.3(b) and (c).

The loads may be applied manually by hanging weights on the beam or by a testing machine. Deflections are measured by a dial gauge placed underneath the beam. From the recorded results a load–deflection diagram is plotted.

For most ductile materials the test beams continue to deform without failure and fracture does not occur. Thus plastic properties, e.g. the ultimate strength in bending, cannot be determined for such materials. In the case of brittle materials, including cast iron, timber and various plastics, failure does occur, so that plastic properties can be evaluated. For such materials the ultimate strength in bending is defined by the *modulus of rupture.* This is taken to be the maximum direct stress in bending, $\sigma_{x,u}$, corresponding to the ultimate moment M_u, and is assumed to be related to M_u by the elastic relationship

$$\sigma_{x,u} = \frac{M_u}{I} y_{max} \text{ (see Eq. 9.9)}$$

Other bending tests are designed to measure the ductility of a material and involve the bending of a bar round a pin. The angle of bending at which the bar starts to crack is then taken as an indication of its ductility.

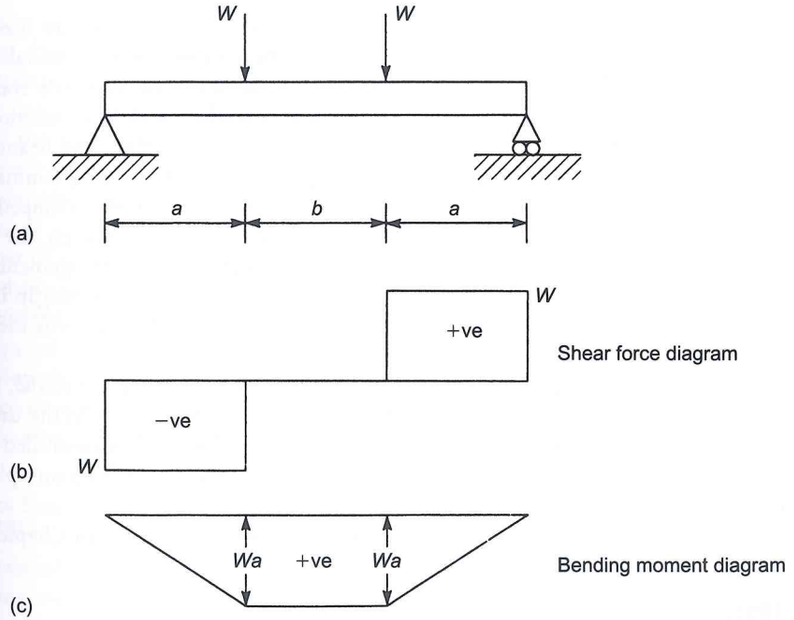

FIGURE 8.2

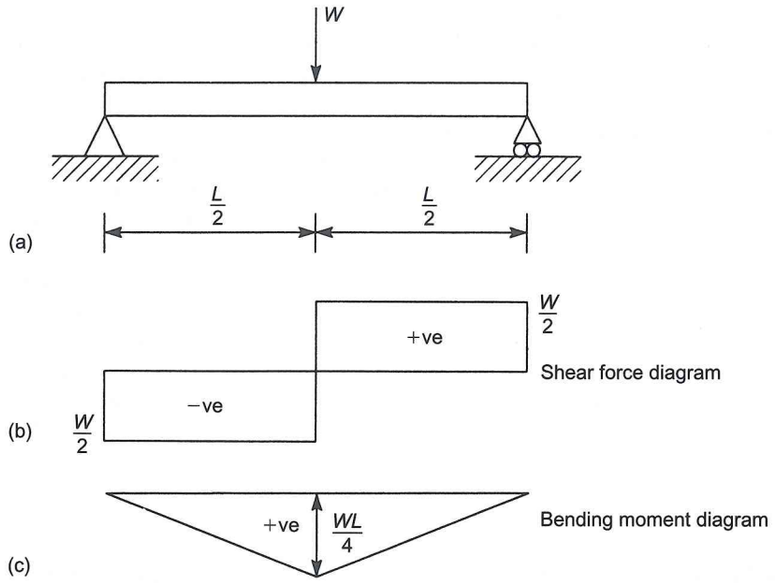

FIGURE 8.3
Bending test on a beam, single load.

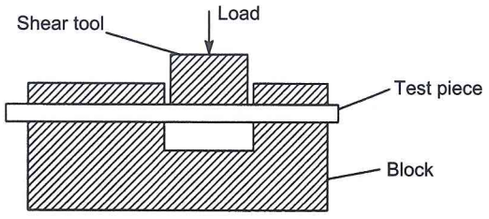

FIGURE 8.4
Shear test.

Shear tests

Two main types of shear test are used to determine the shear properties of materials. One type investigates the direct or transverse shear strength of a material and is used in connection with the shear strength of bolts, rivets and beams. A typical arrangement is shown diagrammatically in Fig. 8.4 where the test piece is clamped to a block and the load is applied through the shear tool until failure occurs. In the arrangement shown the test piece is subjected to double shear, whereas if it is extended only partially across the gap in the block it would be subjected to single shear. In either case the average shear strength is taken as the maximum load divided by the shear resisting area.

The other type of shear test is used to evaluate the basic shear properties of a material, such as the shear modulus, G (Eq. (7.9)), the shear stress at yield and the ultimate shear stress. In the usual form of test a solid circular-section test piece is placed in a torsion machine and twisted by controlled increments of torque. The corresponding angles of twist are recorded and torque–twist diagrams plotted from which the shear properties of the material are obtained. The method is similar to that used to determine the tensile properties of a material from a tensile test and uses relationships derived in Chapter 11.

Hardness tests

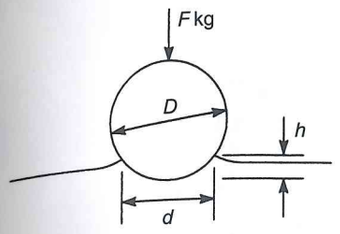

FIGURE 8.5
Brinell hardness test.

tensile strength so that hardness tests may be used to determine the properties of a finished structural member where tensile and other tests would be impracticable. Hardness tests are also used to investigate the effects of heat treatment, hardening and tempering and of cold forming. Two types of hardness test are in common use: *indentation tests* and *scratch and abrasion tests.*

Indentation tests may be subdivided into two classes: static and dynamic. Of the static tests the *Brinell* is the most common. In this a hardened steel ball is pressed into the material under test by a static load acting for a fixed period of time. The load in kg divided by the spherical area of the indentation in mm^2 is called the *Brinell Hardness Number* (BHN). Thus in Fig. 8.5, if D is the diameter of the ball, F the load in kg, h the depth of the indentation, and d the diameter of the indentation, then

$$\text{BHN} = \frac{F}{\pi D h} = \frac{2F}{\pi D\left[D - \sqrt{D^2 - d^2}\right]}$$

In practice the hardness number of a given material is found to vary with F and D so that for uniformity the test is standardized. For steel and hard materials $F = 3000$ kg and $D = 10$ mm while for soft materials $F = 500$ kg and $D = 10$ mm; in addition the load is usually applied for 15 s.

In the Brinell test the dimensions of the indentation are measured by means of a microscope. To avoid this rather tedious procedure, direct reading machines have been devised of which the *Rockwell* is typical. The indenting tool, again a hardened sphere, is first applied under a definite light load. This indenting tool is then replaced by a diamond cone with a rounded point which is then applied under a specified indentation load. The difference between the depth of the indentation under the two loads is taken as a measure of the hardness of the material and is read directly from the scale.

A typical dynamic hardness test is performed by the *Shore Scleroscope* which consists of a small hammer approximately 20 mm long and 6 mm in diameter fitted with a blunt, rounded, diamond point. The hammer is guided by a vertical glass tube and allowed to fall freely from a height of 25 cm onto the specimen, which it indents before rebounding. A certain proportion of the energy of the hammer is expended in forming the indentation so that the height of the rebound, which depends upon the energy still possessed by the hammer, is taken as a measure of the hardness of the material.

A number of tests have been devised to measure the 'scratch hardness' of materials. In one test, the smallest load in grams which, when applied to a diamond point, produces a scratch visible to the naked eye on a polished specimen of material is called its hardness number. In other tests the magnitude of the load required to produce a definite width of scratch is taken as the measure of hardness. Abrasion tests, involving the shaking over a period of time of several specimens placed in a container, measure the resistance to wear of some materials. In some cases there appears to be a connection between wear and hardness number although the results show no level of consistency.

Impact tests

It has been found that certain materials, particularly heat-treated steels, are susceptible to failure under shock loading whereas an ordinary tensile test on the same material would show no abnormality. Impact tests measure the ability of materials to withstand shock loads and provide an indication of their

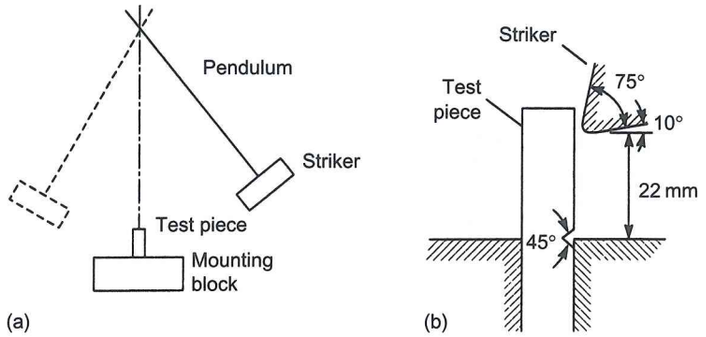

FIGURE 8.6
Izod impact test.

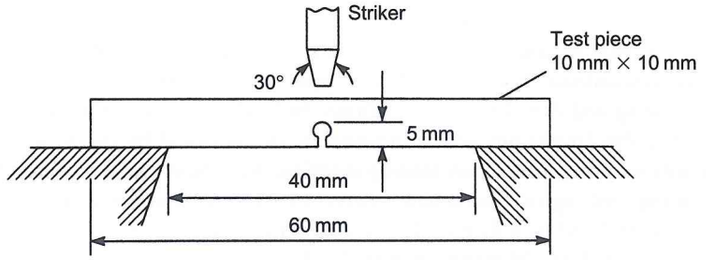

FIGURE 8.7
Charpy impact test.

Both tests rely on a striker or weight attached to a pendulum. The pendulum is released from a fixed height, the weight strikes a notched test piece and the angle through which the pendulum then swings is a measure of the toughness of the material. The arrangement for the Izod test is shown diagrammatically in Fig. 8.6(a). The specimen and the method of mounting are shown in detail in Fig. 8.6(b). The Charpy test is similar in operation except that the test piece is supported in a different manner as shown in the plan view in Fig. 8.7.

8.3 Stress–strain curves

We shall now examine in detail the properties of the different materials used in civil engineering construction from the viewpoint of the results obtained from tensile and compression tests.

Low carbon steel (mild steel)

A nominal stress–strain curve for mild steel, a ductile material, is shown in Fig. 8.8. From 0 to 'a' the stress–strain curve is linear, the material in this range obeying Hooke's law. Beyond 'a', the *limit of proportionality*, stress is no longer proportional to strain and the stress–strain curve continues to 'b', the *elastic limit*, which is defined as the maximum stress that can be applied to a material without produc-

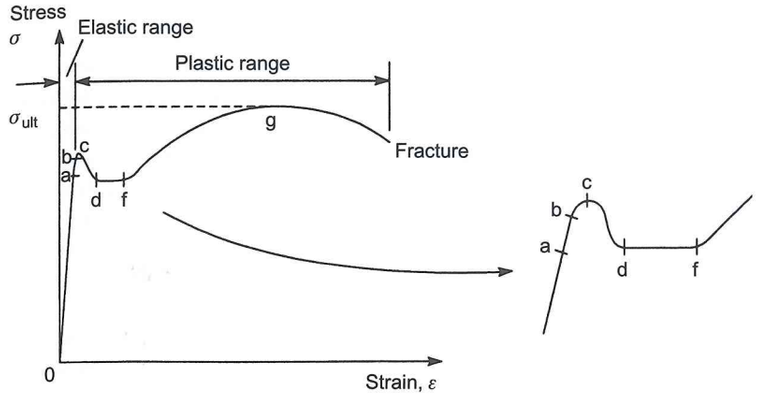

FIGURE 8.8
Stress–strain curve for mild steel.

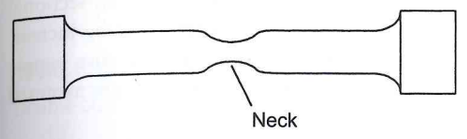

FIGURE 8.9
'Necking' of a test piece in the plastic range.

material is stressed beyond 'b' and the load then removed, a residual strain exists at zero load. For many materials it is impossible to detect a difference between the limit of proportionality and the elastic limit. From 0 to 'b' the material is said to be in the *elastic range* while from 'b' to fracture the material is in the *plastic range*. The transition from the elastic to the plastic range may be explained by considering the arrangement of crystals in the material. As the load is applied, slipping occurs between the crystals which are aligned most closely to the direction of load. As the load is increased, more and more crystals slip with each equal load increment until appreciable strain increments are produced and the plastic range is reached.

A further increase in stress from 'b' results in the mild steel reaching its *upper yield point* at 'c' followed by a rapid fall in stress to its *lower yield point* at 'd'. The existence of a lower yield point for mild steel is a peculiarity of the tensile test wherein the movement of the ends of the test piece produced by the testing machine does not proceed as rapidly as its plastic deformation; the load therefore decreases, as does the stress. From 'd' to 'f' the strain increases at a roughly constant value of stress until *strain hardening* (see Section 8.4) again causes an increase in stress. This increase in stress continues, accompanied by a large increase in strain to 'g', the *ultimate stress*, σ_{ult}, of the material. At this point the test piece begins, visibly, to 'neck' as shown in Fig. 8.9. The material in the test piece in the region of the 'neck' is almost perfectly plastic at this stage and from this point, onwards to fracture, there is a reduction in nominal stress.

For mild steel, yielding occurs at a stress of the order of 300 N/mm^2. At fracture the strain (i.e. the elongation) is of the order of 30%. The gradient of the linear portion of the stress–strain curve gives a value for Young's modulus in the region of 200 000 N/mm^2.

The characteristics of the fracture are worthy of examination. In a cylindrical test piece the two halves of the fractured test piece have ends which form a 'cup and cone' (Fig. 8.10). The actual failure planes in this case are inclined at approximately 45° to the axis of loading and coincide with planes of maximum shear stress (Section 14.2). Similarly, if a flat tensile specimen of mild steel is polished and

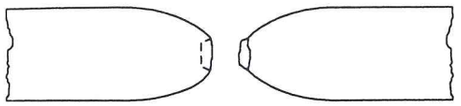

FIGURE 8.10

'Cup-and-cone' failure of a mild steel test piece.

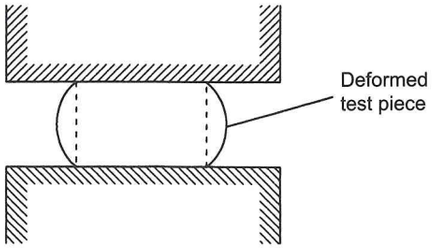

FIGURE 8.11

'Barrelling' of a mild steel test piece in compression.

then stressed, a pattern of fine lines appears on the polished surface at yield. These lines, which were first discovered by Lüder in 1854, intersect approximately at right angles and are inclined at 45° to the axis of the specimen, thereby coinciding with planes of maximum shear stress. These forms of yielding and fracture suggest that the crystalline structure of the steel is relatively weak in shear with yielding taking the form of the sliding of one crystal plane over another rather than the tearing apart of two crystal planes.

The behaviour of mild steel in compression is very similar to its behaviour in tension, particularly in the elastic range. In the plastic range it is not possible to obtain ultimate and fracture loads since, due to compression, the area of cross section increases as the load increases producing a 'barrelling' effect as shown in Fig. 8.11. This increase in cross-sectional area tends to decrease the true stress, thereby increasing the load resistance. Ultimately a flat disc is produced. For design purposes the ultimate stresses of mild steel in tension and compression are assumed to be the same.

The ductility of mild steel is often an advantage in that structures fabricated from mild steel do not generally suffer an immediate and catastrophic collapse if the yield stress of a member is exceeded. The member will deform in such a way that loads are redistributed to other adjacent members and at the same time will exhibit signs of distress thereby giving a warning of a probable impending collapse.

Higher grades of steel have greater strengths than mild steel but are not as ductile. They also possess the same Young's modulus so that the higher stresses are accompanied by higher strains.

Steel structures are very susceptible to rust which forms on surfaces exposed to oxygen and moisture (air and rain) and this can seriously weaken a member as its cross-sectional area is eaten away. Generally, exposed surfaces are protected by either *galvanizing*, in which they are given a coating of zinc, or by painting. The latter system must be properly designed and usually involves shot blasting the steel to remove the loose steel flakes, or millscale, produced in the hot rolling process, priming, undercoating and painting. Cold-formed sections do not suffer from millscale so that protective treatments are more easily applied.

Aluminium

Aluminium and some of its alloys are also ductile materials, although their stress–strain curves do not have the distinct yield stress of mild steel. A typical stress–strain curve is shown in Fig. 8.12. The points 'a' and 'b' again mark the limit of proportionality and elastic limit, respectively, but are difficult to determine experimentally. Instead a *proof stress* is defined which is the stress required to produce a given permanent strain on removal of the load. In Fig. 8.12, a line drawn parallel to the linear portion of the stress–strain curve from a strain of 0.001 (i.e. a strain of 0.1%) intersects the stress–strain curve at the 0.1% proof stress. For elastic design this, or the 0.2% proof stress, is taken as the working stress.

Beyond the limit of proportionality the material extends plastically, reaching its ultimate stress, σ_{ult},

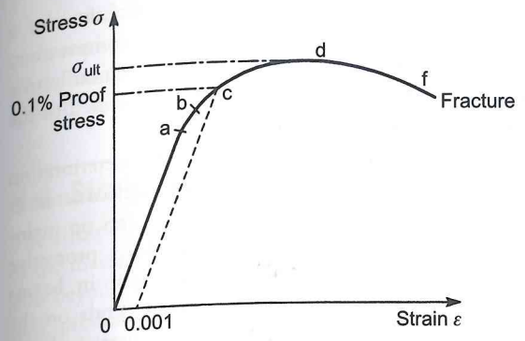

FIGURE 8.12

Stress–strain curve for aluminium.

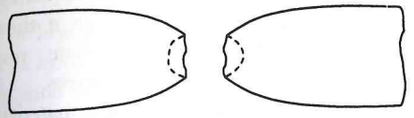

FIGURE 8.13

'Double-cup' failure of an aluminium alloy test piece.

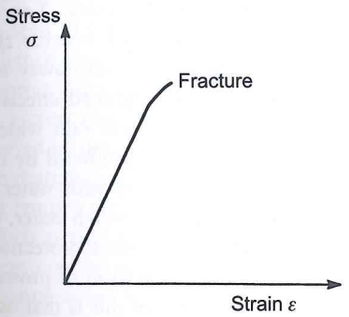

FIGURE 8.14

Stress–strain curve for a brittle material.

A feature of the fracture of aluminium alloy test pieces is the formation of a 'double cup' as shown in Fig. 8.13, implying that failure was initiated in the central portion of the test piece while the outer surfaces remained intact. Again considerable 'necking' occurs.

In compression tests on aluminium and its ductile alloys similar difficulties are encountered to those experienced with mild steel. The stress–strain curve is very similar in the elastic range to that obtained in a tensile test but the ultimate strength in compression cannot be determined; in design its value is assumed to coincide with that in tension.

Aluminium and its alloys can suffer a form of corrosion particularly in the salt laden atmosphere of coastal regions. The surface becomes pitted and covered by a white furry deposit. This can be prevented by an electrolytic process called *anodizing* which covers the surface with an inert coating. Aluminium alloys will also corrode if they are placed in direct contact with other metals, such as steel. To prevent this, plastic is inserted between the possible areas of contact.

Brittle materials

These include cast iron, high-strength steel, concrete, timber, ceramics, glass, etc. The plastic range for brittle materials extends to only small values of strain. A typical stress–strain curve for a brittle material under tension is shown in Fig. 8.14. Little or no yielding occurs and fracture takes place very shortly after the elastic limit is reached.

The fracture of a cylindrical test piece takes the form of a single failure plane approximately perpendicular to the direction of loading with no visible 'necking' and an elongation of the order of 2–3%.

In compression the stress–strain curve for a brittle material is very similar to that in tension except that failure occurs at a much higher value of stress; for concrete the ratio is of the order of 10: 1. This is thought to be due to the presence of microscopic cracks in the material, giving rise to high stress concentrations which are more likely to have a greater effect in reducing tensile strength than compressive strength.

The form of the fracture of brittle materials under compression is clear and visible. For example, a cast-iron cylinder cracks on a diagonal plane as shown in Fig. 8.15(a) while failure of a concrete cube is

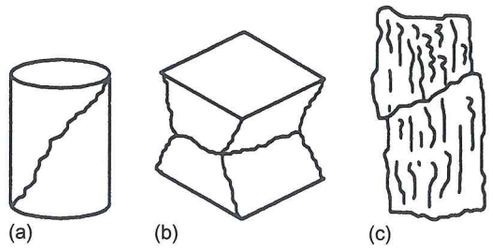

FIGURE 8.15

Failure of brittle materials.

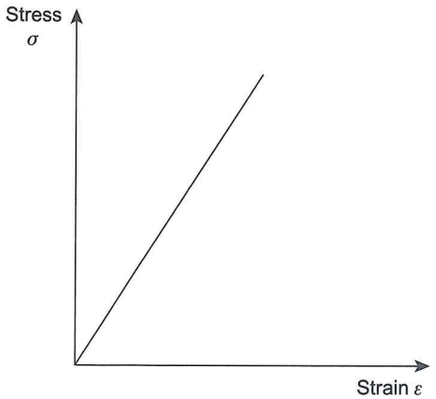

FIGURE 8.16

Stress–strain curve for a fibre composite.

Figure 8.15(c) shows a typical failure of a rectangular block of timber in compression. Failure in all these cases is due primarily to a breakdown in shear on planes inclined to the direction of compression.

Brittle materials can suffer deterioration in hostile environments although concrete is very durable and generally requires no maintenance. Concrete also provides a protective cover for the steel reinforcement in beams where the amount of cover depends on the diameter of the reinforcing bars and the degree of exposure of the beam. In some situations, e.g. in foundations, concrete is prone to chemical attack from sulphates contained in groundwater although if these are known to be present sulphate resisting cement can be used in the concrete.

Brick and stone are durable materials and can survive for hundreds of years as evidenced by the many medieval churches and Jacobean houses which still exist. There are, of course, wide variations in durability. For example, granite is extremely hard whereas the much softer sandstone can be worn away over periods of time by the combined effects of wind and rain, particularly acid rain which occurs when sulphur dioxide, produced by the burning of fossil fuels, reacts with water to form sulphuric acid. Bricks and stone are vulnerable to repeated wetting and freezing in which water, penetrating any surface defect, can freeze causing parts of the surface to flake off or *spall.* Some protection can be provided by masonry paints but these require frequent replacement. An alternative form of protection is a sealant which can be sprayed onto the surface of the masonry. The disadvantage of this is that, while preventing moisture penetrating the building, it also prevents water vapour from leaving. The ideal solution is to use top quality materials, do not apply any treatment and deal with any problem as it arises.

Timber, as we noted in Chapter 1, can be protected from fungal and insect attacks by suitable treatments.

Composites

Fibre composites have stress–strain characteristics which indicate that they are brittle materials (Fig. 8.16). There is little or no plasticity and the modulus of elasticity is less than that of steel and aluminium alloy. However, the fibres themselves can have much higher values of strength and modulus of elasticity than the composite. For example, carbon fibres have a tensile strength of the order 2400 N/mm^2 and a modulus of elasticity of 400 000 N/mm^2.

Fibre composites are highly durable, require no maintenance and can be used in hostile chemical

All the stress–strain curves described in the preceding discussion are those produced in tensile or compression tests in which the strain is applied at a negligible rate. A rapid strain application would result in significant changes in the apparent properties of the materials giving possible variations in yield stress of up to 100%.

8.4 Strain hardening

The stress–strain curve for a material is influenced by the *strain history*, or the loading and unloading of the material, within the plastic range. For example, in Fig. 8.17 a test piece is initially stressed in tension beyond the yield stress at, 'a', to a value at 'b'. The material is then unloaded to 'c' and reloaded to 'f' producing an increase in yield stress from the value at 'a' to the value at 'd'. Subsequent unloading to 'g' and loading to 'j' increases the yield stress still further to the value at 'h'. This increase in strength resulting from the loading and unloading is known as *strain hardening.* It can be seen from Fig. 8.17 that the stress–strain curve during the unloading and loading cycles forms loops (the shaded areas in Fig. 8.17). These indicate that strain energy is lost during the cycle, the energy being dissipated in the form of heat produced by internal friction. This energy loss is known as *mechanical hysteresis* and the loops as *hysteresis loops.* Although the ultimate stress is increased by strain hardening it is not influenced to the same extent as yield stress. The increase in strength produced by strain hardening is accompanied by decreases in toughness and ductility.

8.5 Creep and relaxation

We have seen in Chapter 7 that a given load produces a calculable value of stress in a structural member and hence a corresponding value of strain once the full value of the load is transferred to the member. However, after this initial or 'instantaneous' stress and its corresponding value of strain have been attained, a great number of structural materials continue to deform slowly and progressively under load over a period of time. This behaviour is known as *creep.* A typical creep curve is shown in Fig. 8.18.

Some materials, such as plastics and rubber, exhibit creep at room temperatures but most structural materials require high temperatures or long-duration loading at moderate temperatures. In some 'soft' metals, such as zinc and lead, creep occurs over a relatively short period of time, whereas materials such as concrete may be subject to creep over a period of years. Creep occurs in steel to a slight extent at normal temperatures but becomes very important at temperatures above 316°C.

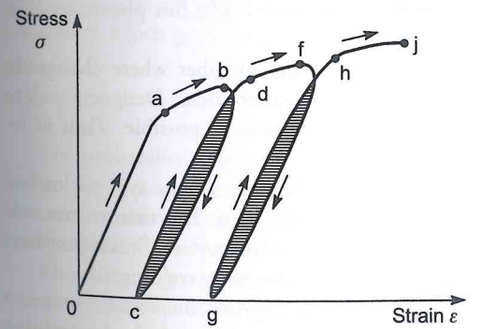

FIGURE 8.17

Strain hard...

Closely related to creep is *relaxation.* Whereas creep involves an increase in strain under constant stress, relaxation is the decrease in stress experienced over a period of time by a material subjected to a constant strain.

8.6 Fatigue

Structural members are frequently subjected to repetitive loading over a long period of time. For example, the members of a bridge structure suffer variations in loading possibly thousands of times a day as traffic moves over the bridge. In these cir-

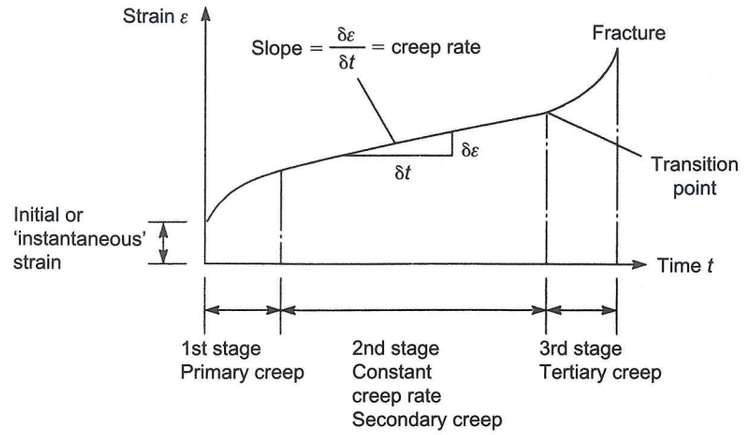

FIGURE 8.18

Typical creep curve.

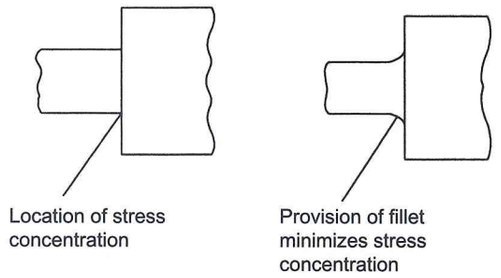

FIGURE 8.19

Stress concentration location.

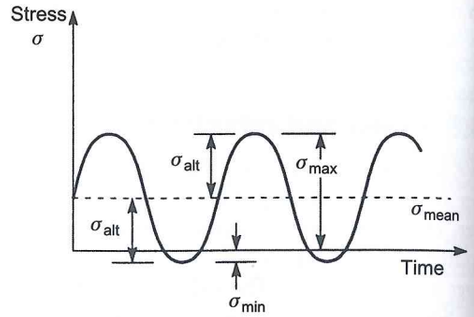

FIGURE 8.20

Alternating stress in fatigue loading.

level of stress substantially below the ultimate stress for non-repetitive static loads; this phenomenon is known as *fatigue.*

Fatigue cracks are most frequently initiated at sections in a structural member where changes in geometry, e.g. holes, notches or sudden changes in section, cause *stress concentrations.* Designers seek to eliminate such areas by ensuring that rapid changes in section are as smooth as possible. Thus at re-entrant corners, fillets are provided as shown in Fig. 8.19.

Other factors which affect the failure of a material under repetitive loading are the type of loading (fatigue is primarily a problem with repeated tensile stresses due, probably, to the fact that microscopic cracks can propagate more easily under tension), temperature, the material, surface finish (machine marks are potential crack propagators), corrosion and residual stresses produced by welding.

Frequently in structural members an alternating stress, σ_{alt}, is superimposed on a static or mean stress, σ_{mean}, as illustrated in Fig. 8.20. The value of σ_{alt} is the most important factor in determining the number of cycles of load that produce failure. The stress, σ_{alt}, that can be withstood for a specified

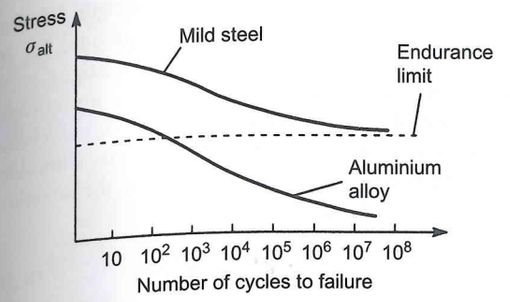

FIGURE 8.21

Stress-endurance curves.

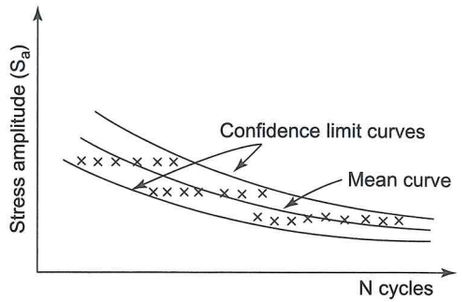

FIGURE 8.22

S-N diagram

a stress level that can be withstood for an indefinite number of cycles. This stress is known as the *endurance limit* of the material; no such limit has been found for aluminium and its alloys. Fatigue data are frequently presented in the form of an $S-n$ curve or stress-endurance curve as shown in Fig. 8.21.

The stress-endurance curves shown in Fig. 8.21 correspond to the average value of N at each stress amplitude since the given stress has a wide range of values of N; even under carefully controlled conditions the ratio of maximum N to minimum N may be as high as 10:1. Two other curves may therefore be drawn as shown in Fig. 8.22 enveloping all, or nearly all, the experimental results; these curves are known as the *confidence limits.* If 99.9 % of all the results lie between the curves, that is, only 1 in 1000 falls outside, they represent the 99.9% confidence limits. If 99.99999% of results lie between the curves only 1 in 10^7 results falls outside them and they represent the 99.99999% confidence limits.

The results from tests on a number of specimens may be represented as histograms in which the number of specimens failing within certain ranges R of N is plotted against N. Then, if N_{av} is the average value of N at a given stress amplitude, the probability of failure occurring at N cycles is given by

$$p(N) = [1/(\sigma\sqrt{2\pi})] \exp\{-(N - N_{av})/\sigma]^2/2\} \tag{8.1}$$

in which σ is the standard deviation of the whole population of N values. The derivation of Eq. (8.1) depends on the histogram approaching the profile of a continuous function close to the *normal distribution* which it does as the interval of N_{av}/R becomes smaller and the number of tests increases. The *cumulative probability*, which gives the probability that a particular specimen fails at or below N cycles, is defined as

$$P(N) = \int_{-\infty}^{N} p(N)\, dN \tag{8.2}$$

The probability that a specimen endures more than N cycles is then $1 - P(N)$. The normal distribution allows negative values of N which is clearly impossible in a fatigue testing situation. Other distributions, *extreme value distributions*, are more realistic and allow the existence of minimum fatigue endurances and fatigue limits.

The damaging portion of a fluctuating load cycle occurs when the stress is tensile; this causes cracks to open and grow. Therefore, if a steady tensile stress is superimposed on a cyclic stress the maximum tensile stress during the cycle increases and the number of cycles to failure decreases. An approximate method of assessing the effect of a steady mean value of stress is provided by a Goodman diagram

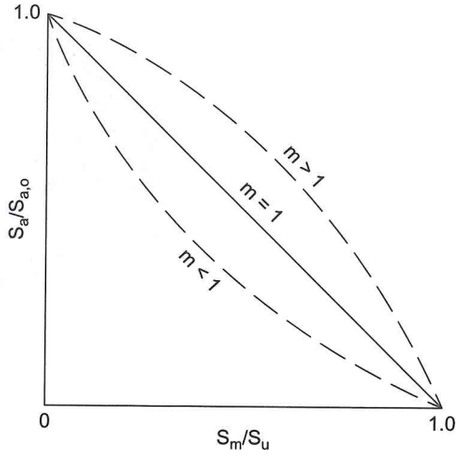

FIGURE 8.23
Goodman diagram

mean stress levels to give a constant fatigue life. In Fig. 8.23 S_a is the allowable stress amplitude, $S_{a,0}$ is the stress amplitude required to produce fatigue at N cycles with zero mean stress, S_m is the mean stress and S_u the ultimate tensile stress. If $S_m = S_u$ any cyclic stress causes failure while if $S_m = 0$ the allowable stress amplitude is $S_{a,0}$. The equation of the straight-line portion of the diagram is

$$(S_a/S_{a,0}) = [1 - (S_m/S_u)] \qquad (8.3)$$

Experimental evidence suggests a non-linear relationship for particular materials. Equation (8.3) then becomes

$$(S_a/S_{a,0}) = [1 - (S_m/S_u)^m] \qquad (8.4)$$

where m lies between 0.6 and 2. The relationship for the case of $m = 2$ is known as the *Gerber parabola.*

EXAMPLE 8.1

The allowable stress amplitude for a low-carbon steel is ± 225 N/mm^2 and its ultimate tensile stress is 750 N/mm^2. The steel is subjected to a repeated cycle of stress in which the minimum stress is zero. Calculate the safe range of stress based on the Goodman and Gerber predictions.

For the Goodman prediction Eq. (8.3) applies in which $S_{a,0} = 450$ N/mm^2 and $S_m = S_a/2$. Then

$$S_a = 450[1 - (S_a/2 \times 750)]$$

from which

$$S_a = 346 \text{ N/mm}^2$$

For the Gerber prediction $m = 2$ in Eq. (8.4). Then

$$S_a = 450[1 - (S_a/2 \times 750)^2]$$

which simplifies to

$$S_a^2 + 5000S_a - 2.25 \times 10^6 = 0$$

Solving gives

$$S_a = 415 \text{ N/mm}^2$$

EXAMPLE 8.2

If the steel in Ex. 8.1 is subjected to an alternating cycle of tensile stress about a mean stress of 180 N/mm^2 calculate the safe range of stress based on the Goodman prediction and also the maximum stress values.

From Eq. (8.3)

$$S_a = 450[1 - (180/750)]$$

which gives

$$S_a = 342 \text{ N/mm}^2$$

Now

$$S_a = \sigma_{max} - \sigma_{min} \qquad \text{(i)}$$

and

$$S_m = (\sigma_{max} + \sigma_{min})/2 \qquad \text{(ii)}$$

Adding Eqs (i) and (ii)

$$S_a + 2S_m = 2\sigma_{max}$$

that is

$$342 + 2 \times 180 = 2\sigma_{max}$$

so that

$$\sigma_{max} = 351 \text{ N/mm}^2$$

Then, from Eq. (i)

$$\sigma_{min} = 351 - 342 = 9 \text{ N/mm}^2$$

In many practical situations the amplitude of the alternating stress varies and is frequently random in nature. The S–n curve does not, therefore, apply directly and an alternative means of predicting failure is required. *Miner's cumulative damage theory* suggests that failure will occur when

$$\frac{n_1}{N_1} + \frac{n_2}{N_2} + \cdots + \frac{n_r}{N_r} = 1 \qquad (8.5)$$

where $n_1, n_2, \ldots, n_r$ are the number of applications of stresses σ_{alt}, σ_{mean} and $N_1, N_2, \ldots, N_r$ are the number of cycles to failure of stresses σ_{alt}, σ_{mean}.

EXAMPLE 8.3

In a fatigue test a steel specimen is subjected to a reversed cyclic loading in a continuous sequence of four stages as follows:

200 cycles at ± 150 N/mm^2
250 cycles at ± 125 N/mm^2
400 cycles at ± 120 N/mm^2
550 cycles at ± 100 N/mm^2

If the loading is applied at the rate of 80 cycles/hour and the fatigue lives at these stress levels are 10^4, 10^5, 1.5×10^5 and 2×10^5, respectively, calculate the life of the specimen.

Suppose that the specimen fails after P sequences of the four stages. Then, from Eq. (8.6)

$$P[(200/10^4) + (250/10^5) + (400/1.5 \times 10^5) + (550/2 \times 10^5)] = 1$$

which gives

$$P = 35.8$$

The total number of cycles in the four stages is 1400 so that for a loading rate of 80 cycles/hour the total number of hours to fracture is given by

$$\text{Total hours to fracture} = 35.8 \times 1400/80 = 626.5$$

Crack propagation

We have noted that the fatigue life of a structural member can be severely compromised by the presence of cracks. It is useful, therefore, for a designer to be able to predict the rate at which a perceived crack will propagate until it reaches proportions at which the member will fail.

There are three basic modes of crack growth and these are shown in Fig. 8.24.

Generally, the stress field in the region of the crack tip is described by a two-dimensional model which may be used as an approximation for many practical three-dimensional loading cases. Texts on fracture mechanics suggest that the stress system at a distance r ($r \leq a$) from the tip of the crack of length $2a$, as shown in Fig. 8.25, can be expressed in the form

$$S_r, S_\theta, S_{r,\theta} = [K/(2\pi r)^{1/2}]f(\theta) \tag{8.6}$$

in which $f(\theta)$ is a different function for each of the three stresses and K is the *stress concentration factor*; K is a function of the nature and magnitude of the applied stress levels and also of the crack size. The terms $(2\pi r)^{1/2}$ and $f(\theta)$ map the stress field in the vicinity of the crack and are the same for all cracks under external loads that cause crack openings of the same type.

Equation (8.6) applies to all modes of crack opening with K having different values depending on the geometry of the structure, the nature of the applied loads and the type of crack.

Experimental data show that crk growth and residual strength data are better correlated using K than any other parameter. K may be expressed as a function of the nominal applied stress, S, and the crack length in the form

$$K = S(\pi a)^{1/2}\alpha \tag{8.7}$$

in which α is a non-dimensional coefficient usually expressed as the ratio of crack length to any convenient local dimension in the plane of the component; for a crack in an infinite plate under an applied uniform stress level, S, remote from the crack, $\alpha = 1.0$. Alternatively, in cases where opposing loads, P, are applied at points close to the crack

$$K = P\alpha/(\pi a)^{1/2} \tag{8.8}$$

in which P is the load/unit thickness. Equations (8.7) and (8.8) may be rewritten as

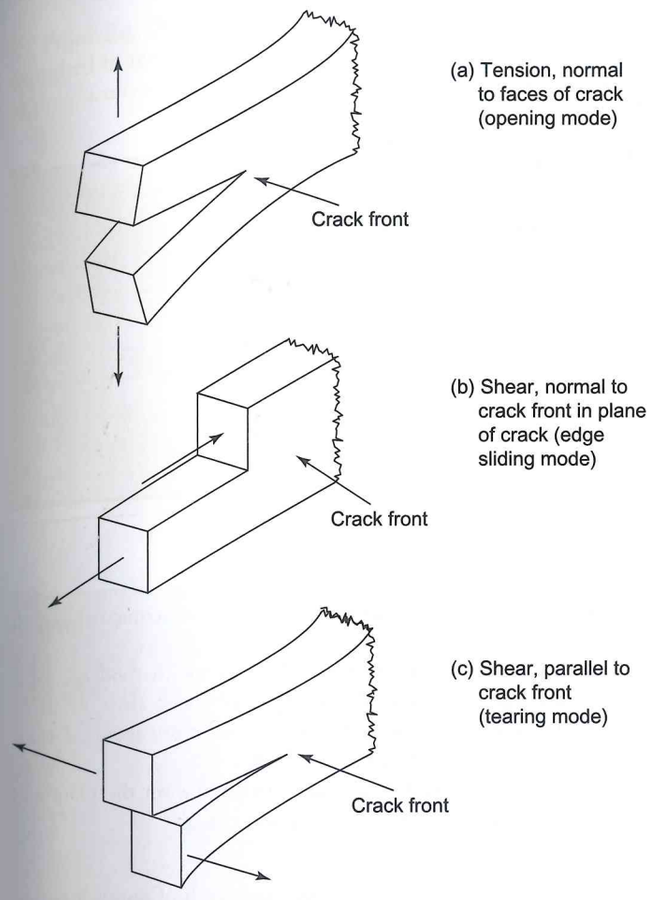

FIGURE 8.24
Basic modes of crack growth

where K_0 is a reference value of the stress concentration factor which depends on the loading. For the simple case of a remotely loaded plate in tension

$$K_0 = S(\pi a)^{1/2} \tag{8.10}$$

and Eqs (8.9) and (8.7) are identical so that, for a given ratio of crack length to plate width, α is the same in both formulations. In more complex cases, for example the in-plane bending of a plate of width $2b$ and having a central crack of length $2a$

$$K_0 = (3Ma/4b^3)(\pi a)^{1/2} \tag{8.11}$$

in which M is the bending moment per unit thickness. Comparing Eqs (8.11) and (8.7) we see that $S = 3Ma/4b^3$ which is the value of direct stress given by basic bending theory at a point a distance $\pm a/2$ from the central axis (see Chapter 9). However, if S is specified as the bending stress in the outer fibres of the plate, that is at $\pm b$, then $S = 3M/2b^2$; clearly the different specifications of S require different values of α. On the other hand the final value of K must be independent of the form of presentation used. [illegible]

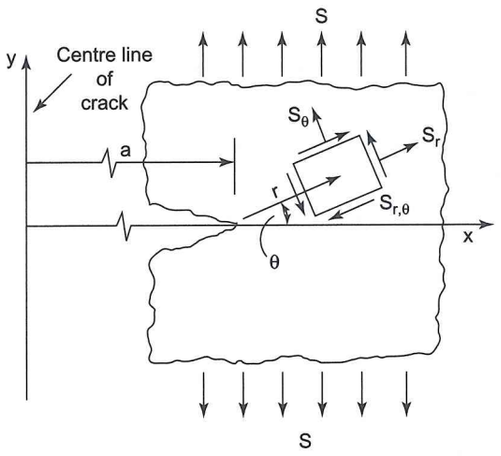

FIGURE 8.25
Stress field in the vicinity of a crack

to ensure that the formula used and the way in which the nominal stress is defined are compatible with those used in the derivation of α.

A number of methods are available for determining the values of K and α. In one method the solution for a structural member subjected to more than one type of loading is obtained from available standard solutions using superposition or, if the geometry is not covered, two or more standard solutions may be compounded. Alternatively a finite element analysis may be used.

The coefficient α in Eq. (8.7) has, as we have noted, different values depending on the plate and crack geometries. The following are values of α for some of the more common cases.

i. A semi-infinite plate having an edge crack of length a; $\alpha = 1.12$.

ii. An infinite plate having an embedded circular crack or a semi-circular crack each of radius a and lying in a plane normal to the applied stress; $\alpha = 0.64$.

iii. An infinite plate having an embedded elliptical crack of axes $2a$ and $2b$ or a semi-elliptical crack of width $2b$ in which the depth a is less than half the plate thickness, each lying in a plane normal to the applied stress; $\alpha = 1.12\Phi$ in which Φ varies with the ratio b/a as follows:

b/a	0	0.2	0.4	0.6	0.8
Φ	1.0	1.05	1.15	1.28	1.42

For $b/a = 1$ the situation is identical to case (ii).

iv. A plate of finite width w having a central crack of length $2a$ where $a \leq 0.3w$;

$$\alpha = [\sec(a\pi/w)]^{1/2}.$$

v. For a plate of finite width w having two symmetrical edge cracks each of depth $2a$, Eq. (8.7) becomes

From Eq. (8.6) it can be seen that the stress concentration at a point ahead of a crack can be expressed in terms of the parameter K. Failure occurs when K reaches a critical value K_c. This is known as the *fracture toughness* of the material and has units $MN/m^{3/2}$ or $N/mm^{3/2}$.

EXAMPLE 8.4

An infinite plate has a fracture toughness of 3300 $N/mm^{3/2}$. If the plate contains an embedded circular crack of 3 mm radius calculate the maximum allowable stress that could be applied around the boundary of the plate.

In this case Eq. (8.7) applies with $\alpha = 0.64$. Then,

$$S = 3300/[(\pi \times 3)^{1/2} \times 0.64]$$

which gives

$$S = 1680 \text{ N/mm}^2$$

EXAMPLE 8.5

If the steel plate of Ex. 8.4 develops an elliptical crack of length 6 mm and width 2.4 mm calculate the allowable stress that could be applied around the boundary of the plate.

In this case $b/a = 1.2/3 = 0.4$. Then $\alpha = 1.12 \times 1.15 = 1.164$ and from Eq. (8.7)

$$S = 3300/[(\pi \times 3)^{1/2} \times 1.164]$$

so that

$$S = 931.5 \text{ N/mm}^2$$

EXAMPLE 8.6

Suppose that the plate of Ex. 8.4 has a finite width of 50 mm and develops a central crack of length 6 mm. What then is the allowable stress that could be applied around the boundary of the plate?

For this case

$$\alpha = [\sec(\pi a/w)]^{1/2} = [\sec(\pi \times 3/50)]^{1/2} = 1.018$$

so that

$$S = 3300/[(\pi \times 3)^{1/2} \times 1.018]$$

which gives

$$S = 1056 \text{ N/mm}^2$$

Having obtained values of the stress concentration factor and the coefficient α fatigue propagation rates may be estimated. From these the life of a structure containing cracks or crack-like defects may be determined. Alternatively the loading condition may be modified or inspection periods arranged so that the crack is detected before failure. The following summarises the results detailed in specialised texts on fracture mechanics.

Under constant amplitude loading the rate of crack propagation may be represented graphically by curves described in general terms by the law

$$(da/dN) = f(R, \Delta K) \tag{8.12}$$

in which ΔK is the stress concentration factor range and $R = S_{min}/S_{max}$. If Eq. (8.7) is used

$$\Delta K = (S_{max} - S_{min})(\pi a)^{1/2}\alpha \tag{8.13}$$

The curves represented by Eq. (8.12) may be divided into three regions. The first corresponding to a very slow crack growth rate ($<10^{-8}$ m/cycle) where the curves approach a threshold value of stress concentration factor ΔK^{th} corresponding to 4×10^{-11} m/cycle, that is, no crack growth. In the second region ($10^{-8} - 10^{-6}$ m/cycle) much of the crack life takes place and, for small ranges of ΔK, Eq. (8.12) may be represented by

$$(da/dN) = C(\Delta K)^n \tag{8.14}$$

in which C and n depend on the material properties; over small ranges of da/dN and ΔK, C and n remain approximately constant. The third region corresponds to crack growth rates $>10^{-6}$ m/cycle where instability and final failure occur.

An attempt has been made to describe the complete set of curves by the relationship

$$(da/dN) = C\,(\Delta K)^n/[(1 - R)K_c - \Delta K] \tag{8.15}$$

in which K_c is the fracture toughness of the material obtained from toughness tests. Integration of Eq. (8.14) or (8.15) analytically or graphically gives an estimate of the crack growth life of the structure, that is the number of cycles required for a crack to grow from an initial size to an unacceptable length or the crack growth rate for failure whichever is the design criterion. Thus, for example, integration of Eq. (8.14) gives, for an infinite width plate for which $\alpha = 1.0$

$$[N]_{Ni}^{Nf} = \left[(a^{(1-n/2)})/(1 - n/2)\right]_{ai}^{af}/C[(S_{max} - S_{min})\pi^{1/2}]^n \tag{8.16}$$

and for which $n > 2$. An analytical integration may only be carried out if n is an integer and α is in the form of a polynomial otherwise graphical or numerical techniques must be employed. Substituting the limits in Eq. (8.16) and taking $N_i = 0$, the number of cycles to failure is given by

$$N_f = 2[(1/a_i^{(n-2)/2}) - (1/a_f^{(n-2)/2})]/\{C(n - 2)[(S_{max} - S_{min})\pi^{1/2}]^n\} \tag{8.17}$$

EXAMPLE 8.7

An infinite plate contains a crack having an initial length of 0.2 mm and is subjected to a cyclic repeated stress range of 175 N/mm^2. If the fracture toughness of the plate is 1708 N/mm$^{3/2}$ and the rate of crack growth is 40×10^{-15} $(\Delta K)^4$ mm/cycle determine the number of cycles to failure.

The crack length at failure is given by Eq. (8.7) in which $\alpha = 1$, $K = 1708$ N/mm$^{3/2}$ and $S = 175$ N/mm^2. Then

$$a_f = 1708^2/(\pi \times 175^2) = 30.3 \text{ mm}$$

Also, it can be seen from Eq. (8.14) that $C = 40 \times 10^{-15}$ and $n = 4$. Substituting the relevant parameters in Eq. (8.17) gives

$$N_f = \{1/[40 \times 10^{-15}(175 \times \pi^{1/2})^4]\}[(1/0.1) - (1/30.3)]$$

From which

$$N_f = 26919 \text{ cycles}$$

8.7 Design methods

In Section 8.3 we examined stress–strain curves for different materials and saw that, generally, there are two significant values of stress: the yield stress, σ_Y, and the ultimate stress, σ_{ult}. Either of these two stresses may be used as the basis of design which must ensure, of course, that a structure will adequately perform the role for which it is constructed. In any case the maximum stress in a structure should be kept below the elastic limit of the material otherwise a permanent set will result when the loads are applied and then removed.

Two design approaches are possible. The first, known as *elastic design*, uses either the yield stress (for ductile materials), or the ultimate stress (for brittle materials) and establishes a *working* or *allowable stress* within the elastic range of the material by applying a suitable factor of safety whose value depends upon a number of considerations. These include the type of material, the type of loading (fatigue loading would require a larger factor of safety than static loading which is obvious from Section 8.6) and the degree of complexity of the structure. Therefore for materials such as steel, the working stress, σ_w, is given by

$$\sigma_w = \frac{\sigma_Y}{n} \tag{8.18}$$

where n is the factor of safety, a typical value being 1.65. For a brittle material, such as concrete, the working stress would be given by

$$\sigma_w = \frac{\sigma_{ult}}{n} \tag{8.19}$$

in which n is of the order of 2.5.

Elastic design has been superseded for concrete by *limit state* or *ultimate load* design and for steel by *plastic design* (or limit, or ultimate load design). In this approach the structure is designed with a given factor of safety against complete collapse which is assumed to occur in a concrete structure when the stress reaches σ_{ult} and occurs in a steel structure when the stress at one or more points reaches σ_Y (see Section 9.10). In the design process working or actual loads are determined and then factored to give the required ultimate or collapse load of the structure. Knowing σ_{ult} (for concrete) or σ_Y (for steel) the appropriate section may then be chosen for the structural member.

The factors of safety used in ultimate load design depend upon several parameters. These may be grouped into those related to the material of the member and those related to loads. Thus in the ultimate load design of a reinforced concrete beam the values of σ_{ult} for concrete and σ_Y for the reinforcing steel are factored by *partial safety factors* to give *design strengths* that allow for variations of workmanship or quality of control in manufacture. Typical values for the partial safety factors are 1.5 for concrete and 1.15

for the reinforcement. Note that the design strength in both cases is less than the actual strength. In addition, as stated above, design loads are obtained in which the actual loads are increased by multiplying the latter by a partial safety factor which depends upon the type of load being considered.

As well as strength, structural members must possess sufficient stiffness, under normal working loads, to prevent deflections being excessive and thereby damaging adjacent parts of the structure. Another consideration related to deflection is the appearance of a structure which can be adversely affected if large deflections cause cracking of protective and/or decorative coverings. This is particularly critical in reinforced concrete beams where the concrete in the tension zone of the beam cracks; this does not affect the strength of the beam since the tensile stresses are withstood by the reinforcement. However, if deflections are large the crack widths will be proportionately large and the surface finish and protection afforded by the concrete to the reinforcement would be impaired.

Codes of Practice limit deflections of beams either by specifying maximum span/depth ratios or by fixing the maximum deflection in terms of the span. A typical limitation for a reinforced concrete beam is that the total deflection of the beam should not exceed span/250. An additional proviso is that the deflection that takes place after the construction of partitions and finishes should not exceed span/350 or 20 mm, whichever is the lesser. A typical value for a steel beam is span/360.

It is clear that the deflections of beams under normal working loads occur within the elastic range of the material of the beam no matter whether elastic or ultimate load theory has been used in their design. Deflections of beams, therefore, are checked using elastic analysis.

8.8 Material properties

Table 8.1 lists some typical properties of the more common engineering materials.

Table 8.1

Material	Density (kN/m^3)	Modulus of Elasticity, E (N/mm^2)	Shear Modulus, G (N/mm^2)	Yield Stress, σ_Y (N/mm^2)	Ultimate Stress, σ_{ult} (N/mm^2)	Poissons Ratio v
Aluminium alloy	27.0	70 000	40 000	290	440	0.33
Brass	82.5	103 000	41 000	103	276	
Bronze	87.0	103 000	45 000	138	345	
Cast iron	72.3	103 000	41 000		552 (compression) 138 (tension)	0.25
Concrete (medium strength)	22.8	21 400			20.7 (compression)	0.13
Copper	80.6	117000	41 000	245	345	
Steel (mild)	77.0	200 000	79 000	250	410–550	0.27
Steel (high carbon)	77.0	200 000	79 000	414	690	0.27
Prestressing wire		200 000			1570	
Timber						
softwood		7000			16	
hardwood	6.0	12000			30	
Composite (glass fibre)		20 000			250	

PROBLEMS

P.8.1. Describe a simple tensile test and show, with the aid of sketches, how measures of the ductility of the material of the specimen may be obtained. Sketch typical stress–strain curves for mild steel and an aluminium alloy showing their important features.

P.8.2. A bar of metal 25 mm in diameter is tested on a length of 250 mm. In tension the following results were recorded:

Table P.8.2(a)

Load (kN)	10.4	31.2	52.0	72.8
Extension (mm)	0.036	0.089	0.140	0.191

A torsion test gave the following results:

Table P.8.2(b)

Torque (kNm)	0.051	0.152	0.253	0.354
Angle of twist (degrees)	0.24	0.71	1.175	1.642

Represent these results in graphical form and hence determine Young's modulus, E, the modulus of rigidity, G, Poisson's ratio, v, and the bulk modulus, K, for the metal. (Note: see Chapter 11 for torque–angle of twist relationship).

Ans. $E \simeq 205\,000$ N/mm^2, $G \simeq 80\,700$ N/mm^2, $v \simeq 0.27$, $K \simeq 148\,500$ N/mm^2.

P.8.3. The actual stress–strain curve for a particular material is given by $\sigma = C\varepsilon^n$ where C is a constant. Assuming that the material suffers no change in volume during plastic deformation, derive an expression for the nominal stress–strain curve and show that this has a maximum value when $\varepsilon = n/(1-n)$.

Ans. σ (nominal) $= C\varepsilon^n/(1+\varepsilon)$.

P.8.4. A structural member is to be subjected to a series of cyclic loads which produce different levels of alternating stress as shown below. Determine whether or not a fatigue failure is probable.

Ans. Not probable ($n_1/N_1 + n_2/N_2 + \cdots = 0.39$).

Table P.8.4

Loading	Number of Cycles	Number of Cycles to Failure
1	10^4	5×10^4
2	10^5	10^6
3	10^6	24×10^7
4	10^7	12×10^7

P.8.5. A material has a fatigue limit of ± 230 N/mm^2 and an ultimate tensile strength of 870 N/mm^2. If the safe range of stress is determined by the Goodman prediction calculate its value.

Ans. 363 N/mm^2

P.8.6. A more accurate estimate for the safe range of stress for the material of P.8.5 is given by the Gerber prediction. Calculate its value.

Ans. 432 N/mm^2.

P.8.7. A steel component is subjected to a reversed cyclic loading of 100 cycles/day over a period of time in which $\pm$ 160 N/mm^2 is applied for 200 cycles, $\pm$ 140 N/mm^2 is applied for 200 cycles and $\pm$ 100 N/mm^2 is applied for 600 cycles. If the fatigue life of the material of the component at each of these stress levels is 10^4, 10^5 and 2×10^5 cycles respectively, estimate the life of the component using Miner's law.

Ans. 400 days.

P.8.8. An infinite steel plate has a fracture toughness 3320 N/mm$^{3/2}$ and contains a 4 mm long crack. Calculate the maximum allowable design stress that could be applied around the boundary of the plate.

Ans. 1324 N/mm^2.

P.8.9. A semi-infinite plate has an edge crack of length 0.4 mm. If the plate is subjected to a cyclic repeated stress loading of 180 N/mm^2, its fracture toughness is 1800 N/mm$^{3/2}$ and the rate of crack growth is 30×10^{-15} $(\Delta K)^4$ mm/cycle determine the crack length at failure and the number of cycles to failure.

Ans. 25.4 mm, 7916 cycles.

P.8.10. A steel plate 50 mm wide is 5 mm thick and carries an in-plane bending moment. If the plate develops an elliptical crack of length 6 mm and width 2.4 mm calculate the maximum bending moment the plate can withstand if the fracture toughness of the steel is 3500 N/mm$^{3/2}$.

Ans. 4300 Nmm.

CHAPTER

Bending of Beams

9

In Chapter 7 we saw that an axial load applied to a member produces a uniform direct stress across the cross section of the member (Fig. 7.2). A different situation arises when the applied loads cause a beam to bend which, if the loads are vertical, will take up a sagging or hogging shape (Section 3.2). This means that for loads which cause a beam to sag the upper surface of the beam must be shorter than the lower surface as the upper surface becomes concave and the lower one convex; the reverse is true for loads which cause hogging. The strains in the upper regions of the beam will, therefore, be different to those in the lower regions and since we have established that stress is directly proportional to strain (Eq. (7.7)) it follows that the stress will vary through the depth of the beam.

The truth of this can be demonstrated by a simple experiment. Take a reasonably long rectangular rubber eraser and draw three or four lines on its longer faces as shown in Fig. 9.1(a); the reason for this will become clear a little later. Now hold the eraser between the thumb and forefinger at each end and apply pressure as shown by the direction of the arrows in Fig. 9.1(b). The eraser bends into the shape shown and the lines on the side of the eraser *remain straight* but are now further apart at the top than at the bottom. Reference to Section 2.2 shows that a couple, or pure moment, has been applied to each end of the eraser and, in this case, has produced a hogging shape.

Since, in Fig. 9.1(b), the upper fibres have been stretched and the lower fibres compressed there will be fibres somewhere in between which are neither stretched nor compressed; the plane containing these fibres is called the *neutral plane.*

Now rotate the eraser so that its shorter sides are vertical and apply the same pressure with your fingers. The eraser again bends but now requires much less effort. It follows that the geometry and orientation of a beam section must affect its *bending stiffness.* This is more readily demonstrated with a

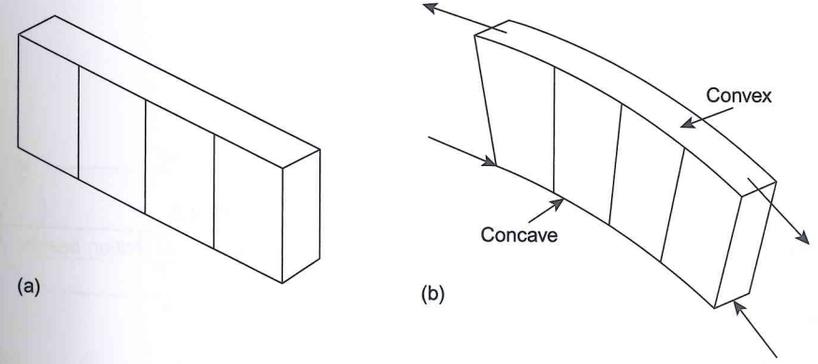

FIGURE 9.1
Bending of a rubber eraser.

plastic ruler. When flat it requires hardly any effort to bend it but when held with its width vertical it becomes almost impossible to bend. What does happen is that the lower edge tends to move sideways (for a hogging moment) but this is due to a type of instability which we shall investigate later.

We have seen in Chapter 3 that bending moments in beams are produced by the action of either pure bending moments or shear loads. Reference to problem P.3.7 also shows that two symmetrically placed concentrated shear loads on a simply supported beam induce a state of pure bending, i.e. bending without shear, in the central portion of the beam. It is also possible, as we shall see in Section 9.2, to produce bending moments by applying loads parallel to but offset from the centroidal axis of a beam. Initially, however, we shall concentrate on beams subjected to pure bending moments and consider the corresponding internal stress distributions.

9.1 Symmetrical bending

Although symmetrical bending is a special case of the bending of beams of arbitrary cross section, we shall investigate the former first, so that the more complex general case may be more easily understood.

Symmetrical bending arises in beams which have either singly or doubly symmetrical cross sections; examples of both types are shown in Fig. 9.2.

Suppose that a length of beam, of rectangular cross section, say, is subjected to a pure, sagging bending moment, M, applied in a vertical plane. The length of beam will bend into the shape shown in Fig. 9.3(a) in which the upper surface is concave and the lower convex. It can be seen that the upper longitudinal fibres of the beam are compressed while the lower fibres are stretched. It follows that, as in the case of the eraser, between these two extremes there are fibres that remain unchanged in length.

Thus the direct stress varies through the depth of the beam from compression in the upper fibres to tension in the lower. Clearly the direct stress is zero for the fibres that do not change in length; we have called the plane containing these fibres the *neutral plane.* The line of intersection of the neutral plane and any cross section of the beam is termed the *neutral axis* (Fig. 9.3(b)).

The problem, therefore, is to determine the variation of direct stress through the depth of the beam, the values of the stresses and subsequently to find the corresponding beam deflection.

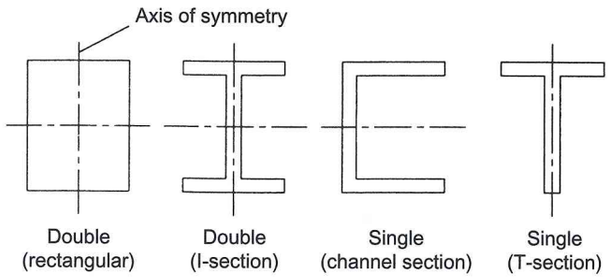

FIGURE 9.2
Symmetrical section beams.

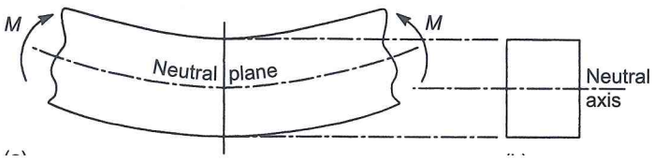

FIGURE 9.3
Beam subjected to a pure sagging

Assumptions

The primary assumption made in determining the direct stress distribution produced by pure bending is that plane cross sections of the beam remain plane and normal to the longitudinal fibres of the beam after bending. Again, we saw this from the lines on the side of the eraser. We shall also assume that the material of the beam is linearly elastic, i.e. it obeys Hooke's law, and that the material of the beam is homogeneous. Cases of composite beams are considered in Chapter 12.

Direct stress distribution

Consider a length of beam (Fig. 9.4(a)) that is subjected to a pure, sagging bending moment, M, applied in a vertical plane; the beam cross section has a vertical axis of symmetry as shown in Fig. 9.3(b). The bending moment will cause the length of beam to bend in a similar manner to that shown in Fig. 9.3(a) so that a neutral plane will exist which is, as yet, unknown distances y_1 and y_2 from the top and bottom of the beam, respectively. Coordinates of all points in the beam are referred to axes $Oxyz$ (see Section 3.2) in which the origin O lies in the neutral plane of the beam. We shall now investigate the behaviour of an elemental length, δx, of the beam formed by parallel sections MIN and PGQ (Fig. 9.4(a)) and also the fibre ST of cross-sectional area δA a distance y above the neutral plane. Clearly, before bending takes place MP = IG = ST = NQ = δx.

The bending moment M causes the length of beam to bend about a *centre of curvature* C as shown in Fig. 9.5(a). Since the element is small in length and a pure moment is applied we can take the curved shape of the beam to be circular with a *radius of curvature* R measured to the neutral plane. This is a useful reference point since, as we have seen, strains and stresses are zero in the neutral plane.

The previously parallel plane sections MIN and PGQ remain plane as we have demonstrated but are now inclined at an angle $\delta\theta$ to each other. The length MP is now shorter than δx as is ST while NQ is longer; IG, being in the neutral plane, is still of length δx. Since the fibre ST has changed in length it has suffered a strain ε_x which is given by

$$\varepsilon_x = \frac{\text{change in length}}{\text{original length}} \quad \text{(see Eq. (7.4))}$$

Then

$$\varepsilon_x = \frac{(R-y)\delta\theta - \delta\theta}{\delta x}$$

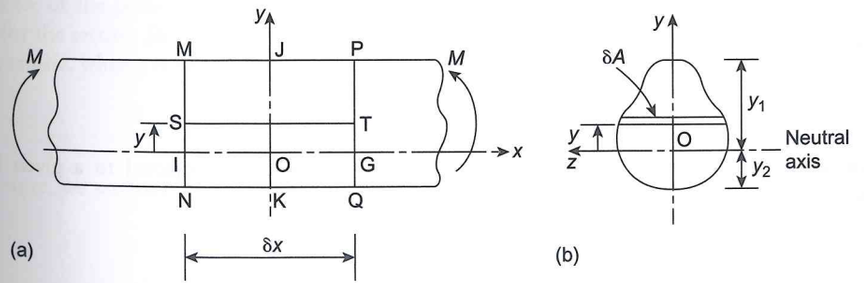

FIGURE 9.4
Bending of

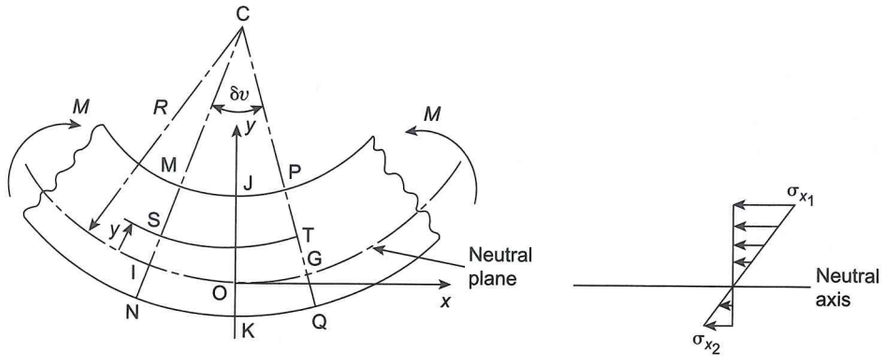

FIGURE 9.5
Length of beam subjected to a pure bending moment.

i.e.

$$\varepsilon_x = \frac{(R-y)\delta\theta - R\delta\theta}{R\delta x}$$

so that

$$\varepsilon_x = -\frac{y}{R} \tag{9.1}$$

The negative sign in Eq. (9.1) indicates that fibres in the region where y is positive will shorten when the bending moment is positive. Then, from Eq. (7.7), the direct stress σ_x in the fibre ST is given by

$$\sigma_x = -E\frac{y}{R} \tag{9.2}$$

The direct or normal force on the cross section of the fibre ST is $\sigma_x \delta A$. However, since the direct stress in the beam section is due to a pure bending moment, in other words there is no axial load, the resultant normal force on the complete cross section of the beam must be zero. Then

$$\int_A \sigma_x \, \mathrm{d}A = 0 \tag{9.3}$$

where A is the area of the beam cross section.

Substituting for σ_x in Eq. (9.3) from Eq. (9.2) gives

$$-\frac{E}{R}\int_A y \, \mathrm{d}A = 0 \tag{9.4}$$

in which both E and R are constants for a beam of a given material subjected to a given bending moment. Thus

$$\int_A y \, \mathrm{d}A = 0 \tag{9.5}$$

Equation (9.5) states that the first moment of the area of the cross section of the beam with respect

centroid of area of the cross section. Since the y axis in this case is also an axis of symmetry, it must also pass through the centroid of the cross section. Hence the origin, O, of the coordinate axes, coincides with the centroid of area of the cross section.

Equation (9.2) shows that for a sagging (i.e. positive) bending moment the direct stress in the beam section is negative (i.e. compressive) when y is positive and positive (i.e. tensile) when y is negative.

Consider now the elemental strip δA in Fig. 9.4(b); this is, in fact, the cross section of the fibre ST. The strip is above the neutral axis so that there will be a *compressive* force acting on its cross section of $\sigma_x \delta A$ which is *numerically* equal to $(Ey/R)\delta A$ from Eq. (9.2). Note that this force will act at all sections along the length of ST. At S this force will exert a clockwise moment $(Ey/R)y\delta A$ about the neutral axis while at T the force will exert an identical anticlockwise moment about the neutral axis. Considering either end of ST we see that the moment resultant about the neutral axis of the stresses on all such fibres must be *equivalent* to the applied moment M, i.e.

$$M = \int_A E\frac{y^2}{R} \, \mathrm{d}A$$

or

$$M = \frac{E}{R}\int_A y^2 \, \mathrm{d}A \tag{9.6}$$

The term $\int_A y^2 \, \mathrm{d}A$ is known as the *second moment of area* of the cross section of the beam about the neutral axis and is given the symbol I. Rewriting Eq. (9.6) we have

$$M = \frac{EI}{R} \tag{9.7}$$

or, combining this expression with Eq. (9.2)

$$\frac{M}{I} = \frac{E}{R} = -\frac{\sigma_x}{y} \tag{9.8}$$

From Eq. (9.8) we see that

$$\sigma_x = -\frac{My}{I} \tag{9.9}$$

The direct stress, σ_x, at any point in the cross section of a beam is therefore directly proportional to the distance of the point from the neutral axis and so varies linearly through the depth of the beam as shown, for the section JK, in Fig. 9.5(b). Clearly, for a positive, or sagging, bending moment σ_x is positive, i.e. tensile, when y is negative and compressive (i.e. negative) when y is positive. Thus in Fig. 9.5(b)

$$\sigma_{x,1} = \frac{My_1}{I} \text{ (compression)} \quad \sigma_{x,2} = \frac{My_2}{I} \text{ (tension)} \tag{9.10}$$

Furthermore, we see from Eq. (9.7) that the curvature, $1/R$, of the beam is given by

$$\frac{1}{R} = \frac{M}{EI} \tag{9.11}$$

and is therefore directly proportional to the applied bending moment and inversely proportional to the product EI which is known as the *flexural rigidity* of the beam.

Elastic section modulus

Equation (9.10) may be written in the form

$$\sigma_{x,1} = \frac{M}{Z_{e,1}} \quad \sigma_{x,2} = \frac{M}{Z_{e,2}} \tag{9.12}$$

in which the terms $Z_{e,1}(=I/y_1)$ and $Z_{e,2}(=I/y_2)$ are known as the *elastic section moduli* of the cross section. For a beam section having the z axis as an axis of symmetry, say, $y_1 = y_2$ and $Z_{e,1} = Z_{e,2} = Z_e$. Then, numerically

$$\sigma_{x,1} = \sigma_{x,2} = \frac{M}{Z_e} \tag{9.13}$$

Expressing the extremes of direct stress in a beam section in this form is extremely useful in elastic design where, generally, a beam of a given material is required to support a given bending moment. The maximum allowable stress in the material of the beam is known and a minimum required value for the section modulus, Z_e, can be calculated. A suitable beam section may then be chosen from handbooks which list properties and dimensions, including section moduli, of standard structural shapes.

The selection of a beam cross section depends upon many factors; these include the type of loading and construction, the material of the beam and several others. However, for a beam subjected to bending and fabricated from material that has the same failure stress in compression as in tension, it is logical to choose a doubly symmetrical beam section having its centroid (and therefore its neutral axis) at mid-depth. Also it can be seen from Fig. 9.5(b) that the greatest values of direct stress occur at points furthest from the neutral axis so that the most efficient section is one in which most of the material is located as far as possible from the neutral axis. Such a section is the I-section shown in Fig. 9.2.

EXAMPLE 9.1

A simply supported beam, 6 m long, is required to carry a uniformly distributed load of 10 kN/m. If the allowable direct stress in tension and compression is 155 N/mm^2, select a suitable cross section for the beam.

From Fig. 3.16(d) we see that the maximum bending moment in a simply supported beam of length L carrying a uniformly distributed load of intensity w is given by

$$M_{max} = \frac{wL^2}{8} \tag{i}$$

Therefore in this case

$$M_{max} = \frac{10 \times 6^2}{8} = 45 \text{ kN m}$$

The required section modulus of the beam is now obtained using Eq. (9.13), thus

$$Z_{e,min} = \frac{M_{max}}{\sigma_{x,max}} = \frac{45 \times 10^6}{155} = 290\,323 \text{ mm}^3$$

From tables of structural steel sections it can be seen that a Universal Beam, 254 mm × 102 mm × 28 kg/m, has a section modulus (about a centroidal axis parallel to its flanges) of 307 600 mm^3. This is the smallest beam section having a section modulus greater than that required and allows a margin for the increased load due to the self-weight of the beam. However, we must now check that the allowable stress is not exceeded due to self-weight. The total load intensity produced by the applied load and self-weight is

$$10 + \frac{28 \times 9.81}{10^3} = 10.3 \text{ kN/m}$$

Hence, from Eq. (i)

$$M_{max} = \frac{10.3 \times 6^2}{8} = 46.4 \text{ kN m}$$

Therefore from Eq. (9.13)

$$\sigma_{x,max} = \frac{46.4 \times 10^3 \times 10^3}{307\,600} = 150.8 \text{ N/mm}^2$$

The allowable stress is 155 N/mm^2 so that the Universal Beam, 254 mm × 102 mm × 28 kg/m, is satisfactory.

EXAMPLE 9.2

The cross section of a beam has the dimensions shown in Fig. 9.6(a). If the beam is subjected to a sagging bending moment of 100 kN m applied in a vertical plane, determine the distribution of direct stress through the depth of the section.

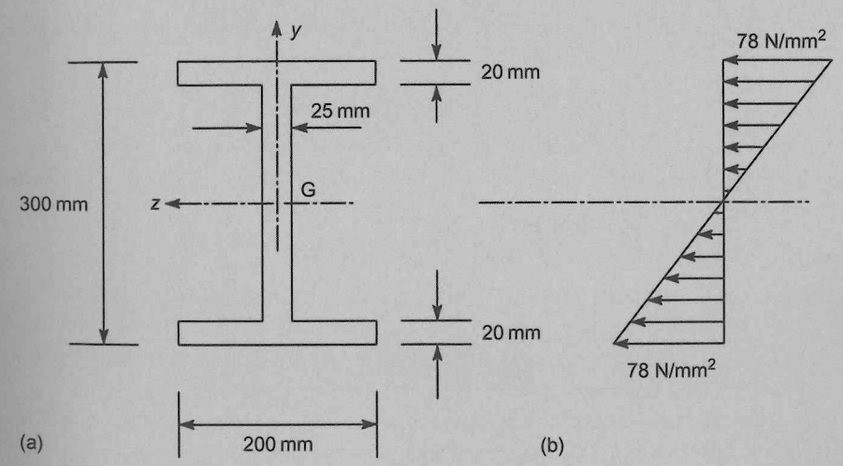

FIGURE 9.6
Direct stress distribution in beam of Ex. 9.2.

The cross section of the beam is doubly symmetrical so that the centroid, G, of the section, and therefore the origin of axes, coincides with the mid-point of the web. Furthermore, the bending moment is applied to the beam section in a vertical plane so that the z axis becomes the neutral axis of the beam section; we therefore need to calculate the second moment of area, I_z, about this axis. Thus

$$I_z = \frac{200 \times 300^3}{12} - \frac{175 \times 260^3}{12} = 193.7 \times 10^6 \text{ mm}^4 \quad \text{(see Section 9.6)}$$

From Eq. (9.9) the distribution of direct stress, σ_x, is given by

$$\sigma_x = -\frac{100 \times 10^6}{193.7 \times 10^6} y = -0.52y \tag{i}$$

The direct stress, therefore, varies linearly through the depth of the section from a value

$$-0.52 \times (+150) = -78 \text{ N/mm}^2 \text{ (compression)}$$

at the top of the beam to

$$-0.52 \times (-150) = +78 \text{ N/mm}^2 \text{ (tension)}$$

at the bottom as shown in Fig. 9.6(b).

EXAMPLE 9.3

Now determine the distribution of direct stress in the beam of Ex. 9.2 if the bending moment is applied in a horizontal plane and in a clockwise sense about Gy when viewed in the direction Gy.

In this case the beam will bend about the vertical y axis which therefore becomes the neutral axis of the section. Thus Eq. (9.9) becomes

$$\sigma_x = -\frac{M}{I_y} z \tag{i}$$

where I_y is the second moment of area of the beam section about the y axis. Again from Section 9.6

$$I_y = 2 \times \frac{20 \times 200^3}{12} + \frac{260 \times 25^3}{12} = 27.0 \times 10^6 \text{ mm}^4$$

Hence, substituting for M and I_y in Eq. (i)

$$\sigma_x = -\frac{100 \times 10^6}{27.0 \times 10^6} z = -3.7z$$

We have not specified a sign convention for bending moments applied in a horizontal plane; clearly in this situation the sagging/hogging convention loses its meaning. However, a physical appreciation of the problem shows that the left-hand edges of the beam are in tension while the right-hand edges are in compression. Again the distribution is linear and varies from $3.7 \times (+100) = 370 \text{ N/mm}^2$ (tension) at the left-hand edges of each flange to $3.7 \times (-100) = -370 \text{ N/mm}^2$ (compression) at the right-hand edges.

We note that the maximum stresses in this example are very much greater than those in Ex. 9.2. This is due to the fact that the bulk of the material in the beam section is concentrated in the region of the neutral axis where the stresses are low. The use of an I-section in this manner would therefore be structurally inefficient.

EXAMPLE 9.4

The beam section of Ex. 9.2 is subjected to a bending moment of 100 kN m applied in a plane parallel to the longitudinal axis of the beam but inclined at 30° to the left of vertical. The sense of the bending moment is clockwise when viewed from the left-hand edge of the beam section. Determine the distribution of direct stress.

The bending moment is first resolved into two components, M_z in a vertical plane and M_y in a horizontal plane. Equation (9.9) may then be written in two forms

$$\sigma_x = -\frac{M_z}{I_z} y \quad \sigma_x = -\frac{M_y}{I_y} z \tag{i}$$

The separate distributions can then be determined and superimposed. A more direct method is to combine the two equations (i) to give the total direct stress at any point (y, z) in the section. Thus

$$\sigma_x = -\frac{M_z}{I_z} y - \frac{M_y}{I_y} z \tag{ii}$$

Now

$$\left.\begin{aligned} M_z &= 100 \cos 30° = 86.6 \text{ kN m} \\ M_y &= 100 \sin 30° = 50.0 \text{ kN m} \end{aligned}\right\} \tag{iii}$$

M_z is, in this case, a negative bending moment producing tension in the upper half of the beam where y is positive. Also M_y produces tension in the left-hand half of the beam where z is positive; we shall therefore call M_y a negative bending moment. Substituting the values of M_z and M_y from Eq. (iii) but with the appropriate sign in Eq. (ii) together with the values of I_z and I_y from Exs 9.2 and 9.3 we obtain

$$\sigma_x = \frac{86.6 \times 10^6}{193.7 \times 10^6} y + \frac{50.0 \times 10^6}{27.0 \times 10^6} z \tag{iv}$$

or

$$\sigma_x = 0.45y + 1.85z \tag{v}$$

Equation (v) gives the value of direct stress at any point in the cross section of the beam and may also be used to determine the distribution over any desired portion. Thus on the upper edge of the top flange $y = +150$ mm, $100 \text{ mm} \geq z \geq -100$ mm, so that the direct stress varies linearly with z. At the top left-hand corner of the top flange

$$\sigma_x = 0.45 \times (+150) + 1.85 \times (+100) = +252.5 \text{ N/mm}^2 \text{ (tension)}$$

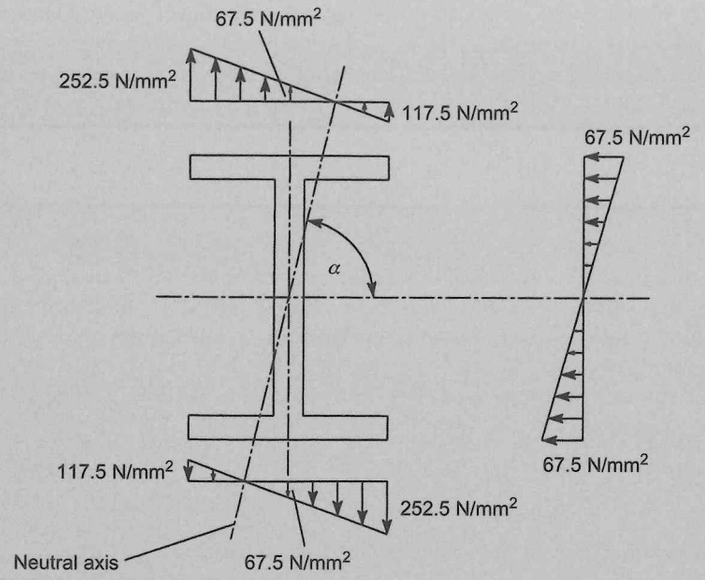

FIGURE 9.7

Direct stress distribution in beam of Ex. 9.4.

At the top right-hand corner

$$\sigma_x = 0.45 \times (+150) + 1.85 \times (-100) = -117.5 \ N/mm^2 \text{ (compression)}$$

The distributions of direct stress over the outer edge of each flange and along the vertical axis of symmetry are shown in Fig. 9.7. Note that the neutral axis of the beam section does not in this case coincide with either the z or y axes, although it still passes through the centroid of the section. Its inclination, α, to the z axis, say, can be found by setting $\sigma_x = 0$ in Eq. (v). Thus

$$0 = 0.45y + 1.85z$$

or

$$-\frac{y}{z} = \frac{1.85}{0.45} = 4.11 = \tan\alpha$$

which gives

$$\alpha = 76.3°$$

Note that α may be found in general terms from Eq. (ii) by again setting $\sigma_x = 0$. Hence

$$\frac{y}{z} = -\frac{M_y I_z}{M_z I_y} = \tan\alpha \tag{9.14}$$

or

$$\tan\alpha = \frac{M_y I_z}{M_z I_y}$$

EXAMPLE 9.5

A beam, 6 m long, is simply supported at its left-hand end and at 1.5 m from its right-hand end. If the cross section of the beam is that shown in Fig. 9.8 and it carries a uniformly distributed load of 7.5 kN/m over its full length calculate the maximum tensile and compressive stresses in the beam.

The first step is to find the position of the centroid of area, G, of the beam section. This will lie on the vertical axis of symmetry and is a distance $\bar{y}$ from the top of the flange.

Taking moments of area about the top of the flange

$$(125 \times 25 + 125 \times 25)\,\bar{y} = 125 \times 25 \times 12.5 + 125 \times 25 \times 87.5$$

which gives

$$\bar{y} = 50 \text{ mm}$$

Since the loading is applied in the vertical plane of symmetry the direct stress distribution is given by Eq. (9.9) in which I is the second moment of area of the beam cross section about the z axis. Then, using the method described in Section 9.6

$$I_z = \frac{125 \times 25^3}{12} + 125 \times 25 \times 37.5^2 + \frac{25 \times 125^3}{12} + 25 \times 125 \times 37.5^2$$

which gives

$$I_z = 13.02 \times 10^6 \text{ mm}^4$$

It is clear from Ex. 3.9 that the maximum sagging bending moment in the beam will occur at a section between the support points and that the maximum hogging bending moment will occur at the right-hand support. Referring to Fig. 9.9 and taking moments about B

$$R_A \times 4.5 - 7.5 \times 6.0 \times 1.5 = 0$$

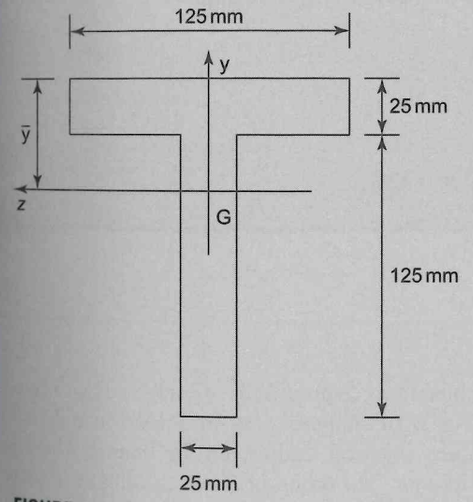

FIGURE 9.8

Beam section of Ex. 9.5.

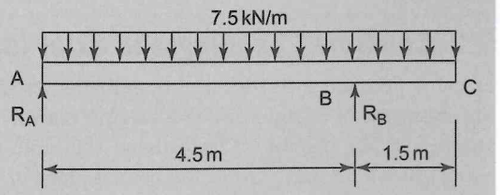

FIGURE 9.9

Beam of Ex. 9.5.

from which

$$R_A = 15 \text{ kN}$$

From Eq. (3.4) we see that the bending moment diagram will have a mathematical maximum between A and B when the shear force is zero. Then

$$S_{AB} = R_A - 7.5x = 15 - 7.5x = 0$$

so that $S_{AB} = 0$ when $x = 2$ m. The maximum sagging bending moment is therefore given by

$$M_z \text{ (max.sagging)} = 15 \times 2.0 - \frac{7.5 \times 2.0^2}{2} = 15.0 \text{ kNm}$$

The maximum hogging bending moment occurs at B and is given by

$$M_z \text{ (max.hogging)} = -\frac{7.5 \times 1.5^2}{2} = -8.45 \text{ kNm}$$

The maximum sagging bending moment will produce a direct compressive stress at the top of the flange and a direct tensile stress at the base of the leg. Then, from Eq. (9.9)

$$\sigma_x \text{ (top of flange)} = -\frac{15 \times 10^6 \times 50}{13.02 \times 10^6} = -57.6 \text{ N/mm}^2$$

$$\sigma_x \text{ (base of leg)} = -\frac{15 \times 10^6 \times (-100)}{13.02 \times 10^6} = +115.2 \text{ N/mm}^2$$

Similarly, due to the maximum hogging bending moment

$$\sigma_x \text{ (top of flange)} = -\frac{(-8.45) \times 10^6 \times 50}{13.02 \times 10^6} = +32.5 \text{ N/mm}^2$$

$$\sigma_x \text{ (base of leg)} = -\frac{(-8.45) \times 10^6 \times (-100)}{13.02 \times 10^6} = -64.9 \text{ N/mm}^2$$

Therefore the maximum tensile stress in the beam is 115.2 N/mm^2 occurring at a section 2 m from the left-hand support and the maximum compressive stress is 64.9 N/mm^2 occurring at the right-hand support.

9.2 Combined bending and axial load

In many practical situations beams and columns are subjected to combinations of axial loads and bending moments. For example, the column shown in Fig. 9.10 supports a beam seated on a bracket attached to the column. The loads on the beam produce a vertical load, P, on the bracket, the load being offset a distance e from the neutral plane of the column. The action of P on the column is therefore equivalent to an axial load, P, plus a bending moment, Pe. The direct stress at any point in the cross section of the column is therefore the algebraic sum of the direct stress due to the axial load and

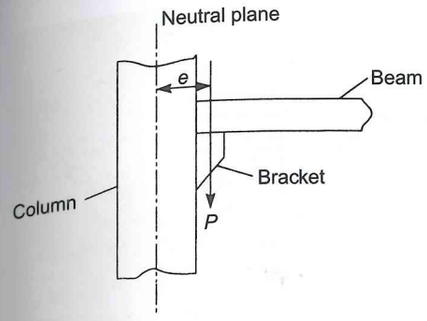

FIGURE 9.10
Combined bending and axial load on a column.

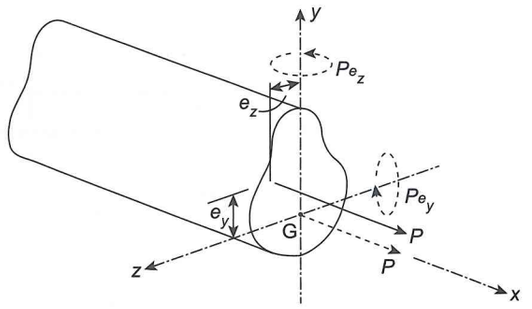

FIGURE 9.11
Combined bending and axial load on a beam section.

Consider now a length of beam having a vertical plane of symmetry and subjected to a tensile load, P, which is offset by positive distances e_y and e_z from the z and y axes, respectively (Fig. 9.11). It can be seen that P is equivalent to an axial load P plus bending moments Pe_y and Pe_Z about the z and y axes, respectively. The moment Pe_y is a negative or hogging bending moment while the moment Pe_z induces tension in the region where z is positive; Pe_z is, therefore, also regarded as a negative moment. Thus at any point (y,z) the direct stress, σ_x, due to the combined force system, using Eqs (7.1) and (9.9), is

$$\sigma_x = \frac{P}{A} + \frac{Pe_y}{I_z}y + \frac{Pe_z}{I_y}z \tag{9.15}$$

Equation (9.15) gives the value of σ_x at any point (y,z) in the beam section for any combination of signs of P, e_z, e_y.

EXAMPLE 9.6

A beam has the cross section shown in Fig. 9.12(a). It is subjected to a normal tensile force, P, whose line of action passes through the centroid of the horizontal flange. Calculate the maximum allowable value of P if the maximum direct stress is limited to ± 150 N/mm^2.

The first step in the solution of the problem is to determine the position of the centroid, G, of the section. Thus, taking moments of areas about the top edge of the flange we have

$$(200 \times 20 + 200 \times 20)\bar{y} = 200 \times 20 \times 10 + 200 \times 20 \times 120$$

from which

$$\bar{y} = 65 \text{ mm}$$

The second moment of area of the section about the z axis is then obtained using the methods of Section 9.6 and is

$$I_z = \frac{200 \times 65^3}{3} - \frac{180 \times 45^3}{3} + \frac{20 \times 155^3}{3} = 37.7 \times 10^6 \text{ mm}^4$$

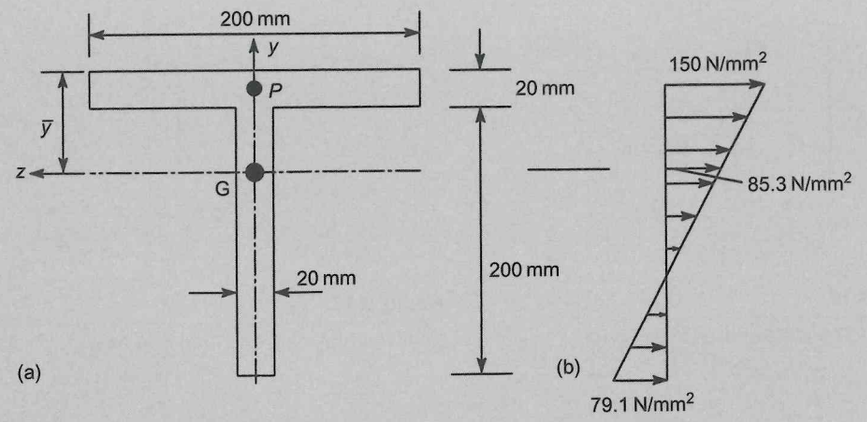

FIGURE 9.12

Direct stress distribution in beam section of Ex. 9.5.

Since the line of action of the load intersects the y axis, e_z in Eq. (9.15) is zero so that

$$\frac{P}{A} + \frac{Pe_y}{I_z}y \tag{i}$$

Also $e_y = +55$ mm so that $Pe_y = +55\,P$ and Eq. (i) becomes

$$\sigma_x = P\left(\frac{1}{8000} + \frac{55}{37.7 \times 10^6}y\right)$$

or

$$\sigma_x = P(1.25 \times 10^{-4} + 1.46 \times 10^{-6}y) \tag{ii}$$

It can be seen from Eq. (ii) that σ_x varies linearly through the depth of the beam from a tensile value at the top of the flange where y is positive to either a tensile or compressive value at the bottom of the leg depending on whether the bracketed term is positive or negative. Therefore at the top of the flange

$$+150 = P[1.25 \times 10^{-4} + 1.46 \times 10^{-6} \times (+65)]$$

which gives the limiting value of P as 682 kN.

At the bottom of the leg of the section $y = -155$ mm so that the right-hand side of Eq. (ii) becomes

$$P[1.25 \times 10^{-4} + 1.46 \times 10^{-6} \times (-155)] \equiv -1.01 \times 10^{-4}P$$

which is negative for a tensile value of P. Hence the resultant direct stress at the bottom of the leg is compressive so that for a limiting value of P

$$-150 = -1.01 \times 10^{-4}P$$

from which

$$P = 1485 \text{ kN}$$

Therefore, we see that the maximum allowable value of P is 682 kN, giving the direct stress distribution shown in Fig. 9.12(b).

Core of a rectangular section

In some structures, such as brick-built chimneys and gravity dams which are fabricated from brittle materials, it is inadvisable for tension to be developed in any cross section. Clearly, from our previous discussion, it is possible for a compressive load that is offset from the neutral axis of a beam section to induce a resultant tensile stress in some regions of the cross section if the tensile stress due to bending in those regions is greater than the compressive stress produced by the axial load. Therefore, we require to impose limits on the eccentricity of such a load so that no tensile stresses are induced.

Consider the rectangular section shown in Fig. 9.13 subjected to an eccentric compressive load, P, applied parallel to the longitudinal axis in the positive yz quadrant. Note that if P were inclined at some angle to the longitudinal axis, then we need only consider the component of P normal to the section since the in-plane component would induce only shear stresses. Since P is a compressive load and therefore negative, Eq. (9.15) becomes

$$\sigma_x = \frac{P}{A} - \frac{Pe_y}{I_z}y - \frac{Pe_z}{I_y}z \tag{9.16}$$

Note that both Pe_y and Pe_z are positive moments according to the sign convention we have adopted. In the region of the cross section where z and y are negative, tension will develop if

$$\left|\frac{Pe_y}{I_z}y + \frac{Pe_z}{I_y}z\right| > \left|\frac{P}{A}\right|$$

The limiting case arises when the direct stress is zero at the corner of the section, i.e. when $z = -b/2$ and $y = -d/2$. Therefore, substituting these values in Eq. (9.16) we have

$$0 = -\frac{P}{A} - \frac{Pe_y}{I_z}\left(-\frac{d}{2}\right) - \frac{Pe_z}{I_y}\left(-\frac{b}{2}\right)$$

or, since $A = bd$, $I_z = bd^3/12$, $I_y = db^3/12$ (see Section 9.6)

$$0 = -bd + 6be_y + 6de_z$$

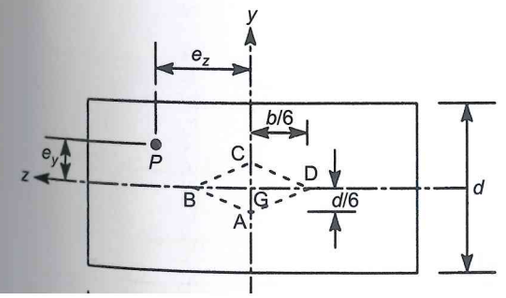

which gives

$$be_y + de_z = \frac{bd}{6}$$

Rearranging we obtain

$$e_y = -\frac{d}{b}e_z + \frac{d}{6} \tag{9.17}$$

Equation (9.17) defines the line BC in Fig. 9.13 which sets the limit for the eccentricity of P from both the z and y axes. It follows that P can be applied at any point in the region BCG for there to be no tension developed anywhere in the section.

Since the section is doubly symmetrical, a similar argument applies to the regions GAB, GCD and GDA; the rhombus ABCD is known as the *core of the section* and has diagonals BD = $b/3$ and AC = $d/3$.

Core of a circular section

Bending, produced by an eccentric load P, in a circular cross section always takes place about a diameter that is perpendicular to the radius on which P acts. It is therefore logical to take this diameter and the radius on which P acts as the coordinate axes of the section (Fig. 9.14).

Suppose that P in Fig. 9.14 is a compressive load. The direct stress, σ_x, at any point (z, y) is given by Eq. (9.15) in which $e_y = 0$. Hence

$$\sigma_x = -\frac{P}{A} - \frac{Pe_z}{I_y}z \tag{9.18}$$

Tension will occur in the region where z is negative if

$$\left|\frac{Pe_z}{I_y}z\right| > \left|\frac{P}{A}\right|$$

The limiting case occurs when $\sigma_x = 0$ and $z = -R$; hence

$$0 = -\frac{P}{A} - \frac{Pe_z}{I_y}(-R)$$

Now $A = \pi R^2$ and $I_y = \pi R^4/4$ (see Section 9.6) so that

$$0 = -\frac{1}{\pi R^2} + \frac{4e_z}{\pi R^3}$$

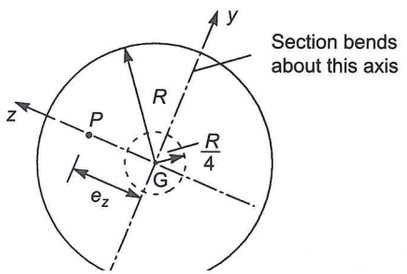

FIGURE 9.14

from which

$$e_z = \frac{R}{4}$$

Thus the core of a circular section is a circle of radius $R/4$.

EXAMPLE 9.7

A free-standing masonry wall is 7 m high, 0.6 m thick and has a density of 2000 kg/m^3. Calculate the maximum, uniform, horizontal wind pressure that can occur without tension developing at any point in the wall.

Consider a 1 m length of wall. The forces acting are the horizontal resultant, P, of the uniform wind pressure, p, and the weight, W, of the 1 m length of wall (Fig. 9.15).

Clearly the base section is the one that experiences the greatest compressive normal load due to self-weight and also the greatest bending moment due to wind pressure.

It is also the most critical section since the bending moment that causes tension is a function of the square of the height of the wall, whereas the weight causing compression is a linear function of wall height. From Fig. 9.13 it is clear that the resultant, R, of P and W must lie within the central 0.2 m of the base section, i.e. within the middle third of the section, for there to be no tension developed anywhere in the base cross section. The reason for this is that R may be resolved into vertical and horizontal components at any point in its line of action. At the base of the wall the vertical component is then a compressive load parallel to the vertical axis of the wall (i.e. the same situation as in Fig. 9.13) and the horizontal component is a shear load which has no effect as far as tension in the wall is concerned. The limiting case arises when R passes through m, one of the middle third points, in which case the direct stress at B is zero and the moment of R (and therefore the sum of the moments of P and W) about m is zero. Hence

$$3.5P = 0.1W \tag{i}$$

where

$$P = p \times 7 \times 1\text{N if } p \text{ is in N/m}^2$$

and

$$W = 2000 \times 9.81 \times 0.6 \times 7 \text{ N}$$

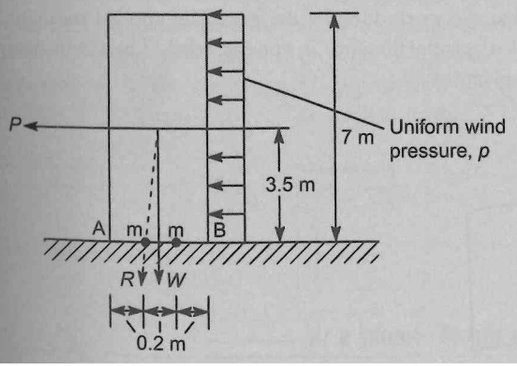

FIGURE 9.15
Masonry wall of Ex. 9.7.

Substituting for P and W in Eq. (i) and solving for p gives

$$p = 336.3 \text{ N/m}^2$$

9.3 Anticlastic bending

In the rectangular beam section shown in Fig. 9.16(a) the direct stress distribution due to a positive bending moment applied in a vertical plane varies from compression in the upper half of the beam to tension in the lower half (Fig. 9.16(b)). However, due to the Poisson effect (see Section 7.8) the compressive stress produces a lateral elongation of the upper fibres of the beam section while the tensile stress produces a lateral contraction of the lower. The section does not therefore remain rectangular but distorts as shown in Fig. 9.16(c); the effect is known as *anticlastic bending*.

Anticlastic bending is of interest in the analysis of thin-walled box beams in which the cross sections are maintained by stiffening ribs. The prevention of anticlastic distortion induces local variations in stress distributions in the webs and covers of the box beam and also in the stiffening ribs.

9.4 Strain energy in bending

A positive bending moment applied to a length of beam causes the upper longitudinal fibres to be compressed and the lower ones to stretch as shown in Fig. 9.5(a). The bending moment therefore does work on the length of beam and this work is absorbed by the beam as strain energy.

Suppose that the bending moment, M, in Fig. 9.5(a) is gradually applied so that when it reaches its final value the angle subtended at the centre of curvature by the element δx is $\delta\theta$. From Fig. 9.5(a) we see that

$$R\,\delta\theta = \delta x$$

Substituting in Eq. (9.7) for R we obtain

$$M = \frac{EI_z}{\delta x}\delta\theta \tag{9.19}$$

so that $\delta\theta$ is a linear function of M. It follows that the work done by the gradually applied moment M is $M\,\delta\theta/2$ subject to the condition that the limit of proportionality is not exceeded. The strain energy, δU, of the elemental length of beam is therefore given by

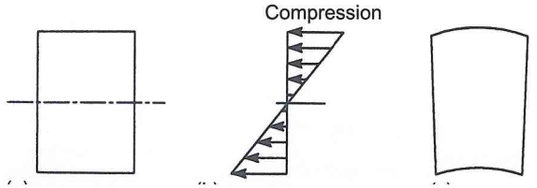

FIGURE 9.16

$$\delta U = \frac{1}{2}M\,\delta\theta \tag{9.20}$$

or, substituting for $\delta\theta$ from Eq. (9.19) in Eq. (9.20)

$$\delta U = \frac{1}{2}\frac{M^2}{EI_z}\delta x$$

The total strain energy, U, due to bending in a beam of length L is therefore

$$U = \int_L \frac{M^2}{2EI_z}\,dx \tag{9.21}$$

9.5 Unsymmetrical bending

Frequently in civil engineering construction beam sections do not possess any axes of symmetry. Typical examples are shown in Fig. 9.17 where the angle section has legs of unequal length and the Z-section possesses anti- or skew symmetry about a horizontal axis through its centroid, but not symmetry. We shall now develop the theory of bending for beams of arbitrary cross section.

Assumptions

We shall again assume, as in the case of symmetrical bending, that plane sections of the beam remain plane after bending and that the material of the beam is homogeneous and linearly elastic.

Sign conventions and notation

Since we are now concerned with the general case of bending we may apply loading systems to a beam in any plane. However, no matter how complex these loading systems are, they can always be resolved into components in planes containing the three coordinate axes of the beam. We shall use an identical system of axes to that shown in Fig. 3.6, but our notation for loads must be extended and modified to allow for the general case.

As far as possible we shall adopt sign conventions and a notation which are consistent with those shown in Fig. 3.6. Thus, in Fig. 9.18, the externally applied shear load W_y is parallel to the y axis but vertically downwards, i.e. in the negative y direction as before; similarly we take W_z to act in the negative z direction. The distributed loads $w_y(x)$ and $w_z(x)$ can be functions of x and are also applied in the negative directions of the axes. The bending moment M_z in the vertical xy plane is, as before, a sagging (i.e. positive) moment and will produce compressive direct stresses in the positive yz quadrant of the beam section. In the same way M_y is positive when it produces compressive stresses in the positive yz quadrant of the beam section. The applied torque T is positive when anticlockwise when viewed in the

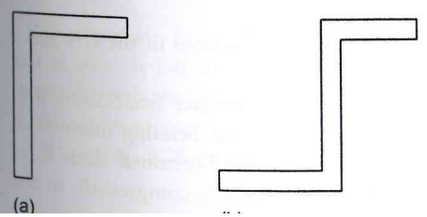

FIGURE 9.17

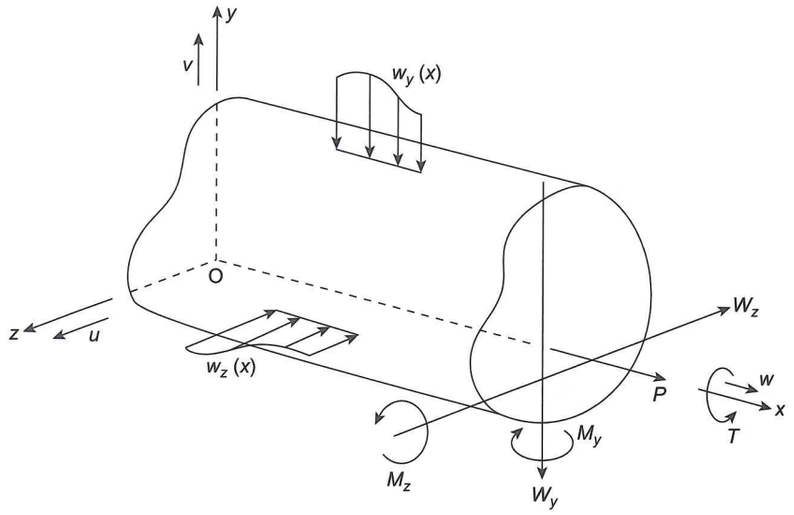

FIGURE 9.18

Sign conventions and notation.

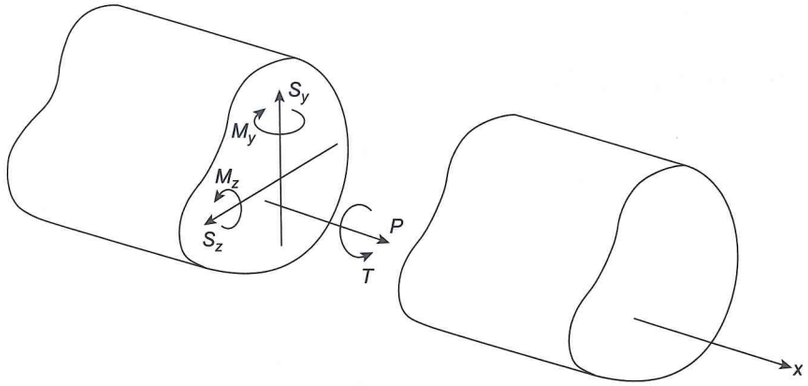

FIGURE 9.19

Internal force system.

direction xO and the displacements, u, v and w are positive in the positive directions of the z, y and x axes, respectively.

The positive directions and senses of the internal forces acting on the positive face (see Section 3.2) of a beam section are shown in Fig. 9.19 and agree, as far as the shear force and bending moment in the vertical xy plane are concerned, with those in Fig. 3.7. The positive internal horizontal shear force S_z is in the positive direction of the z axis while the internal moment M_y produces compression in the

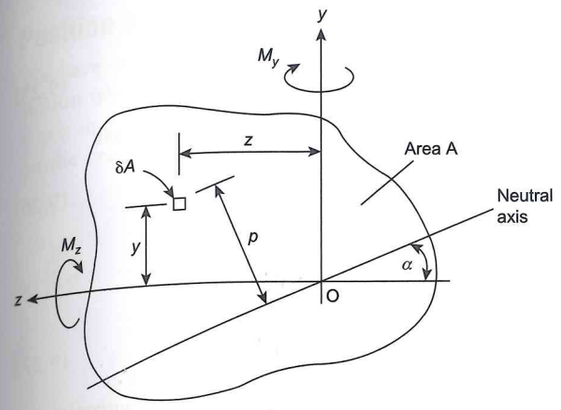

FIGURE 9.20

Bending of an unsymmetrical section beam.

Direct stress distribution

Figure 9.20 shows the positive face of the cross section of a beam which is subjected to positive internal bending moments M_z and M_y. Suppose that the origin O of the y and z axes lies on the neutral axis of the beam section; as yet the position of the neutral axis and its inclination to the z axis are unknown.

We have seen in Section 9.1 that a beam bends about the neutral axis of its cross section so that the radius of curvature, R, of the beam is perpendicular to the neutral axis. Therefore, by direct comparison with Eq. (9.2) it can be seen that the direct stress, σ_x, on the element, δA, a perpendicular distance p from the neutral axis, is given by

$$\sigma_x = -E\frac{p}{R} \tag{9.22}$$

The beam section is subjected to a pure bending moment so that the resultant direct load on the section is zero. Hence

$$\int_A \sigma_x \, dA = 0$$

Replacing σ_x in this equation from Eq. (9.22) we have

$$-\int_A E\frac{p}{R} \, dA = 0$$

or, for a beam of a given material subjected to a given bending moment

$$\int_A p \, dA = 0 \tag{9.23}$$

Qualitatively Eq. (9.23) states that the first moment of area of the beam section about the neutral axis is zero. It follows that in problems involving the pure bending of beams the neutral axis always passes through the centroid of the beam section. We shall therefore choose the centroid, G, of a section as the origin of axes.

From Fig. 9.20 we see that

$$p = z\sin\alpha + y\cos\alpha \tag{9.24}$$

so that from Eq. (9.22)

$$\sigma_x = -\frac{E}{R}(z\sin\alpha + y\cos\alpha) \tag{9.25}$$

The moment resultants of the direct stress distribution are equivalent to M_z and M_y so that

$$M_z = \int_A \sigma_x y\,\mathrm{d}A \quad M_y = -\int_A \sigma_x z\,\mathrm{d}A \quad \text{(see Section 9.1)} \tag{9.26}$$

Substituting for σ_x from Eq. (9.25) in Eq. (9.26), we obtain

$$\left.\begin{aligned} M_z &= \frac{E\sin\alpha}{R}\int_A zy\;\mathrm{d}A + \frac{E\cos\alpha}{R}\int_A y^2\,\mathrm{d}A \\ M_y &= \frac{E\sin\alpha}{R}\int_A z^2\,\mathrm{d}A + \frac{E\cos\alpha}{R}\int_A zy\,\mathrm{d}A \end{aligned}\right\} \tag{9.27}$$

In Eq. (9.27)

$$\int_A zy\,\mathrm{d}A = I_{zy} \quad \int_A y^2\,\mathrm{d}A = I_z \quad \int_A z^2\,\mathrm{d}A = I_y$$

where I_{zy} is the product second moment of area of the beam section about the z and y axes, I_z is the second moment of area about the z axis and I_y is the second moment of area about the y axis. Equation (9.27) may therefore be rewritten as

$$\left.\begin{aligned} M_z &= \frac{E\sin\alpha}{R}I_{zy} + \frac{E\cos\alpha}{R}I_z \\ M_y &= \frac{E\sin\alpha}{R}I_y + \frac{E\cos\alpha}{R}I_{zy} \end{aligned}\right\} \tag{9.28}$$

Solving Eq. (9.28)

$$\frac{E\sin\alpha}{R} = \frac{M_yI_z - M_zI_{zy}}{I_zI_y - I_{zy}^2} \tag{9.29}$$

$$\frac{E\cos\alpha}{R} = \frac{M_zI_y - M_yI_{zy}}{I_zI_y - I_{zy}^2} \tag{9.30}$$

Now substituting these expressions in Eq. (9.25)

$$\sigma_x = -\left(\frac{M_yI_z - M_zI_{zy}}{I_zI_y - I_{zy}^2}\right)z - \left(\frac{M_zI_y - M_yI_{zy}}{I_zI_y - I_{zy}^2}\right)y \tag{9.31}$$

In the case where the beam section has either Oz or Oy (or both) as an axis of symmetry $I_{zy} = 0$ (see Section 9.6) and Eq. (9.31) reduces to

$$\sigma_x = -\frac{M_y}{I_y}z - \frac{M_z}{I_z}y \tag{9.32}$$

which is identical to Eq. (ii) in Ex. 9.4.

Position of the neutral axis

We have established that the neutral axis of a beam section passes through the centroid of area of the section whether the section has an axis of symmetry or not. The inclination α of the neutral axis to the z axis in Fig. 9.20 is obtained from Eq. (9.31) using the fact that the direct stress is zero at all points on the neutral axis. Then, for a point (z_{NA}, y_{NA})

$$0 = (M_zI_{zy} - M_yI_z)z_{NA} + (M_yI_{zy} - M_zI_y)y_{NA}$$

so that

$$\frac{y_{NA}}{z_{NA}} = -\frac{(M_zI_{zy} - M_yI_z)}{(M_yI_{zy} - M_zI_y)}$$

or, referring to Fig. 9.20

$$\tan\alpha = \frac{(M_zI_{zy} - M_yI_z)}{(M_yI_{zy} - M_zI_y)} \tag{9.33}$$

since α is positive when y_{NA} is positive and z_{NA} is negative. Again, for a beam having a cross section with either Oy or Oz as an axis of symmetry, $I_{zy} = 0$ and Eq. (9.33) reduces to

$$\tan\alpha = \frac{M_yI_z}{M_zI_y} \quad \text{(see Eq. (9.14))}$$

9.6 Calculation of section properties

It will be helpful at this stage to discuss the calculation of the various section properties required in the analysis of beams subjected to bending. Initially, however, two useful theorems are quoted.

Parallel axes theorem

Consider the beam section shown in Fig. 9.21 and suppose that the second moment of area, I_G, about an axis through its centroid G is known. The second moment of area, I_N, about a parallel axis, NN, a distance b from the centroidal axis is then given by

$$I_N = I_G + Ab^2 \tag{9.34}$$

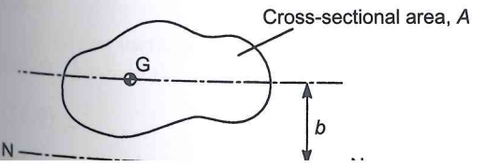

FIGURE 9.21

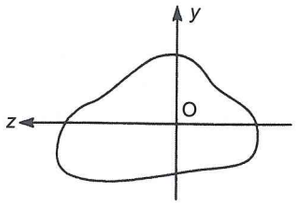

FIGURE 9.22
Theorem of perpendicular axes.

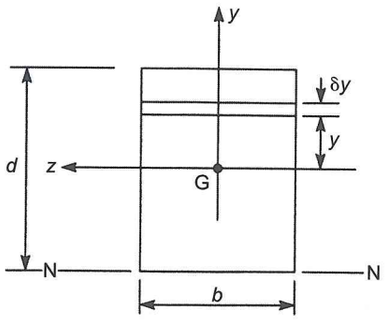

FIGURE 9.23
Second moments of area of a rectangular section.

Theorem of perpendicular axes

In Fig. 9.22 the second moments of area, I_z and I_y, of the section about Oz and Oy are known. The second moment of area about an axis through O perpendicular to the plane of the section (i.e. a *polar second moment of area)* is then

$$I_o = I_z + I_y \tag{9.35}$$

Second moments of area of standard sections

Many sections in use in civil engineering such as those illustrated in Fig. 9.2 may be regarded as comprising a number of rectangular shapes. The problem of determining the properties of such sections is simplified if the second moments of area of the rectangular components are known and use is made of the parallel axes theorem. Thus, for the rectangular section of Fig. 9.23

$$I_z = \int_A y^2 \, dA = \int_{-d/2}^{d/2} by^2 \, dy = b\left[\frac{y^3}{3}\right]_{-d/2}^{d/2}$$

which gives

$$I_z = \frac{bd^3}{12} \tag{9.36}$$

Similarly

$$I_y = \frac{db^3}{12} \tag{9.37}$$

Frequently it is useful to know the second moment of area of a rectangular section about an axis which coincides with one of its edges. Thus in Fig. 9.23, and using the parallel axes theorem

$$I_N = \frac{bd^3}{12} + bd\left(-\frac{d}{2}\right)^2 = \frac{bd^3}{3} \tag{9.38}$$

EXAMPLE 9.8

Determine the second moments of area I_z and I_y of the I-section shown in Fig. 9.24.

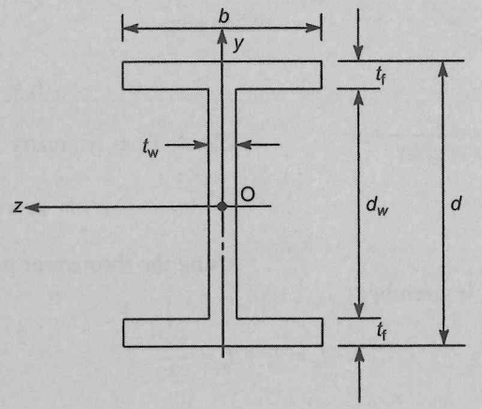

FIGURE 9.24
Second moments of area of an I-section.

Using Eq. (9.36)

$$I_z = \frac{bd^3}{12} - \frac{(b - t_w)d_w^3}{12}$$

Alternatively, using the parallel axes theorem in conjunction with Eq. (9.36)

$$I_z = 2\left[\frac{bt_f^3}{12} + bt_f\left(\frac{d_w + t_f}{2}\right)^2\right] + \frac{t_w d_w^3}{12}$$

The equivalence of these two expressions for I_z is most easily demonstrated by a numerical example. Also, from Eq. (9.37)

$$I_y = 2\frac{t_f b^3}{12} + \frac{d_w t_w^3}{12}$$

It is also useful to determine the second moment of area, about a diameter, of a circular section. In Fig. 9.25 where the z and y axes pass through the centroid of the section

$$I_z = \int y^2 \, dA = \int^{d/2} 2\left(\frac{d}{2}\cos\theta\right) y^2 \, dy \tag{9.39}$$

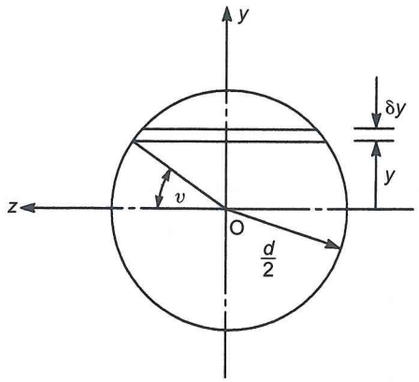

FIGURE 9.25
Second moments of area of a circular section.

Integration of Eq. (9.39) is simplified if an angular variable, θ, is used. Thus

$$I_z = \int_{-\pi/2}^{\pi/2} d\cos\theta\left(\frac{d}{2}\sin\theta\right)^2 \frac{d}{2}\cos\theta\,\mathrm{d}\theta$$

i.e.

$$I_z = \frac{d^4}{8}\int_{-\pi/2}^{\pi/2} \cos^2\theta\sin^2\theta\,\mathrm{d}\theta$$

which gives

$$I_z = \frac{\pi d^4}{64} \tag{9.40}$$

Clearly from symmetry

$$I_y = \frac{\pi d^4}{64} \tag{9.41}$$

Using the theorem of perpendicular axes, the polar second moment of area, I_o, is given by

$$I_o = I_z + I_y = \frac{\pi d^4}{32} \tag{9.42}$$

Product second moment of area

The product second moment of area, I_{zy}, of a beam section with respect to z and y axes is defined by

$$I_{zy} = \int_A zy\,\mathrm{d}A \tag{9.43}$$

Thus each element of area in the cross section is multiplied by the product of its coordinates and the integration is taken over the complete area. Although second moments of area are always positive since elements of area are multiplied by the square of one of their coordinates, it is possible for I_{zy} to be negative if the section lies predominantly in the second and fourth quadrants of the axes system. Such a situation would arise in the case of the Z-section of Fig. 9.26(a) where the product second moment of area of each flange is clearly negative.

A special case arises when one (or both) of the coordinate axes is an axis of symmetry so that for any element of area, δA, having the product of its coordinates positive, there is an identical element for which the product of its coordinates is negative (Fig. 9.26(b)).

Summation (i.e. integration) over the entire section of the product second moment of area of all such pairs of elements results in a zero value for I_{zy}.

We have shown previously that the parallel axes theorem may be used to calculate second moments of area of beam sections comprising geometrically simple components. The theorem can be extended to the calculation of product second moments of area. Let us suppose that we wish to calculate the product second moment of area, I_{zy}, of the section shown in Fig. 9.26(c) about axes zy when I_{ZY} about its

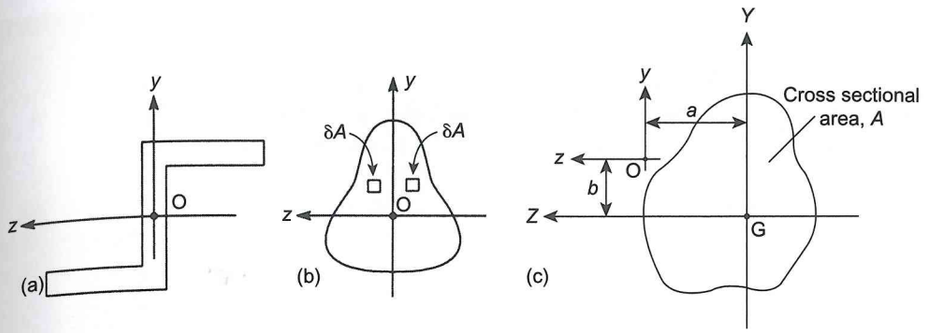

FIGURE 9.26
Product second moment of area.

$$I_{zy} = \int_A zy\,\mathrm{d}A$$

or

$$I_{zy} = \int_A (Z-a)(Y-b)\,\mathrm{d}A$$

which, on expanding, gives

$$I_{zy} = \int_A ZY\,\mathrm{d}A - b\int_A Z\,\mathrm{d}A - a\int_A Y\,\mathrm{d}A + ab\int_A \mathrm{d}A$$

If Z and Y are centroidal axes then $\int_A Z\,\mathrm{d}A = \int_A Y\,\mathrm{d}A = 0$. Hence

$$I_{zy} = I_{ZY} + abA \tag{9.44}$$

It can be seen from Eq. (9.44) that if either GZ or GY is an axis of symmetry, i.e. $I_{ZY} = 0$, then

$$I_{zy} = abA \tag{9.45}$$

Thus for a section component having an axis of symmetry that is parallel to either of the section reference axes the product second moment of area is the product of the coordinates of its centroid multiplied by its area.

A table of the properties of a range of beam sections is given in Appendix A.

EXAMPLE 9.9

A beam having the cross section shown in Fig. 9.27 is subjected to a hogging bending moment of 1500 Nm in a vertical plane. Calculate the maximum direct stress due to bending stating the point at which it acts.

The position of the centroid, G, of the section may be found by taking moments of areas about some convenient point. Thus

$$(120\times 8 + 80\times 8)\bar{y} = 120\times 8\times 4 + 80\times 8\times 48$$

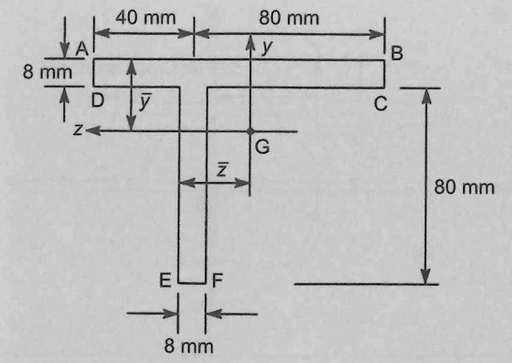

FIGURE 9.27
Beam section of Ex. 9.9.

which gives

$$\bar{y} = 21.6 \text{ mm}$$

and

$$(120 \times 8 + 80 \times 8)\bar{z} = 80 \times 8 \times 4 + 120 \times 8 \times 24$$

giving

$$\bar{z} = 16 \text{ mm}$$

The second moments of area referred to axes Gzy are now calculated.

$$I_z = \frac{120 \times (8)^3}{12} + 120 \times 8 \times (17.6)^2 + \frac{8 \times (80)^3}{12} + 80 \times 8 \times (26.4)^2$$

$$= 1.09 \times 10^6 \text{ mm}^4$$

$$I_y = \frac{8 \times (120)^3}{12} + 120 \times 8 \times (8)^2 + \frac{80 \times (8)^3}{12} + 80 \times 8 \times (12)^2$$

$$= 1.31 \times 10^6 \text{ mm}^4$$

$$I_{zy} = 120 \times 8 \times (-8) \times (+17.6) + 80 \times 8 \times (+12) \times (-26.4)$$

$$= -0.34 \times 10^6 \text{ mm}^4$$

Since $M_z = -1500$ Nm and $M_y = 0$ we have from Eq. (9.31)

$$\sigma_x = -\frac{1500 \times 10^3 \times (-0.34 \times 10^6)z + 1500 \times 10^3 \times (1.31 \times 10^6)y}{1.09 \times 10^6 \times 1.31 \times 10^6 - (-0.34 \times 10^6)^2}$$

i.e.

$$\sigma_x = 0.39z + 1.5y \qquad \text{(i)}$$

Note that the denominator in both the terms in Eq. (9.31) is the same.
Inspection of Eq. (i) shows that σ_x is a maximum at F where $z = 8$ mm, $y = -66.4$ mm. Hence

$$\sigma_{x,\max} = -96.5 \text{ N/mm}^2 \text{ (compressive)}$$

Approximations for thin-walled sections

Modern civil engineering structures frequently take the form of thin-walled cellular box beams which combine the advantages of comparatively low weight and high strength, particularly in torsion. Other forms of thin-walled structure consist of 'open' section beams such as a plate girder which is constructed from thin plates stiffened against instability. In addition to these there are the cold-formed sections which we discussed in Chapter 1.

There is no clearly defined line separating 'thick' and 'thin-walled' sections; the approximations allowed in the analysis of thin-walled sections become increasingly inaccurate the 'thicker' a section becomes. However, as a guide, it is generally accepted that the approximations are reasonably accurate for sections for which the ratio

$$\frac{t_{\max}}{b} \leq 0.1$$

where $t_{\max}$ is the maximum thickness in the section and b is a typical cross-sectional dimension.

In the calculation of the properties of thin-walled sections we shall assume that the thickness, t, of the section is small compared with its cross-sectional dimensions so that squares and higher powers of t are neglected. The section profile may then be represented by the mid-line of its wall. Stresses are then calculated at points on the mid-line and assumed to be constant across the thickness.

EXAMPLE 9.10

Calculate the second moment of area, I_z, of the channel section shown in Fig. 9.28(a).

The centroid of the section is located midway between the flanges; its horizontal position is not needed since only I_z is required. Thus

$$I_z = 2\left(\frac{bt^3}{12} + bth^2\right) + t\frac{[2(h - t/2)]^3}{12}$$

which, on expanding, becomes

$$I_z = 2\left(\frac{bt^3}{12} + bth^2\right) + \frac{t}{12}\left[(2)^3\left(h^3 - \frac{3h^2t}{2} + \frac{3ht^2}{4} - \frac{t^3}{8}\right)\right]$$

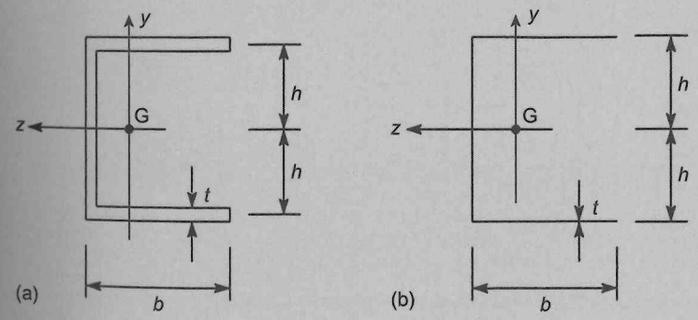

FIGURE 9.28
Calculation of the second moment of area of a thin-walled channel section

Neglecting powers of t^2 and upwards we obtain

$$I_z = 2bth^2 + t\frac{(2h)^3}{12}$$

It is unnecessary for such calculations to be carried out in full since the final result may be obtained almost directly by regarding the section as being represented by a single line as shown in Fig. 9.28(b).

EXAMPLE 9.11

A thin-walled beam has the cross section shown in Fig. 9.29. Determine the direct stress distribution produced by a hogging bending moment M_z.

The beam cross section is antisymmetrical so that its centroid is at the mid-point of the vertical web. Furthermore, $M_y = 0$ so that Eq. (9.31) reduces to

$$\sigma_x = \frac{M_z I_{zy} z - M_z I_y y}{I_z I_y - I_{zy}^2} \tag{i}$$

But M_z is a hogging bending moment and therefore negative. Eq. (i) must then be rewritten as

$$\sigma_x = \frac{-M_z I_{zy} z + M_z I_y y}{I_z I_y - I_{zy}^2} \tag{ii}$$

The section properties are calculated using the previously specified approximations for thin-walled sections; thus

$$I_z = 2\frac{ht}{2}\left(\frac{h}{2}\right)^2 + \frac{th^3}{12} = \frac{h^3 t}{3}$$

$$I_y = 2\frac{t}{2}\left(\frac{h}{2}\right)^3 = \frac{h^3 t}{12}$$

$$I_{zy} = \frac{ht}{2}\left(\frac{h}{4}\right)\left(\frac{h}{2}\right) + \frac{ht}{2}\left(-\frac{h}{4}\right)\left(-\frac{h}{2}\right) = \frac{h^3 t}{8}$$

Substituting these values in Eq. (ii) we obtain

$$\sigma_x = \frac{M_z}{h^3 t}(6.86y - 10.3z) \tag{iii}$$

On the top flange $y = +h/2$, $h/2 \geq z \geq 0$ and the distribution of direct stress is given by

$$\sigma_x = \frac{M_z}{h^3 t}(3.43h - 10.3z)$$

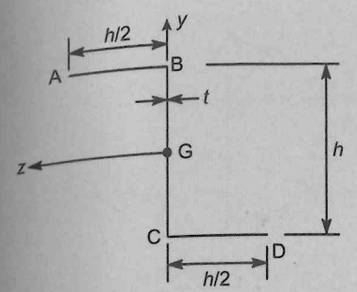

FIGURE 9.29
Beam section of Ex. 9.11.

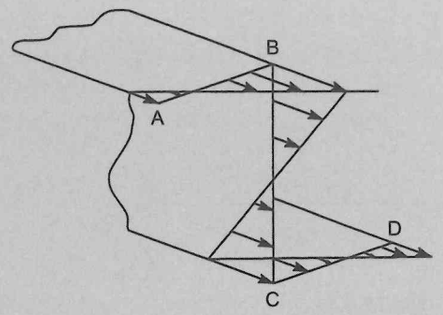

FIGURE 9.30
Distribution of direct stress in beam section of Ex. 9.11.

which is linear. Hence

$$\sigma_{x,A} = -\frac{1.72M_z}{h^2 t}\text{(compressive)}$$

$$\sigma_{x,B} = +\frac{3.43M_z}{h^2 t}\text{(tensile)}$$

In the web $-h/2 \leq y \leq h/2$ and $z = 0$ so that Eq. (iii) reduces to

$$\sigma_x = \frac{6.86M_z}{h^3 t}y$$

Again the distribution is linear and varies from

$$\sigma_{x,B} = +\frac{3.43M_z}{h^2 t}\text{(tensile)}$$

to

$$\sigma_{x,C} = -\frac{3.43M_z}{h^2 t}\text{(compressive)}$$

The distribution in the lower flange may be deduced from antisymmetry. The complete distribution is as shown in Fig. 9.30.

Second moments of area of inclined and curved thin-walled sections

Thin-walled sections frequently have inclined or curved walls which complicate the calculation of section properties. Consider the inclined thin section of Fig. 9.31. The second moment of area of an element δs about a horizontal axis through its centroid G is equal to $t\delta s y^2$. Therefore the total second moment of area of the section about Gz, I_z, is given by

$$I_z = \int_{-a/2}^{a/2} ty^2\,\mathrm{d}s = \int_{-a/2}^{a/2} t(s\sin\beta)^2\,\mathrm{d}s$$

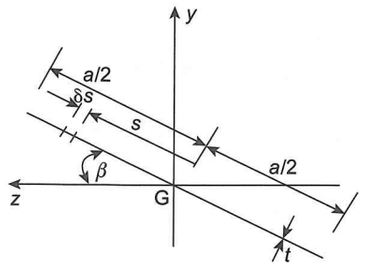

FIGURE 9.31
Second moments of area of an inclined thin-walled section.

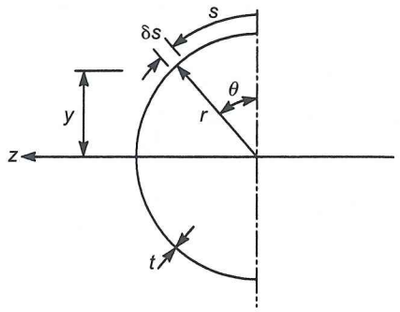

FIGURE 9.32
Second moment of area of a semicircular thin-walled section.

i.e.

$$I_z = \frac{a^3 t \sin^2 \beta}{12}$$

Similarly

$$I_y = \frac{a^3 t \cos^2 \beta}{12}$$

The product second moment of area of the section about Gzy is

$$I_{zy} = \int_{-a/2}^{a/2} tzy \, ds = \int_{-a/2}^{a/2} t(s \cos \beta)(s \sin \beta) \, ds$$

i.e.

$$I_{zy} = \frac{a^3 t \sin 2\beta}{24}$$

Properties of thin-walled curved sections are found in a similar manner. Thus I_z for the semicircular section of Fig. 9.32 is

$$I_z = \int_0^{\pi r} ty^2 \, ds$$

Expressing y and s in terms of a single variable θ simplifies the integration; hence

$$I_z = \int_0^{\pi} t(-r \cos \theta)^2 r \, d\theta$$

from which

$$I_z = \frac{\pi r^3 t}{2}$$

EXAMPLE 9.12

Calculate the second moments of area of the thin-walled beam section shown in Fig. 9.33. Note that the position of the centroid op area of the circular portion of the beam section is given.

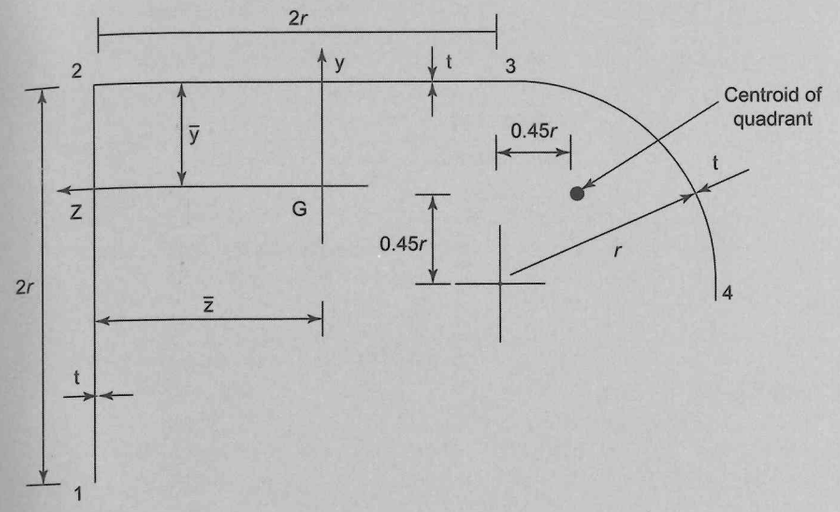

FIGURE 9.33
Beam section of Ex. 9.12.

The first step is to find the position of the centroid of area of the beam section. Therefore, taking moments of area about the flange 12

$$(2rt + 2rt + \pi rt/2)\bar{z} = 2rtr + \pi rt \times 2.45r/2$$

which gives

$$\bar{z} = 1.05r$$

Now taking moments of area about the flange 23

$$(2rt + 2rt + \pi rt/2)\bar{y} = 2rtr + \pi rt \times 0.55r/2$$

from which

$$\bar{y} = 0.51r$$

The second moments of area of the quadrant portion of the section about axes ZY through its own centroid may be found by referring to Fig. 9.34. Then

$$I_Z = \int_0^{\pi/r2} tY^2 \, ds = \int_0^{\pi/2} t(r\cos\theta - 0.45r)^2 r \, d\theta$$

which gives

$$I_Z = 0.7tr^3 = I_Y$$

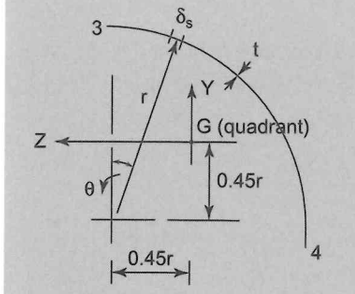

FIGURE 9.34
Quadrant of beam section of Ex. 9.12.

$$I_{ZY} = \int_0^{\pi r/2} tZY\,\mathrm{d}s = \int_0^{\pi/2} t(0.45r - r\sin\theta)(r\cos\theta - 0.45r)r\,\mathrm{d}\theta$$

from which

$$I_{ZY} = 0.58tr^3$$

Now, from Fig. 9.33

$$I_z = \frac{t(2r^3)}{12} + 2rt(0.49r)^2 + 2rt(0.51r)^2 + 0.7tr^3 + \frac{\pi rt}{2}(0.04r)^2$$

so that

$$I_z = 2.87tr^3$$

$$I_y = 2rt(1.05r)^2 + \frac{t(2r)^3}{12} + 2tr(0.05r)^2 + 0.7tr^3 + \frac{\pi rt}{2}(1.4r)^2$$

which gives

$$I_y = 6.65tr^3$$

$$I_{zy} = 2rt(1.05r)(-0.49r) + 2rt(0.05r)(0.51r) + 0.58tr^3 + \frac{\pi rt}{2}(-1.4r)(0.04r)$$

from which

$$I_{zy} = -0.31tr^3$$

9.7 Principal axes and principal second moments of area

In any beam section there is a set of axes, neither of which need necessarily be an axis of symmetry, for which the product second moment of area is zero. Such axes are known as *principal axes* and the second moments of area about these axes are termed principal second moments of area.

Consider the arbitrary beam section shown in Fig. 9.35. Suppose that the second moments of area I_z, I_y and the product second moment of area, I_{zy}, about arbitrary axes Ozy are known. By definition

$$I_z = \int y^2\,\mathrm{d}A \quad I_y = \int z^2\,\mathrm{d}A \quad I_{zy} = \int zy\,\mathrm{d}A \tag{9.46}$$

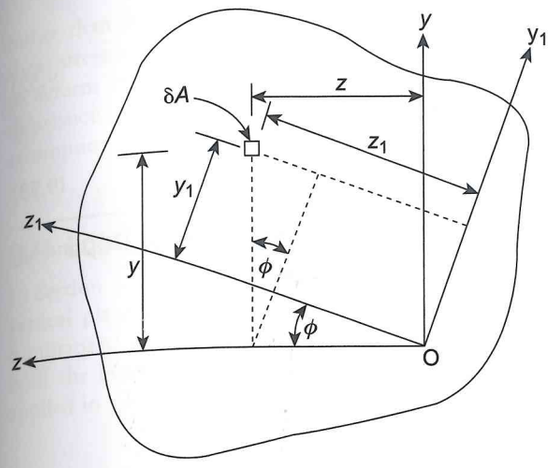

FIGURE 9.35
Principal axes in a beam of arbitrary section.

The corresponding second moments of area about axes Oz_1y_1 are

$$I_{z(1)} = \int_A y_1^2\,\mathrm{d}A \quad I_{y(1)} = \int_A z_1^2\,\mathrm{d}A \quad I_{z(1)y(1)} = \int_A z_1y_1\,\mathrm{d}A \tag{9.47}$$

From Fig. 9.35

$$z_1 = z\cos\phi + y\sin\phi \quad y_1 = y\cos\phi - z\sin\phi$$

Substituting for y_1 in the first of Eq. (9.47)

$$I_{z(1)} = \int_A (y\cos\phi - z\sin\phi)^2\,\mathrm{d}A$$

Expanding, we obtain

$$I_{z(1)} = \cos^2\phi\int_A y^2\,\mathrm{d}A + \sin^2\phi\int_A z^2\mathrm{d}A - 2\cos\phi\sin\phi\int_A zy\,\mathrm{d}A$$

which gives, using Eq. (9.46)

$$I_{z(1)} = I_z\cos^2\phi + I_y\sin^2\phi - I_{zy}\sin 2\phi \tag{9.48}$$

Similarly

$$I_{y(1)} = I_y\cos^2\phi + I_z\sin^2\phi - I_{zy}\sin 2\phi \tag{9.49}$$

and

$$I_{z(1),y(1)} = \left(\frac{I_z - I_y}{2}\right)\sin 2\phi + I_{zy}\cos 2\phi \tag{9.50}$$

Equations (9.48)–(9.50) give the second moments of area and product second moment of area about axes inclined at an angle ϕ to the x axis. In the special case where Oz_1y_1 are principal axes, Oz_p, y_p, $I_{z(p),y(p)} = 0$, $\phi = \phi_p$ and Eqs (9.48) and (9.49) become

$$I_{z(p)} = I_z\cos^2\phi_p + I_y\sin^2\phi_p - I_{zy}\sin 2\phi_p \tag{9.51}$$

and

$$I_{y(\mathrm{p})} = I_y \cos^2 \phi_\mathrm{p} + I_z \sin^2 \phi_\mathrm{p} + I_{zy} \sin 2\phi_\mathrm{p} \tag{9.52}$$

respectively. Furthermore, since $I_{z(1),y(1)} = I_{z(\mathrm{p}),y(\mathrm{p})} = 0$, Eq. (9.50) gives

$$\tan 2\phi_\mathrm{p} = \frac{2I_{zy}}{I_y - I_z} \tag{9.53}$$

The angle ϕ_p may be eliminated from Eqs (9.51) and (9.52) by first determining $\cos 2\phi_\mathrm{p}$ and $\sin 2\phi_\mathrm{p}$ using Eq. (9.53). Thus

$$\cos 2\phi_\mathrm{p} = \frac{(I_y - I_z)/2}{\sqrt{[(I_y - I_z)/2]^2 + I_{xy}^2}} \qquad \sin 2\phi_\mathrm{p} = \frac{I_{zy}}{\sqrt{[(I_y - I_z)/2]^2 + I_{zy}^2}}$$

Rewriting Eq. (9.51) in terms of $\cos 2\phi_\mathrm{p}$ and $\sin 2\phi_\mathrm{p}$ we have

$$I_{z(\mathrm{p})} = \frac{I_z}{2}(1 + \cos 2\phi_\mathrm{p}) + \frac{I_y}{2}(1 - \cos 2\phi_\mathrm{p}) - I_{zy} \sin 2\phi_\mathrm{p}$$

Substituting for $\cos 2\phi_p$ and $\sin 2\phi_p$ from the above we obtain

$$I_{z(\mathrm{p})} = \frac{I_z + I_y}{2} - \frac{1}{2}\sqrt{(I_z - I_y)^2 + 4I_{zy}^2} \tag{9.54}$$

Similarly

$$I_{y(\mathrm{p})} = \frac{I_z + I_y}{2} + \frac{1}{2}\sqrt{(I_z - I_y)^2 + 4I_{zy}^2} \tag{9.55}$$

Note that the solution of Eq. (9.53) gives two values for the inclination of the principal axes, ϕ_p and $\phi_\mathrm{p} + \pi/2$, corresponding to the axes Oz_p and Oy_p.

The results of Eqs (9.48)–(9.55) may be represented graphically by Mohr's circle, a powerful method of solution for this type of problem. We shall discuss Mohr's circle in detail in Chapter 14 in connection with the analysis of complex stress and strain.

Principal axes may be used to provide an apparently simpler solution to the problem of unsymmetrical bending. Referring components of bending moment and section properties to principal axes having their origin at the centroid of a beam section, we see that Eq. (9.31) or Eq. (9.32) reduces to

$$\sigma_x = -\frac{M_{y(\mathrm{p})}}{I_{y(\mathrm{p})}} z_\mathrm{p} - \frac{M_{z(\mathrm{p})}}{I_{z(\mathrm{p})}} y_\mathrm{p} \tag{9.56}$$

However, it must be appreciated that before $I_{z(\mathrm{p})}$ and $I_{y(\mathrm{p})}$ can be determined I_z, I_y and I_{zy} must be known together with ϕ_p. Furthermore, the coordinates (z, y) of a point in the beam section must be transferred to the principal axes as must the components, M_z and M_y, of bending moment. Thus unless the position of the principal axes is obvious by inspection, the amount of computation required by the above method is far greater than direct use of Eq. (9.31) and an arbitrary, but convenient, set of centroidal axes.

9.8 Effect of shear forces on the theory of bending

So far our analysis has been based on the assumption that plane sections remain plane after bending

rather than by shear loads, as is very often the case in practice. The presence of shear loads induces shear stresses in the cross section of a beam which, as shown by elasticity theory, cause the cross section to deform into the shape of a shallow inverted 's'. However, shear stresses in beams, the cross sectional dimensions of which are small in relation to their length, are comparatively low in value so that the assumption of plane sections remaining plane after bending may be used with reasonable accuracy.

9.9 Load, shear force and bending moment relationships, general case

In Section 3.5 we derived load, shear force and bending moment relationships for loads applied in the vertical plane of a beam whose cross section was at least singly symmetrical. These relationships are summarized in Eq. (3.8) and may be extended to the more general case in which loads are applied in both the horizontal *(xz)* and vertical *(yx)* planes of a beam of arbitrary cross section. Thus for loads applied in a horizontal plane Eq. (3.8) become

$$\frac{\partial^2 M_y}{\partial z^2} = -\frac{\partial S_x}{\partial x} = -w_z(x) \tag{9.57}$$

and for loads applied in a vertical plane Eq. (3.8) become

$$\frac{\partial^2 M_z}{\partial x^2} = -\frac{\partial S_y}{\partial x} = -w_y(x) \tag{9.58}$$

In Chapter 18 we shall return to the topic of beams subjected to bending but, instead of considering loads which produce stresses within the elastic range of the material of the beam, we shall investigate the behaviour of beams under loads which cause collapse.

PROBLEMS

P.9.1 A girder 10 m long has the cross section shown in Fig. P.9.1(a) and is simply supported over a span of 6 m (see Fig. P.9.1(b)). If the maximum direct stress in the girder is limited to 150 N/mm^2, determine the maximum permissible uniformly distributed load that may be applied to the girder.

Ans. 84.3 kN/m.

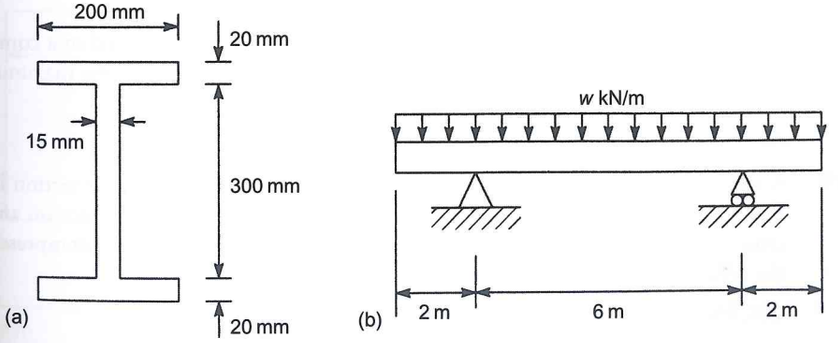

FIGURE P.9.1

P.9.2 A 230 mm × 300 mm timber cantilever of rectangular cross section projects 2.5 m from a wall and carries a load of 13 300 N at its free end. Calculate the maximum direct stress in the beam due to bending.

Ans. 9.6 N/mm^2.

P.9.3 A floor carries a uniformly distributed load of 16 kN/m^2 and is supported by joists 300 mm deep and 110 mm wide; the joists in turn are simply supported over a span of 4 m. If the maximum stress in the joists is not to exceed 7 N/mm^2, determine the distance apart, centre to centre, at which the joists must be spaced.

Ans. 0.36 m.

P.9.4 A wooden mast 15 m high tapers linearly from 250 mm diameter at the base to 100 mm at the top. At what point will the mast break under a horizontal load applied at the top? If the maximum permissible stress in the wood is 35 N/mm^2, calculate the magnitude of the load that will cause failure.

Ans. 5 m from the top, 2320 N.

P.9.5 A main beam in a steel framed structure is 5 m long and simply supported at each end. The beam carries two cross-beams at distances of 1.5 and 3.5 m from one end, each of which transmits a load of 20 kN to the main beam. Design the main beam using an allowable stress of 155 N/mm^2; make adequate allowance for the effect of self-weight.

Ans. Universal Beam, 254 mm × 102 mm × 22 kg/m.

P.9.6 A cantilever beam of length 2.5 m has the cross section shown in Fig. P.9.6 and carries a vertically downward concentrated load of 25 kN at its free end. If the maximum allowable direct stress in the beam is ± 165 N/mm^2 calculate the maximum intensity of uniformly distributed load the beam can carry over its complete length. What are the values of the elastic section moduli of the beam cross section about its horizontal z axis?

Ans. 9.8 kN/m, 563835 mm^3, 1000925 mm^3.

P.9.7 A beam has the singly symmetrical cross section shown in Fig. P.9.7 and is simply supported over a span of 2 m. If the direct stress is limited to ± 155 N/mm^2 and it carries a distributed load which varies in intensity from zero at the left-hand support to w_0 at the right-hand support calculate the maximum allowable value of w_0.

Ans. 308.6 kN/m.

P.9.8 A short column, whose cross section is shown in Fig. P.9.8 is subjected to a compressive load, P, at the centroid of one of its flanges. Find the value of P such that the maximum compressive stress does not exceed 150 N/mm^2.

Ans. 846.4 kN.

P.9.9 A compressive force, P, is applied eccentrically to a column whose cross section is shown in Fig. P.9.9. Find the maximum eccentricity, e, of P if there is to be no tension anywhere in the cross section of the column. For this value of e calculate the maximum compressive stress in the column when $P = 450$ kN.

Ans. 64.2 mm, 160.7 N/mm^2.

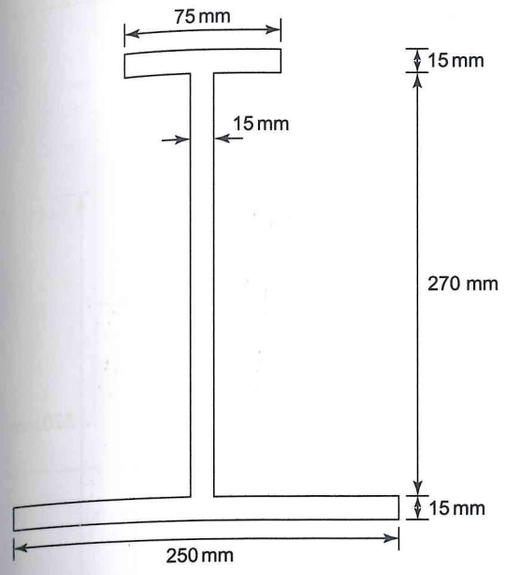

FIGURE P.9.6

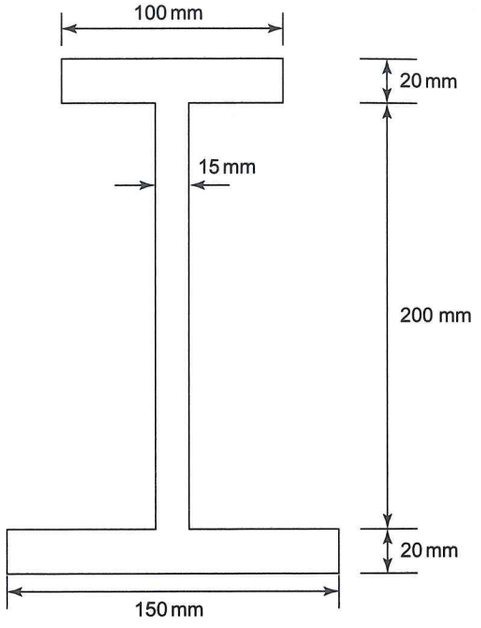

FIGURE P.9.7

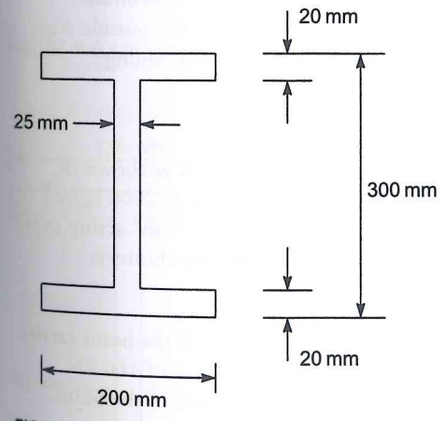

FIGURE P.9.8

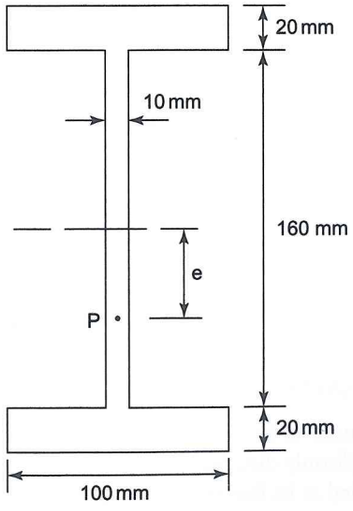

FIGURE P.9.9

P.9.10 The cantilever beam shown in Fig. P.9.10(a) has the hollow cross section shown in Fig. 9.10 (b). If the 130 kN load is applied at the centroid of the end cross section calculate the maximum value of compressive stress in the cross section of the beam.

Ans. 132.1 N/mm^2.

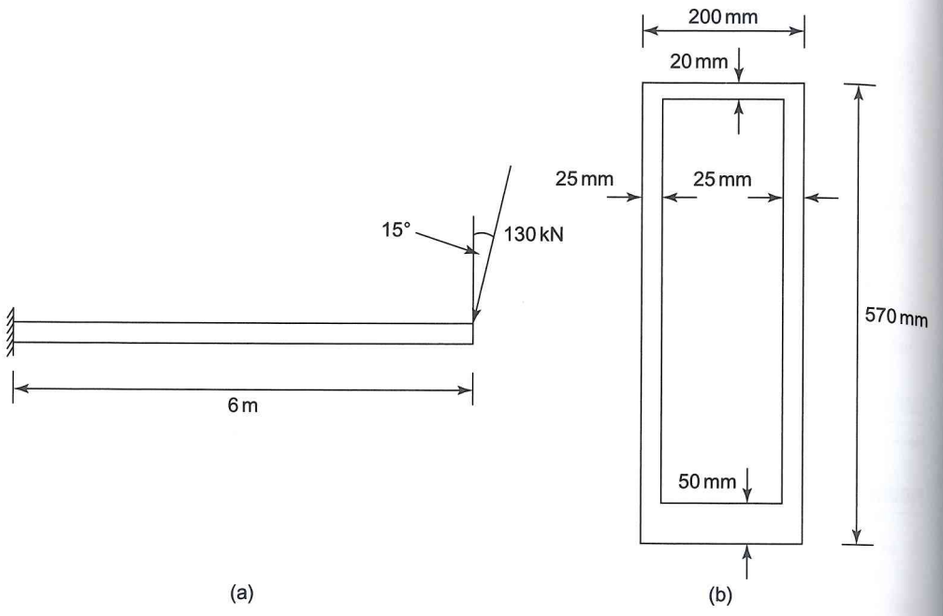

FIGURE P.9.10

P.9.11 A column 3 m high has the cross section shown in Fig. P.9.11 and is subjected to an axial load of 200 kN together with a horizontal load, W, applied in the direction of the web. If the maximum direct stress in the column is limited to 155 N/mm^2 calculate the maximum allowable value of W. If the 200 kN load is moved in the direction of W to the outside edge of a flange but remains in the vertical plane of symmetry calculate the corresponding maximum allowable value of W.

Ans. 20.5 kN, 12.5 kN.

P.9.12 A vertical chimney built in brickwork has a uniform rectangular cross section as shown in Fig. P.9.12(a) and is built to a height of 15 m. The brickwork has a density of 2000 kg/m^3 and the wind pressure is equivalent to a uniform horizontal pressure of 750 N/m^2 acting over one face. Calculate the stress at each of the points A and B at the base of the chimney.

Ans. (A) 0.02 N/mm^2 (compression), (B) 0.60 N/mm^2 (compression).

P.9.13 A cantilever beam of length 2 m has the cross section shown in Fig. P.9.13. If the beam carries a uniformly distributed load of 5 kN/m together with a compressive axial load of 100 kN applied at its free end, calculate the maximum direct stress in the cross section of the beam.

Ans. 121.5 N/mm^2 (compression) at the built-in end and at the bottom of the leg.

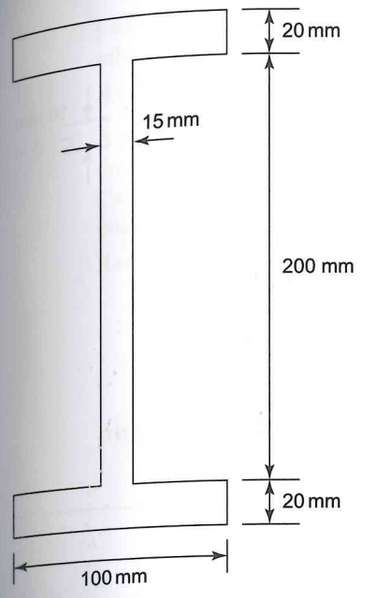

FIGURE P.9.11

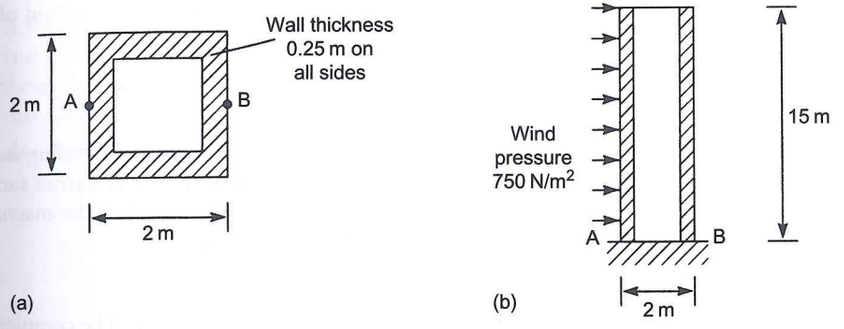

FIGURE P.9.12

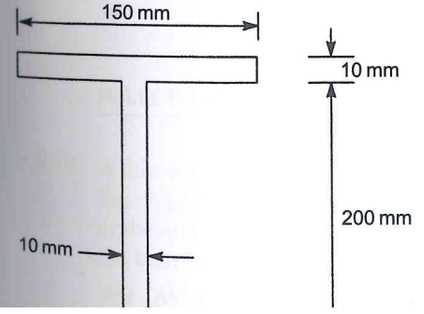

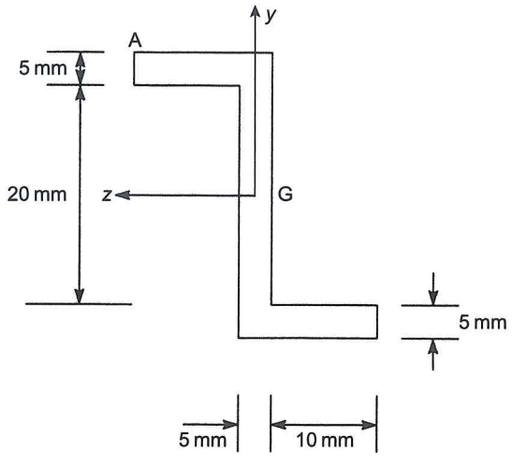

FIGURE P.9.14

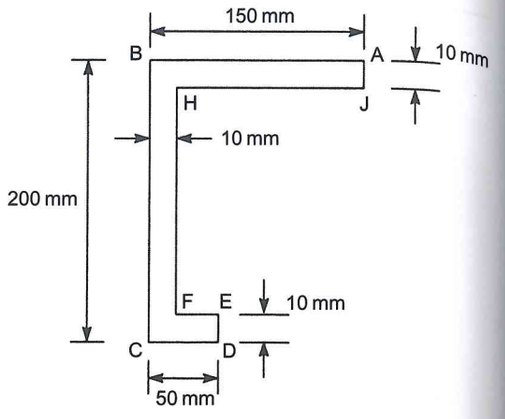

FIGURE P.9.15

P.9.14 The section of a thick beam has the dimensions shown in Fig. P.9.14. Calculate the section properties I_z, I_y and I_{zy} referred to horizontal and vertical axes through the centroid of the section. Determine also the direct stress at the point A due to a bending moment $M_y = 55$ Nm.

Ans. -114 N/mm^2 (compression).

P.9.15 A beam possessing the thick section shown in Fig. P.9.15 is subjected to a bending moment of 12 kN m applied in a plane inclined at 30° to the left of vertical and in a sense such that its components M_z and M_y are negative and positive, respectively. Calculate the magnitude and position of the maximum direct stress in the beam cross section.

Ans. 156.2 N/mm^2 (compression) at D.

P.9.16 The cross section of a beam/floor slab arrangement is shown in Fig. P.9.16. The complete section is simply supported over a span of 10 m and, in addition to its self-weight, carries a concentrated

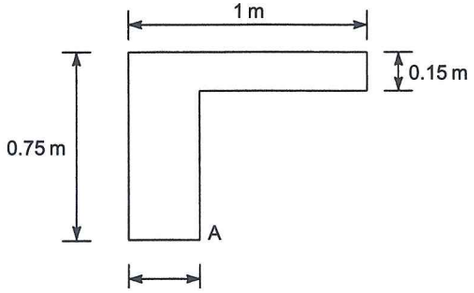

FIGURE P.9.16

load of 25 kN acting vertically downwards at mid-span. If the density of concrete is 2000 kg/m^3, calculate the maximum direct stress at the point A in its cross section.

Ans. 5.4 N/mm^2 (tension).

P.9.17 A precast concrete beam has the cross section shown in Fig. P.9.17 and carries a vertically downward uniformly distributed load of 100 kN/m over a simply supported span of 4 m. Calculate the maximum direct stress in the cross section of the beam, indicating clearly the point at which it acts.

Ans. -27.6 N/mm^2 (compression) at B.

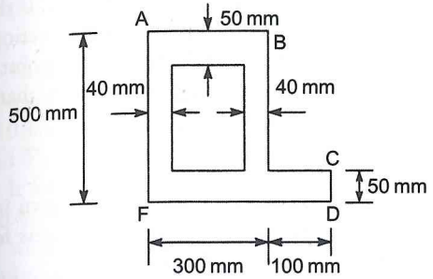

FIGURE P.9.17

P.9.18 A thin-walled, cantilever beam of unsymmetrical cross section supports shear loads at its free end as shown in Fig. P.9.18. Calculate the value of direct stress at the extremity of the lower flange (point A) at a section half-way along the beam if the position of the shear loads is such that no twisting of the beam occurs.

Ans. 194.7 N/mm^2 (tension).

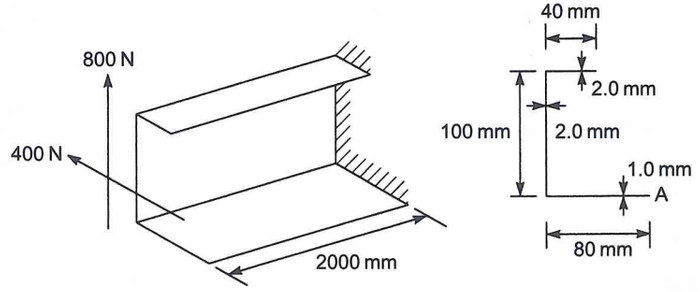

FIGURE P.9.18

P.9.19 A thin-walled cantilever with walls of constant thickness t has the cross section shown in Fig. P.9.19. The cantilever is loaded by a vertical force P at the tip and a horizontal force $2P$ at the mid-section. Determine the direct stress at the points A and B in the cross section at the built-in end.

Ans. (A) $-1.85\ PL/td^2$, (B) $0.1\ PL/td^2$.

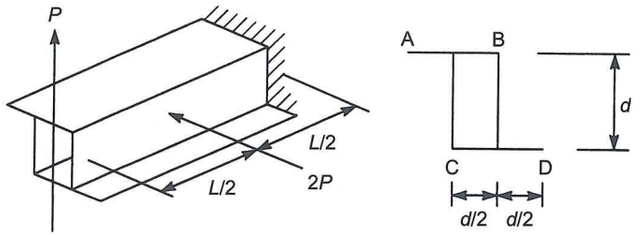

FIGURE P.9.19

P.9.20 A tall building has the cross section shown in Fig. P.9.20 and is subjected to horizontal wind loads which are resisted by an unsymmetrical arrangement of concrete shear walls. If the height of the building is 60 m determine the maximum direct stress in the cross section produced by a uniform wind pressure of 750 N/m^2 acting as shown. Specify the point at which the maximum direct stress acts and assume, for the purposes of calculation, that the shear walls, all of thickness 200 mm, are thin.

Ans. 3.2 N/mm^2 at H.

P.9.21 A cold-formed, thin-walled beam section of constant thickness has the profile shown in Fig. P.9.21. Calculate the position of the neutral axis and the maximum direct stress for a bending moment of 3.5 kN m applied about the horizontal axis G*z*.

Ans. $\alpha = 51.9°$, ± 101.0 N/mm^2.

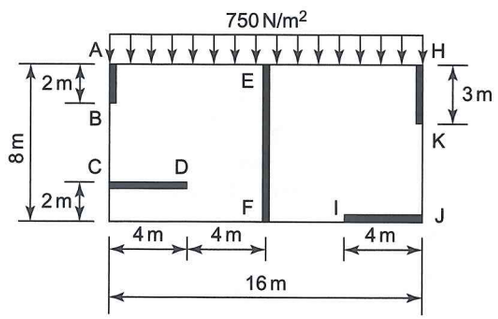

FIGURE P.9.20

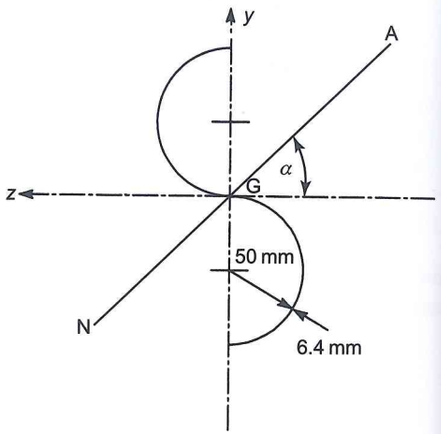

FIGURE P.9.21

CHAPTER

Shear of Beams

10

In Chapter 3 we saw that externally applied shear loads produce internal shear forces and bending moments in cross sections of a beam. The bending moments cause direct stress distributions in beam sections (Chapter 9); we shall now determine the corresponding distributions of shear stress. Initially, however, we shall examine the physical relationship between bending and shear; the mathematical relationship has already been defined in Eq. (3.8).

Suppose that a number of planks are laid one on top of the other and supported at each end as shown in Fig. 10.1(a). Applying a central concentrated load to the planks at mid span will cause them to bend as shown in Fig. 10.1(b). Due to bending the underside of each plank will stretch and the topside will shorten. It follows that there must be a relative sliding between the surfaces in contact. If now the planks are glued together they will bend as shown in Fig. 10.2. The glue has prevented the relative sliding of the adjacent surfaces and is therefore subjected to a shear force. This means that the application of a vertical shear load to a beam not only produces internal shear forces on cross sections of the beam but shear forces on horizontal planes as well. In fact, we have noted this earlier in Section 7.3 where we saw that shear stresses applied in one plane induce equal complementary shear stresses on perpendicular planes which is exactly the same situation as in the connected planks. This is important in the design of the connections between, say, a concrete slab and the flange of a steel I-section beam where the connections, usually steel studs, are subjected to this horizontal shear.

Shear stress distributions in beam cross sections depend upon the geometry of the beam section. We shall now determine this distribution for the general case of an unsymmetrical beam section before extending the theory to the simpler case of beam sections having at least one axis of symmetry. This is the reverse of our approach in Chapter 9 for bending but, here, the development of the theory is only marginally more complicated for the general case.

10.1 Shear stress distribution in a beam of unsymmetrical section

Consider an elemental length, δx, of a beam of arbitrary section subjected to internal shear forces S_z and S_y as shown in Fig. 10.3(a). The origin of the axes *xyz* coincides with the centroid G of the beam section. Let us suppose that the lines of action of S_z and S_y are such that no twisting of the beam occurs (see Section 10.4). The shear stresses induced are therefore due solely to shearing action and are not contributed to by torsion.

Imagine now that a 'slice' of width b_0 is taken through the length of the element. Let τ be the average shear stress along the edge, b_0, of the slice in a direction perpendicular to b_0 and in the plane of the cross section (Fig. 10.3(b)); note that τ is not necessarily the absolute value of shear stress at this position. We saw in Chapter 7 that shear stresses on given planes induce equal, complementary shear stresses on planes perpendicular to the given planes. Thus, τ on the cross-sectional face of the slice induces shear stresses τ on the flat longitudinal face of the slice. In addition, as we saw in Chapter 3, shear loads produce

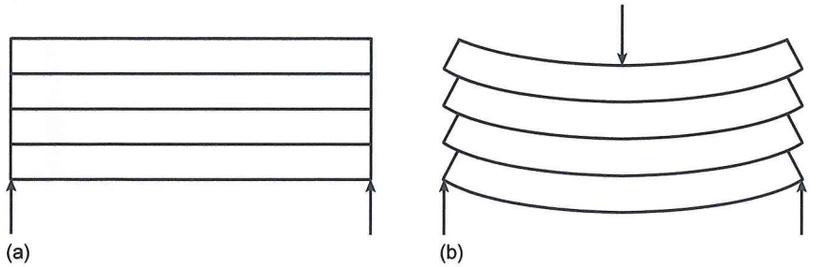

FIGURE 10.1
Bending of unconnected planks.

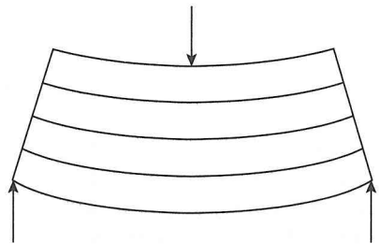

FIGURE 10.2
Bending of connected planks.

internal bending moments which, in turn, give rise to direct stresses in beam cross sections. Therefore on any filament, $\delta A'$, of the slice there is a direct stress σ_x at the section x and a direct stress $\sigma_x + (\partial\sigma_x/\partial x)\delta x$ at the section $x + \delta x$ (Fig. 10.3 (b)). The slice is therefore in equilibrium in the x direction under the combined action of the direct stress due to bending and the complementary shear stress, τ. Hence

$$\tau b_0 \delta x - \int_{A'} \sigma_x \, dA' + \int_{A'} \left(\sigma_x + \frac{\partial \sigma_x}{\partial x} \delta x \right) dA' = 0$$

which, when simplified, becomes

$$\tau b_0 = -\int_{A'} \frac{\partial \sigma_x}{\partial x} dA' \tag{10.1}$$

We shall assume (see Section 9.8) that the direct stresses produced by the bending action of shear loads are given by the theory developed for the pure bending of beams. Therefore, for a beam of unsymmetrical section and for coordinates referred to axes through the centroid of the section

$$\sigma_x = -\left(\frac{M_y I_z - M_z I_{zy}}{I_z I_y - I_{zy}^2} \right) z - \left(\frac{M_z I_y - M_y I_{zy}}{I_z I_y - I_{zy}^2} \right) y \quad (i.e.\ \text{Eq. (9.31)})$$

Then

$$\frac{\partial \sigma_x}{\partial x} = -\left\{ \frac{[(\partial M_y/\partial x) I_z - (\partial M_z/\partial x) I_{zy}]z + [(\partial M_z/\partial x) I_y - (\partial M_y/\partial x) I_{zy}]y}{I_z I_y - I_{zy}^2} \right\}$$

From Eqs (9.57) and (9.58)

$$\frac{\partial M_y}{\partial x} = -S_z \qquad \frac{\partial M_z}{\partial x} = -S_y$$

so that

$$\frac{\partial \sigma_x}{\partial x} = -\left\{ \frac{(-S_z I_z + S_y I_{zy})z + (-S_y I_y + S_z I_{zy})y}{I_z I_y - I^2} \right\}$$

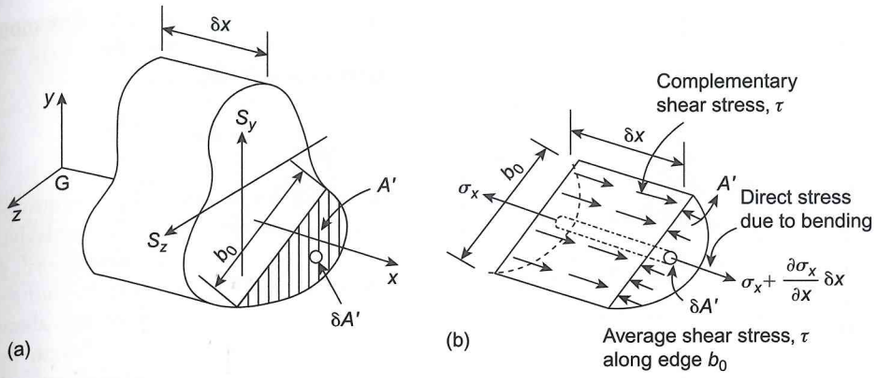

FIGURE 10.3
Determination of shear stress distribution in a beam of arbitrary cross section.

Substituting for $\partial\sigma_x/\partial x$ in Eq. (10.1) we obtain

$$\tau b_0 = \frac{S_y I_{zy} - S_z I_z}{I_z I_y - I_{zy}^2} \int_{A'} z \, dA' + \frac{S_z I_{zy} - S_y I_y}{I_z I_y - I_{zy}^2} \int_{A'} y \, dA'$$

or

$$\tau = \frac{S_y I_{zy} - S_z I_z}{b_0 (I_z I_y - I_{zy}^2)} \int_{A'} z \, dA' + \frac{S_z I_{zy} - S_y I_y}{b_0 (I_z I_y - I_{zy}^2)} \int_{A'} y \, dA' \tag{10.2}$$

The slice may be taken so that the average shear stress in any chosen direction can be determined.

10.2 Shear stress distribution in symmetrical sections

Generally in civil engineering we are not concerned with shear stresses in unsymmetrical sections except where they are of the thin-walled type (see Sections 10.4 and 10.5). 'Thick' beam sections usually possess at least one axis of symmetry and are subjected to shear loads in that direction.

Suppose that the beam section shown in Fig. 10.4 is subjected to a single shear load S_y. Since the y axis is an axis of symmetry, it follows that $I_{zy} = 0$ (Section 9.6). Therefore Eq. 10.2 reduces to

$$\tau = -\frac{S_y}{b_0 I_z} \int_{A'} y \, dA' \tag{10.3}$$

The negative sign arises because the average shear stress τ along the base b_0 of the slice A' is directed towards b_0 from *within the slice* as shown in Fig. 10.3(b). Taking the slice above Gz, as in Fig. 10.4, means that τ is now directed downwards. Clearly a positive shear force S_y produces shear stresses in the positive y direction, hence the negative sign.

Clearly the important shear stresses in the beam section of Fig. 10.4 are in the direction of the load. To find the distribution of this shear stress throughout the depth of the beam we therefore take the slice

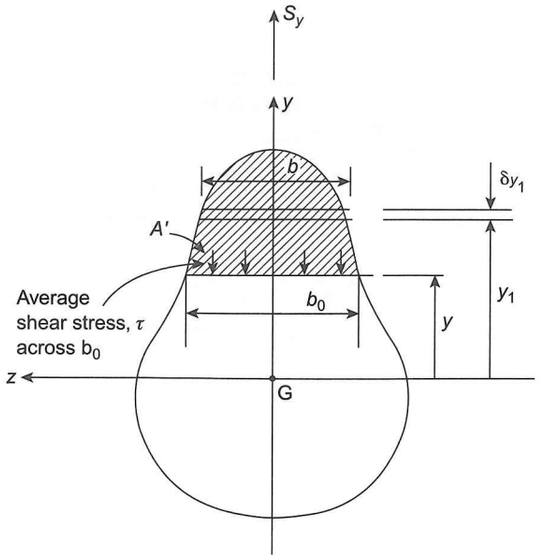

FIGURE 10.4
Shear stress distribution in a symmetrical section beam.

represents, mathematically, the first moment of the shaded area A' about the z axis. We may therefore rewrite Eq. (10.3) as

$$\tau = -\frac{S_y A' \bar{y}}{b_0 I_z} \tag{10.4}$$

where $\bar{y}$ is the distance of the centroid of the area A' from the z axis. Alternatively, if the value of $\bar{y}$ is not easily determined, say by inspection, then $\int_{A'} y dA'$ may be found by calculating the first moment of area about the z axis of an elemental strip of length b, width δy_1 (Fig. 10.4), and integrating over the area A'. Equation (10.3) then becomes

$$\tau = -\frac{S_y}{b_0 I_z} \int_y^{y\ \max} b y_1 \, dy_1 \tag{10.5}$$

Either of Eqs. (10.4) or (10.5) may be used to determine the distribution of vertical shear stress in a beam section possessing at least a horizontal or vertical axis of symmetry and subjected to a vertical shear load. The corresponding expressions for the horizontal shear stress due to a horizontal load are, by direct comparison with Eqs (10.4) and (10.5)

$$\tau = -\frac{S_z A' \bar{z}}{b_0 I_y} \quad \tau = -\frac{S_z}{b_0 I_y} \int_z^{z\ \max} b z_1 \, dz_1 \tag{10.6}$$

in which b_0 is the length of the edge of a vertical slice.

EXAMPLE 10.1

Determine the distribution of vertical shear stress in the beam section shown in Fig. 10.5(a) due to a vertical shear load S_y.

In this example the value of $\bar{y}$ for the slice A' is found easily by inspection so that we may use Eq. (10.4). From Fig. 10.5(a) we see that

$$b_0 = b \quad I_z = \frac{bd^3}{12} \quad A' = b\left(\frac{d}{2} - y\right) \quad \bar{y} = \frac{1}{2}\left(\frac{d}{2} + y\right)$$

Hence

$$\tau = -\frac{12 S_y}{b^2 d^3} b\left(\frac{d}{2} - y\right)\frac{1}{2}\left(\frac{d}{2} + y\right)$$

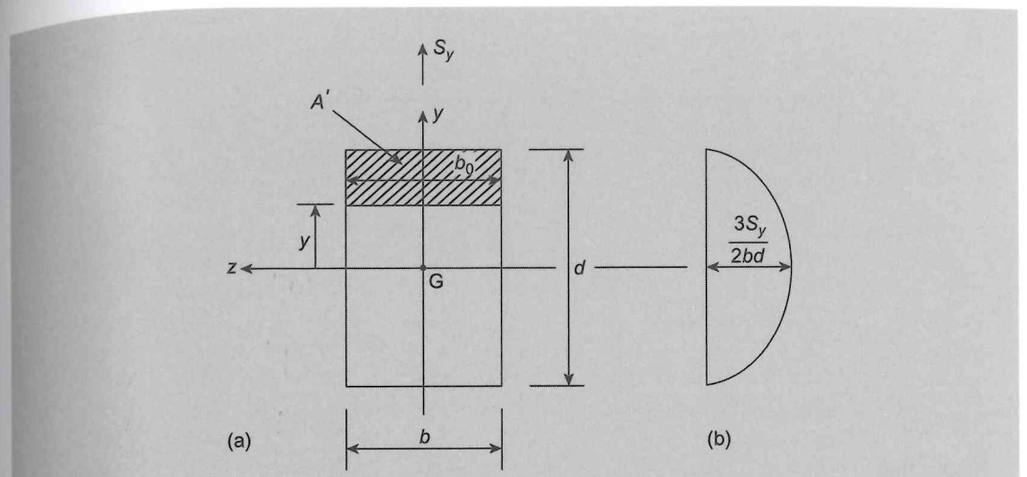

FIGURE 10.5
Shear stress distribution in a rectangular section beam.

which simplifies to

$$\tau = -\frac{6 S_y}{bd^3}\left(\frac{d^2}{4} - y^2\right) \tag{10.7}$$

The distribution of vertical shear stress is therefore parabolic as shown in Fig. 10.5(b) and varies from $\tau = 0$ at $y = \pm d/2$ to $\tau = \tau_{max} = 3S_y/2bd$ at the neutral axis ($y = 0$) of the beam section. Note that $\tau_{max} = 1.5\tau_{av}$, where τ_{av}, the average vertical shear stress over the section, is given by $\tau_{av} = S_y/bd$.

EXAMPLE 10.2

Determine the distribution of vertical shear stress in the I-section beam of Fig. 10.6(a) produced by a vertical shear load, S_y.

It is clear from Fig. 10.6(a) that the geometry of each of the areas A'_f and A'_w formed by taking a slice of the beam in the flange (at $y = y_f$) and in the web (at $y = y_w$), respectively, are different and will therefore lead to different distributions of shear stress. First we shall consider the flange. The area A'_f is rectangular so that the distribution of vertical shear stress, τ_f, in the flange is, by direct comparison with Ex. 10.1

$$\tau_f = -\frac{S_y}{BI_z}\frac{B}{2}\left(\frac{D}{2} - y_f\right)\left(\frac{D}{2} + y_f\right)$$

or

$$\tau_f = -\frac{S_y}{2I_z}\left(\frac{D^2}{4} - y_f^2\right) \tag{10.8}$$

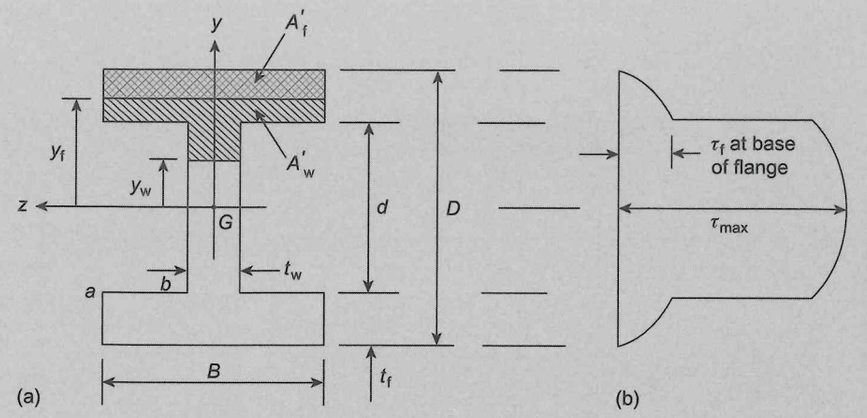

FIGURE 10.6

Shear stress distribution in an I-section beam.

where I_z is the second moment of area of the complete section about the centroidal axis Gz and is obtained by the methods of Section 9.6.

A difficulty arises in the interpretation of Eq. (10.8) which indicates a parabolic distribution of vertical shear stress in the flanges increasing from $\tau_f = 0$ at $y_f = \pm D/2$ to a value

$$\tau_f = -\frac{S_y}{8I_z}(D^2 - d^2) \tag{10.9}$$

at $y_f = \pm d/2$. However, the shear stress must also be zero at the inner surfaces ab, etc., of the flanges. Equation (10.8) therefore may only be taken to give an indication of the vertical shear stress distribution in the flanges *in the vicinity of the web*. Clearly if the flanges are thin so that d is close in value to D then τ_f *in the flanges* at the extremities of the web is small, as indicated in Fig. 10.6(b).

The area A'_w formed by taking a slice in the web at $y = y_w$ comprises two rectangles which may therefore be treated separately in determining $A'\bar{y}$ for the web.

Thus

$$\tau_w = -\frac{S_y}{t_w I_z}\left[B\left(\frac{D}{2} - \frac{d}{2}\right)\frac{1}{2}\left(\frac{D}{2} + \frac{d}{2}\right) + t_w\left(\frac{d}{2} - y_w\right)\frac{1}{2}\left(\frac{d}{2} + y_w\right)\right]$$

which simplifes to

$$\tau_w = -\frac{S_y}{t_w I_z}\left[\frac{B}{8}(D^2 - d^2) + \frac{t_w}{2}\left(\frac{d^2}{4} - y_w^2\right)\right] \tag{10.10}$$

or

$$\tau_w = -\frac{S_y}{I_z}\left[\frac{B}{8t_w}(D^2 - d^2) + \frac{1}{2}\left(\frac{d^2}{4} - y_w^2\right)\right] \tag{10.11}$$

Again the distribution is parabolic and increases from

$$\tau_w = -\frac{S_y}{I_z}\frac{B}{8t_w}(D^2 - d^2) \tag{10.12}$$

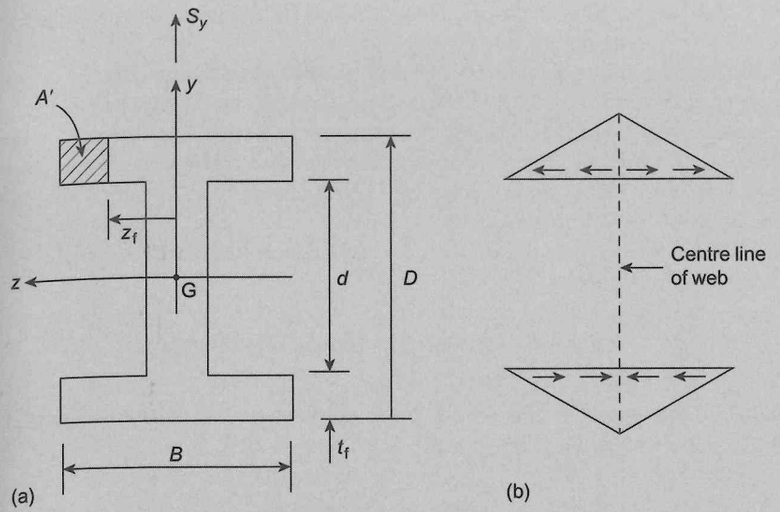

FIGURE 10.7

Distribution of horizontal shear stress in the flanges of an I-section beam.

at $y_w = \pm d/2$ to a maximum value, $\tau_{w,max}$, given by

$$\tau_{w,max} = -\frac{S_y}{I_z}\left[\frac{B}{8t_w}(D^2 - d^2) + \frac{d^2}{8}\right] \tag{10.13}$$

at $y = 0$. Note that the value of τ_w at the extremities of the web (Eq. (10.12)) is greater than the corresponding values of τ_f by a factor B/t_w. The complete distribution is shown in Fig. 10.6(b). Note also that the negative sign indicates that τ is vertically upwards.

The value of $\tau_{w,max}$ (Eq. (10.13)) is not very much greater than that of τ_w at the extremities of the web. In design checks on shear stress values in I-section beams it is usual to assume that the maximum shear stress in the web is equal to the shear load divided by the web area. In most cases the result is only slightly different from the value given by Eq. (10.13). A typical value given in Codes of Practice for the maximum allowable value of shear stress in the web of an I-section, mild steel beam is 100 N/mm^2; this is applicable to sections having web thicknesses not exceeding 40 mm.

We have been concerned so far in this example with the distribution of vertical shear stress. We now consider the situation that arises if we take the slice across one of the flanges at $z = z_f$ as shown in Fig. 10.7(a). Equations (10.4) and (10.5) still apply, but in this case $b_0 = t_f$. Thus, using Eq. (10.4)

$$\tau_{f(h)} = -\frac{S_y}{t_f I_z} t_f\left(\frac{B}{2} - z_f\right)\frac{1}{2}\left(\frac{D}{2} + \frac{d}{2}\right)$$

where $\tau_{f(h)}$ is the distribution of horizontal shear stress in the flange. Simplifying the above equation we obtain

$$\tau_{f(h)} = -\frac{S_y(D + d)}{4I_z}\left(\frac{B}{2} - z_f\right) \tag{10.14}$$

Equation (10.14) shows that the horizontal shear stress varies linearly in the flanges from zero at $z_f = B/2$ to $-S_y(D+d)B/8I_z$ at $z_f = 0$.

We have defined a positive shear stress as being directed towards the edge b_0 of the slice away from the interior of the slice, Fig. 10.3(b). Since Eq. (10.14) is always negative for the upper flange, $\tau_{f(h)}$ in the upper flange is directed towards the edges of the flange. By a similar argument $\tau_{f(h)}$ in the lower flange is directed away from the edges of the flange because y for a slice in the lower flange is negative making Eq. (10.14) always positive. The distribution of horizontal shear stress in the flanges of the beam is shown in Fig. 10.7(b).

From Eq. (10.12) we see that the numerical value of shear stress at the extremities of the web multiplied by the web thickness is

$$\tau_w t_w = \frac{S_y}{I_z}\frac{B}{8}(D+d)(D-d) = \frac{S_y}{I_z}\frac{B}{8}(D+d)2t_f \tag{10.15}$$

The product of horizontal flange stress and flange thickness at the extremities of the web is, from Eq. (10.14)

$$\tau_{f(h)} t_f = \frac{S_y}{I_z}\frac{B}{8}(D+d)\,t_f \tag{10.16}$$

Comparing Eqs (10.15) and (10.16) we see that

$$\tau_w t_w = 2\tau_{f(h)}\,t_f \tag{10.17}$$

The product *stress* × *thickness* gives the *shear force per unit length* in the walls of the section and is known as the *shear flow*, a particularly useful parameter when considering thin-walled sections. In the above example we note that $\tau_{f(h)}t_f$ is the shear flow at the extremities of the web produced by considering one half of the complete flange. From symmetry there is an equal shear flow at the extremities of the web from the other half of the flange. Equation (10.17) therefore expresses the equilibrium of the shear flows at the web/flange junctions. We shall return to a more detailed consideration of shear flow when investigating the shear of thin-walled sections.

In 'thick' I-section beams the horizontal flange shear stress is not of great importance since, as can be seen from Eq. (10.17), it is of the order of half the magnitude of the vertical shear stress at the extremities of the web if $t_w \simeq t_f$. In thin-walled I-sections (and other sections too) this horizontal shear stress can produce shear distortions of sufficient magnitude to redistribute the direct stresses due to bending, thereby seriously affecting the accuracy of the basic bending theory described in Chapter 9. This phenomenon is known as *shear lag*.

EXAMPLE 10.3

A steel beam has the cross section shown in Fig. 10.8(a) and carries a load of W kN in its vertical plane of symmetry. Calculate and sketch the distribution of shear stress in the cross section of the beam and hence determine the maximum allowable value of W if the shear stress in the beam is limited to 100 N/mm^2.

The second moment of area of the beam section about the z axis is given by (see Section 9.6)

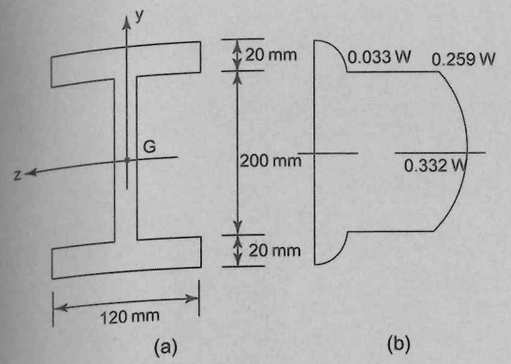

FIGURE 10.8
Shear stress distribution in beam section of Ex. 10.3.

$$I_z = \frac{120\times240^3}{12} - \frac{105\times200^3}{12}$$
$$= 6.8\times10^7\ \text{mm}^4$$

Then, from Eq. (10.8), the shear stress distribution in the flange is

$$\tau_f = -\frac{W\times10^3}{2\times6.8\times10^7}\left(\frac{240^2}{4} - y_f^2\right)$$

so that

$$\tau_f = -7.4\times10^{-6}\,W(120^2 - y_f^2)\text{N/mm}^2 \quad \text{(i)}$$

Then, when $y_f = 120$ mm, $\tau_f = 0$ and when $y_f = 100$ mm, $\tau_f = -0.033$ N/mm^2.

The shear stress distribution in the web is obtained directly from Eq. (10.11) and is

$$\tau_w = -\frac{W\times10^3}{6.8\times10^7}\left[\frac{120}{8\times15}(240^2 - 200^2) + \frac{1}{2}\left(\frac{200^2}{4} - y_w^2\right)\right]$$

which gives

$$\tau_w = -9.8\times10^{-7}(339000 - 7.5\,y_w^2) \quad \text{(ii)}$$

From Eq. (ii), when $y_w = 100$ mm, $\tau_w = -0.259\,W$N/mm^2 and when $y_w = 0$, $\tau_f = -0.332$ N/mm$^2 = \tau_{max}$. The complete distribution is shown in Fig. 10.8(b).

For a limiting value of shear stress of 100 N/mm^2,

$$100 = 0.332W$$

so that

$$W = 301\ \text{kN}.$$

In this example we have applied Eqs (10.8) and (10.11) directly. However, rather than attempt to commit these lengthy formulae to memory it is generally better to work from first principles.

EXAMPLE 10.4

The beam whose cross section is shown in Fig. 10.9(a) is subjected to a shear load of 15 kN applied in its vertical plane of symmetry. Calculate and sketch the distribution of shear stress in the cross section of the beam inserting all principal values.

Initially we need to find the position of the centroid of area, G, which will lie on the vertical axis of symmetry of the beam section. Taking moments of area about the base of the flange

$$(50\times20 + 60\times10)\,\bar{y} = 50\times20\times10 + 60\times10\times50$$

which gives

$$\bar{y} = 25\ \text{mm}$$

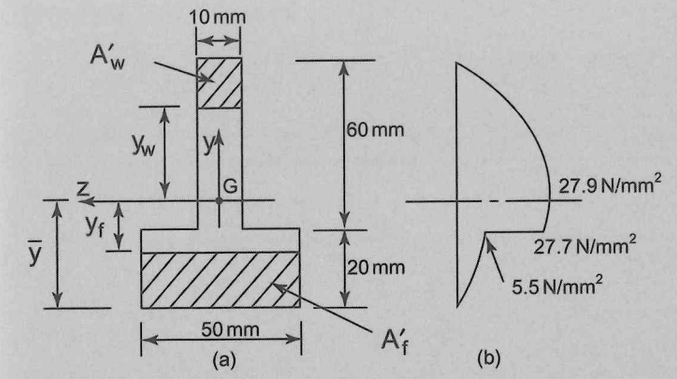

FIGURE 10.9
Shear stress distribution in beam of Ex. 10.4.

The second moment of area of the beam section about Gz is then

$$I_z = \frac{50 \times 20^3}{12} + 50 \times 20 \times 15^2 + \frac{10 \times 60^3}{12} + 10 \times 60 \times 25^2$$

so that

$$I_z = 8.13 \times 10^5 \text{ mm}^4$$

We now take a slice A_w' in the web as shown in Fig. 10.9(a). Then, from Eq. (10.4)

$$\tau_w = -\frac{15 \times 10^3 \times 10}{10 \times 8.13 \times 10^5}(55 - y_w)\frac{1}{2}(55 + y_w)$$

from which

$$\tau_w = -9.23 \times 10^{-3}(55^2 - y_w{}^2) \tag{i}$$

From Eq. (i), when $y_w = 55$ mm, $\tau_w = 0$ and when $y_w = -5$ mm, $\tau_w = -27.7$ N/mm^2. The maximum value of shear stress occurs when $y_w = 0$ and is -27.9 N/mm^2.

To find the shear stress distribution in the flange of the beam section we could consider the inverted T-shape above the slice. However, a simpler solution is obtained by considering the part of the flange below the slice as shown in Fig. 10.9(a). Then, from Eq. (10.4)

$$\tau_f = -\frac{15 \times 10^3 \times 50}{50 \times 8.13 \times 10^5}(25 - y_f)\frac{1}{2}(25 + y_f)$$

which simplifies to

$$\tau_f = -9.23 \times 10^{-3}(25^2 - y_f^2) \tag{ii}$$

From Eq. (ii), when $y_f = -25$ mm, $\tau_f = 0$ and when $y_f = -5$ mm, $\tau_f = -5.54$ N/mm^2. The complete distribution is shown in Fig. 10.9(b).

If the inverted T-shape above the slice in the flange had been considered as A_f' then

$$A_f'\,\bar{y} = 60 \times 10 \times 25 - 50(y_f - 5)(1/2)(y_f + 5)$$

so that

$$A_f'\,\bar{y} = 15000 - 25(y_f{}^2 - 5)$$

Note that the contribution to $A_f'\,\bar{y}$ from the leg of the T- and from the flange have opposite signs due to the fact that their centroids lie on opposite sides of the Gz axis.

EXAMPLE 10.5

Determine the distribution of vertical shear stress in a beam of circular cross section when it is subjected to a shear force S_y (Fig. 10.10).

The area A' of the slice in this problem is a segment of a circle and therefore does not lend itself to the simple treatment of the previous two examples. We shall therefore use Eq. (10.5) to determine the distribution of vertical shear stress. Thus

$$\tau = -\frac{S_y}{b_0 I_z}\int_y^{D/2} b y_1 \, dy_1 \tag{10.18}$$

where

$$I_z = \frac{\pi D^4}{64} \text{ (Eq. (9.40))}$$

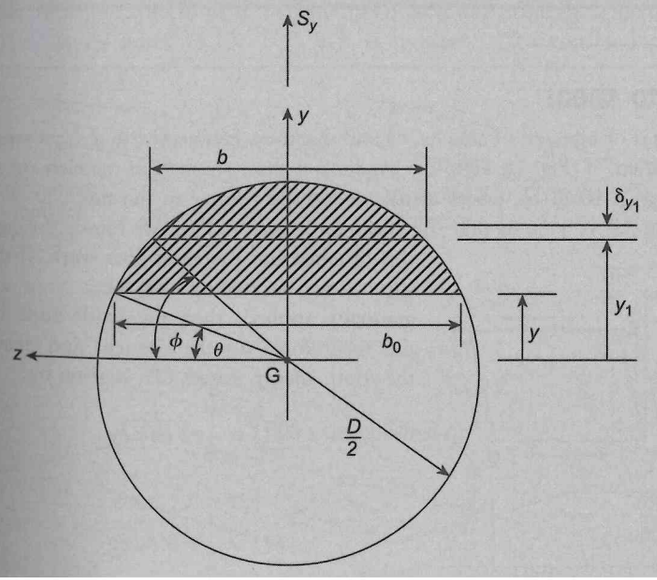

FIGURE 10.10
Distribution of shear stress in a beam of circular cross section.

Integration of Eq. (10.18) is simplified if angular variables are used; thus, from Fig. 10.10

$$b_0 = 2 \times \frac{D}{2}\cos\theta \quad b = 2 \times \frac{D}{2}\cos\phi \quad y_1 = \frac{D}{2}\sin\phi \quad dy_1 = \frac{D}{2}\cos\phi\, d\phi$$

Equation (10.18) then becomes

$$\tau = -\frac{16S_y}{\pi D^2 \cos\theta}\int_\theta^{\pi/2} \cos^2\phi \sin\phi\, d\phi$$

Integrating we obtain

$$\tau = -\frac{16S_y}{\pi D^2 \cos\theta}\left[-\frac{\cos^3\phi}{3}\right]_\theta^{\pi/2}$$

which gives

$$\tau = -\frac{16S_y}{3\pi D^2}\cos^2\theta$$

But

$$\cos^2\theta = 1 - \sin^2\theta = 1 - \left(\frac{y}{D/2}\right)^2$$

Therefore

$$\tau = -\frac{16S_y}{3\pi D^2}\left(1 - \frac{4y^2}{D^2}\right) \tag{10.19}$$

The distribution of shear stress is parabolic with values of $\tau = 0$ at $y = \pm D/2$ and $\tau = \tau_{max} = -16S_y/3\pi D^2$ at $y = 0$, the neutral axis of the section.

10.3 Strain energy due to shear

Consider a small rectangular element of material of side δx, δy and thickness t subjected to a shear stress and complementary shear stress system, τ (Fig. 10.11(a)); τ produces a shear strain γ in the element so that distortion occurs as shown in Fig. 10.11(b), where displacements are relative to the side CD. The horizontal displacement of the side AB is $\gamma\,\delta y$ so that the shear force on the face AB moves through this distance and therefore does work. If the shear loads producing the shear stress are gradually applied, then the work done by the shear force on the element and hence the strain energy stored, δU, is given by

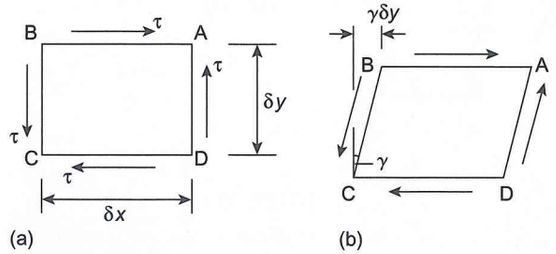

FIGURE 10.11

$$\delta U = \frac{1}{2}\tau t\, \delta x \gamma\, \delta y$$

or

$$\delta U = \frac{1}{2}\tau\gamma t\, \delta x\, \delta y$$

Now $\gamma = \tau/G$, where G is the shear modulus and $t\,\delta x\,\delta y$ is the volume of the element. Hence

$$\delta U = \frac{1}{2}\frac{\tau^2}{G} \times \text{volume of element}$$

The total strain energy, U, due to shear in a structural member in which the shear stress, τ, is uniform is then given by

$$U = \frac{\tau^2}{2G} \times \text{volume of member} \tag{10.20}$$

10.4 Shear stress distribution in thin-walled open section beams

In considering the shear stress distribution in thin-walled open section beams we shall make identical assumptions regarding the calculation of section properties as were made in Section 9.6. In addition we shall assume that shear stresses in the plane of the cross section and parallel to the tangent at any point on the beam wall are constant across the thickness (Fig. 10.12(a)), whereas shear stresses normal to the tangent are negligible (Fig. 10.12(b)). The validity of the latter assumption is evident when it is realized that these normal shear stresses must be zero on the inner and outer surfaces of the section and that the walls are thin. We shall further assume that the wall thickness can vary round the section but is constant along the length of the member.

Figure 10.13 shows a length of a thin-walled beam of arbitrary section subjected to shear loads S_z and S_y which are applied such that no twisting of the beam occurs. In addition to shear stresses, direct stresses due to the bending action of the shear loads are present so that an element $\delta s \times \delta x$ of the beam wall is in equilibrium under the stress system shown in Fig. 10.14(a). The shear stress τ is assumed to be positive in the positive direction of s, the distance round the profile of the section measured from an open edge. Although we have specified that the thickness t may vary with s, this variation is small for most thin-walled sections so that we may reasonably make the approximation that t is constant over the length δs. As stated in Ex. 10.2 it is convenient, when considering thin-walled sections, to work in

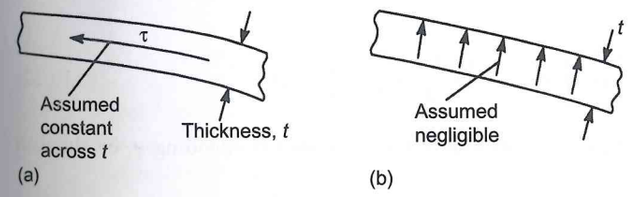

FIGURE 10.12
Assumptions in thin-walled open section beams.

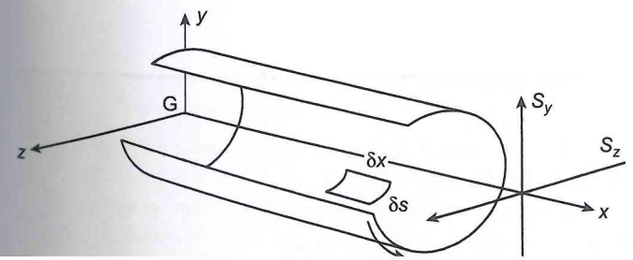

FIGURE 10.13
Shear of a thin-walled open section

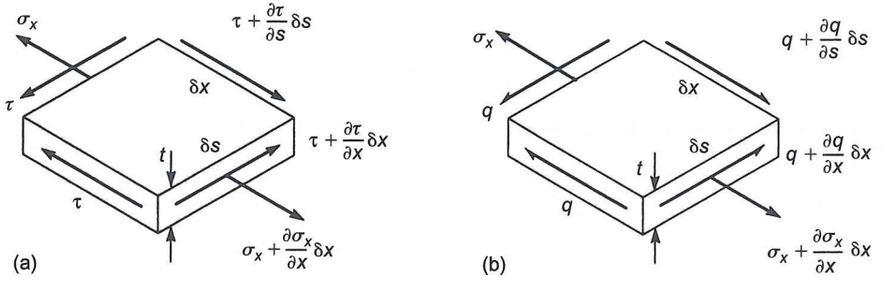

FIGURE 10.14

Equilibrium of beam element.

terms of shear flow to which we assign the symbol q ($=\tau t$). Figure 10.14(b) shows the shear stress system of Fig. 10.14(a) represented in terms of q. Thus for equilibrium of the element in the x direction

$$\left(\sigma_x + \frac{\partial \sigma_x}{\partial x}\delta x\right) t\,\delta s - \sigma_x t\,\delta s + \left(q + \frac{\partial q}{\partial s}\delta s\right)\delta x - q\,\delta x = 0$$

which gives

$$\frac{\partial q}{\partial s} + t\frac{\partial \sigma_x}{\partial x} = 0 \tag{10.21}$$

Again we assume that the direct stresses are given by Eq. (9.31). Then, substituting in Eq. (10.21) for $\partial\sigma x/\partial x$ from the derivation of Eq. (10.2)

$$\frac{\partial q}{\partial s} = \frac{(S_y I_{zy} - S_z I_z)}{I_z I_y - I_{zy}^2} tz + \frac{(S_z I_{zy} - S_y I_y)}{I_z I_y - I_{zy}^2} ty$$

Integrating this expression from $s = 0$ (where $q = 0$ on the open edge of the section) to any point s we have

$$q_s = \frac{(S_y I_{zy} - S_z I_z)}{I_z I_y - I_{zy}^2}\int_0^s tz\,\mathrm{d}s + \frac{(S_z I_{zy} - S_y I_y)}{I_z I_y - I_{zy}^2}\int_0^s ty\,\mathrm{d}s \tag{10.22}$$

The shear stress at any point in the beam section wall is then obtained by dividing q_s by the wall thickness at that point, i.e.

$$\tau_s = \frac{q_s}{t_s} \tag{10.23}$$

EXAMPLE 10.6

Determine the shear flow distribution in the thin-walled Z-section beam shown in Fig. 10.15 produced by a shear load S_y applied in the plane of the web.

The origin for our system of reference axes coincides with the centroid of the section at the midpoint of the web. The centroid is also the centre of antisymmetry of the section so that the shear load, applied through this point, causes no twisting of the section and the shear flow distribution is given by Eq. (10.22) in which $S_z = 0$, i.e

$$q_s = \frac{S_y I_{zy}}{I_z I_y - I_{zy}^2}\int_0^s tz\,\mathrm{d}s - \frac{S_y I_y}{I_z I_y - I_{zy}^2}\int_0^s ty\,\mathrm{d}s \tag{i}$$

The second moments of area of the section about the z and y axes have previously been calculated in Ex. 9.11 and are

$$I_z = \frac{h^3 t}{3} \quad I_y = \frac{h^3 t}{12} \quad I_{zy} = \frac{h^3 t}{8}$$

Substituting these values in Eq. (i) we obtain

$$q_s = \frac{S_y}{h^3}\int_0^s (10.29z - 6.86y)\mathrm{d}s$$

On the upper flange AB, $y = +h/2$ and $z = h/2 - s_A$ where $0 \le s_A \le h/2$. Therefore

$$q_{AB} = \frac{S_y}{h^3}\int_0^{s_A} (1.72\,h - 10.29 s_A)\mathrm{d}s_A$$

which gives

$$q_{AB} = \frac{S_y}{h^3}(1.72 h s_A - 5.15 s_A^2) \tag{ii}$$

Thus at A($s_A = 0$), $q_A = 0$ and at B ($s_A = h/2$), $q_B = -0.43\,S_y/h$. Note that the order of the suffixes of q in Eq. (ii) denotes the positive direction of q (and s_A). An examination of Eq. (ii) shows that the shear flow distribution on the upper flange is parabolic with a change of sign (i.e. direction)

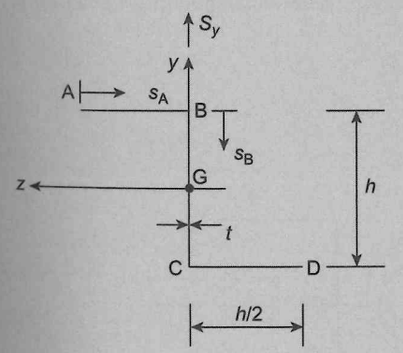

FIGURE 10.15

Beam section of Ex. 10.6.

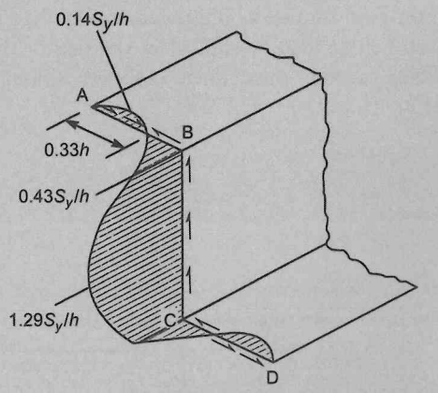

FIGURE 10.16

Shear flow distribution in beam section of Ex. 10.6.

at $s_A = 0.33\,h$. For values of $s_A < 0.33\,h$, q_{AB} is positive and is therefore in the same direction as s_A. Furthermore, q_{AB} has a turning value between $s_A = 0$ and $s_A = 0.33\,h$ at a value of s_A given by

$$\frac{dq_{AB}}{ds_A} = 1.72\,h - 10.29 s_A = 0$$

i.e. at $s_A = 0.17\,h$. The corresponding value of q_{AB} is then, from Eq. (ii), $q_{AB} = 0.14 Sy/h$.

In the web BC, $y = +h/2 - s_B$ where $0 \leq s_B \leq h$ and $z = 0$. Thus

$$q_{BC} = \frac{S_y}{h^3}\int_0^{s_B} (6.86 s_B - 3.43\,h)\,ds_B + q_B \qquad \text{(iii)}$$

Note that in Eq. (iii), q_{BC} is not zero when $s_B = 0$ but equal to the value obtained by inserting $s_A = h/2$ in Eq. (ii), i.e. $q_B = -0.43\,S_y/h$. Integrating the first two terms on the right-hand side of Eq. (iii) we obtain

$$q_{BC} = \frac{S_y}{h^3}(3.43 s_B^2 - 3.43\,h s_B - 0.43\,h^2) \qquad \text{(iv)}$$

Equation (iv) gives a parabolic shear flow distribution in the web, symmetrical about Gz and with a maximum value at $s_B = h/2$ equal to $-1.29 S_y/h$; q_{AB} is negative at all points in the web.

The shear flow distribution in the lower flange may be deduced from antisymmetry; the complete distribution is shown in Fig. 10.16.

Shear centre

We have specified in the previous analysis that the lines of action of the shear loads S_z and S_y must not cause twisting of the section. For this to be the case, S_z and S_y must pass through the *shear centre* of the section. Clearly in many practical situations this is not so and torsion as well as shear is induced. These problems may be simplified by replacing the shear loads by shear loads acting through the shear centre, plus a pure torque, as illustrated in Fig. 10.17 for the simple case of a channel section subjected to a vertical shear load S_y applied in the line of the web. The shear stresses corresponding to the separate loading cases are then added by superposition.

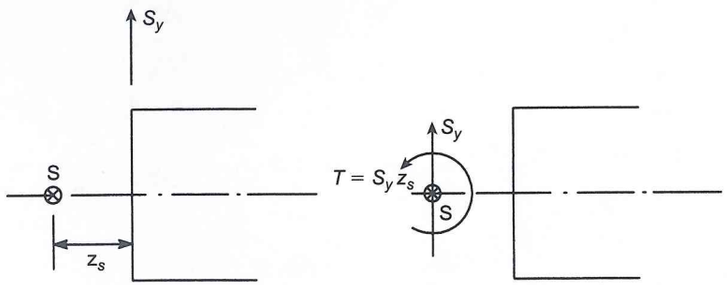

FIGURE 10.17

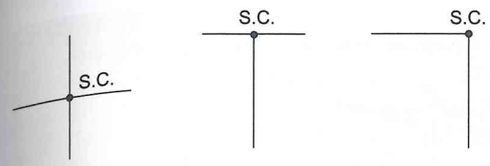

FIGURE 10.18
Special cases of shear centre (S.C.) position.

Where a section possesses an axis of symmetry, the shear centre must lie on this axis. For cruciform, T and angle sections of the type shown in Fig. 10.18 the shear centre is located at the intersection of the walls since the resultant internal shear loads all pass through this point. In fact in any beam section in which the walls are straight and intersect at just one point, that point is the shear centre of the section.

EXAMPLE 10.7

Determine the position of the shear centre of the thin-walled channel section shown in Fig. 10.19.

The shear centre S lies on the horizontal axis of symmetry at some distance z_S, say, from the web. If an arbitrary shear load, S_y, is applied through the shear centre, then the shear flow distribution is given by Eq. (10.22) and the moment about any point in the cross section produced by these shear flows is *equivalent* to the moment of the applied shear load about the same point; S_y appears on both sides of the resulting equation and may therefore be eliminated to leave z_S as the unknown.

For the channel section, G_z is an axis of symmetry so that $I_{zy} = 0$. Equation (10.22) therefore simplifies to

$$q_s = -\frac{S_y}{I_z}\int_0^s ty\,ds$$

where

$$I_z = \frac{th^3}{12} + 2bt\left(\frac{h}{2}\right)^2 = \frac{th^3}{12}\left(1 + 6\frac{b}{h}\right)$$

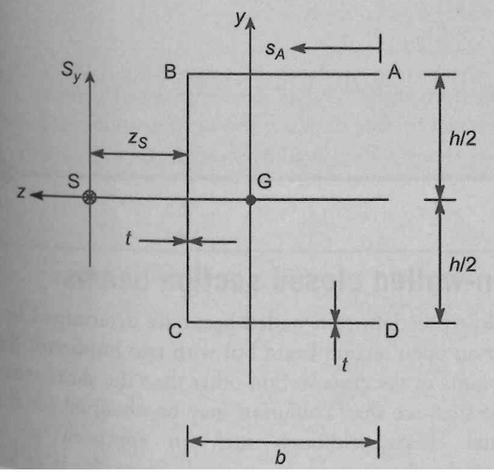

FIGURE 10.19
Channel section beam of Ex. 10.7.

Substituting for I_z and noting that t is constant round the section, we have

$$q_s = -\frac{12S_y}{h^3(1+6b/h)}\int_0^s y\,\mathrm{d}s \tag{i}$$

The solution of this type of problem may be reduced in length by giving some thought to what is required. We are asked, in this case, to obtain the position of the shear centre and not a complete shear flow distribution. From symmetry it can be seen that the moments of the resultant shear forces on the upper and lower flanges about the mid-point of the web are numerically equal and act in the same sense. Furthermore, the moment of the web shear about the same point is zero. Therefore it is only necessary to obtain the shear flow distribution on either the upper or lower flange for a solution. Alternatively, the choice of either flange/web junction as the moment centre leads to the same conclusion.

On the upper flange, $y = +h/2$ so that from Eq. (i) we obtain

$$q_{AB} = -\frac{6S_y}{h^2(1+6b/h)}s_A \tag{ii}$$

Equating the anticlockwise moments of the internal shear forces about the mid-point of the web to the clockwise moment of the applied shear load about the same point gives

$$S_y z_S = -\int_0^b q_{AB}\frac{h}{2}\mathrm{d}s_A$$

Substituting for q_{AB} from Eq. (ii) we have

$$S_y z_S = 2\int_0^b \frac{6S_y}{h^2(1+6b/h)}\frac{h}{2}s_A\,\mathrm{d}s_A$$

from which

$$z_S = \frac{3b^2}{h(1+6b/h)}$$

In the case of an unsymmetrical section, the coordinates (z_S, y_S) of the shear centre referred to some convenient point in the cross section are obtained by first determining z_S in a similar manner to that described above and then calculating y_S by applying a shear load S_z through the shear centre.

10.5 Shear stress distribution in thin-walled closed section beams

The shear flow and shear stress distributions in a closed section, thin-walled beam are determined in a manner similar to that described in Section 10.4 for an open section beam but with two important differences. Firstly, the shear loads may be applied at points in the cross section other than the shear centre so that shear and torsion occur simultaneously. We shall see that a solution may be obtained for this case without separating the shear and torsional effects, although such an approach is an

generally possible to choose an origin for s that coincides with a known value of shear flow. A closed section beam under shear is therefore singly redundant as far as the internal force system is concerned and requires an equation additional to the equilibrium equation (Eq. (10.21)). Identical assumptions are made regarding section properties, wall thickness and shear stress distribution as were made for the open section beam.

The thin-walled beam of arbitrary closed section shown in Fig. 10.20 is subjected to shear loads S_z and S_y applied through any point in the cross section. These shear loads produce direct and shear stresses on any element in the beam wall identical to those shown in Fig. 10.14. The equilibrium equation (Eq. (10.21)) is therefore applicable and is

$$\frac{\partial q}{\partial s} + t\frac{\partial \sigma_x}{\partial x} = 0$$

Substituting for $\partial\sigma_x/\partial x$ from the derivation of Eq. (10.2) and integrating we obtain, in an identical manner to that for an open section beam

$$q_s = \frac{S_y I_{zy} - S_z I_z}{I_z I_y - I_{zy}^2}\int_0^s tz\,\mathrm{d}s + \frac{S_z I_{zy} - S_y I_y}{I_z I_y - I_{zy}^2}\int_0^s ty\,\mathrm{d}s + q_{s,0} \tag{10.24}$$

where $q_{s,0}$ is the value of shear flow at the origin of s.

It is clear from a comparison of Eqs (10.22) and (10.24) that the first two terms of the right-hand side of Eq. (10.24) represent the shear flow distribution in an open section beam with the shear loads applied through its shear centre. We shall denote this 'open section' or 'basic' shear flow distribution by q_b and rewrite Eq. (10.24) as

$$q_s = q_b + q_{s,0}$$

We obtain q_b by supposing that the closed section beam is 'cut' at some convenient point, thereby producing an 'open section' beam as shown in Fig. 10.21(b); we take the 'cut' as the origin for s. The shear flow distribution round this 'open section' beam is given by Eq. (10.22), i.e.

$$q_b = \frac{S_y I_{zy} - S_z I_z}{I_z I_y - I_{zy}^2}\int_0^s tz\,\mathrm{d}s + \frac{S_z I_{zy} - S_y I_y}{I_z I_y - I_{zy}^2}\int_0^s ty\,\mathrm{d}s$$

Equation (10.22) is valid only if the shear loads produce no twist; in other words, S_z and S_y must be applied through the shear centre of the 'open section' beam. Thus by 'cutting' the closed section beam to determine q_b we are, in effect, transferring the line of action of S_z and S_y to the shear centre, $S_{,0}$, of the resulting 'open section' beam. The implication is, therefore, that when we 'cut' the section

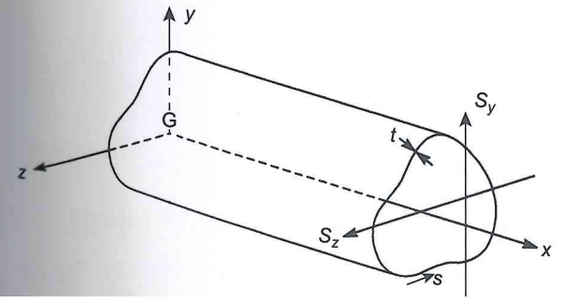

FIGURE 10.20

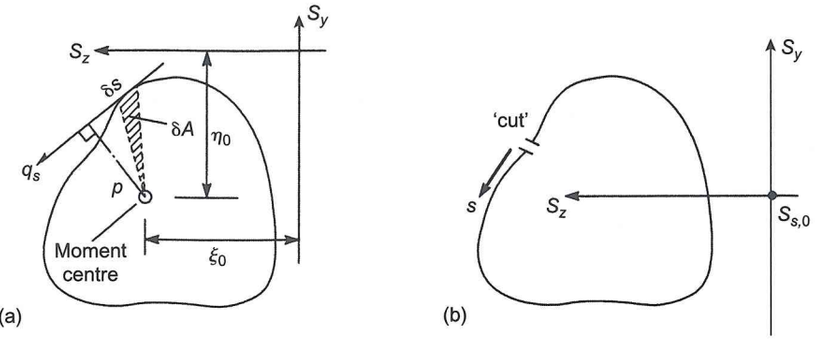

FIGURE 10.21
Determination of shear flow value at the origin for s in a closed section beam.

we must simultaneously introduce a pure torque to compensate for the transference of S_z and S_y. We shall show in Chapter 11 that the application of a pure torque to a closed section beam results in a constant shear flow round the walls of the beam. In this case $q_{s,0}$, which is effectively a constant shear flow round the section, corresponds to the pure torque produced by the shear load transference. Clearly different positions of the 'cut' will result in different values for $q_{s,0}$ since the corresponding 'open section' beams have different shear centre positions.

Equating internal and external moments in Fig. 10.21(a), we have

$$S_z\eta_0 + S_y\xi_0 = \oint pq_s \, ds = \oint pq_b \, ds + q_{s,0} \oint p \, ds$$

where $\oint$ denotes integration taken completely round the section. In Fig. 10.21(a) the elemental area δA is given by

$$\delta A = \frac{1}{2}p\delta s$$

Thus

$$\oint p \, ds = 2 \oint dA$$

or

$$\oint p \, ds = 2A$$

where A is the area enclosed by the mid-line of the section wall. Hence

$$S_x\eta_0 + S_y\xi_0 = \oint pq_b \, ds + 2Aq_{s,0} \tag{10.25}$$

If the moment centre coincides with the lines of action of S_z and S_y then Eq. (10.25) reduces to

$$0 = \oint pq_b \, ds + 2Aq_{s,0} \tag{10.26}$$

The unknown shear flow $q_{s,0}$ follows from either of Eqs. (10.25) or (10.26). Note that the signs of the moment contributions of S_z and S_y on the left-hand side of Eq. (10.25) depend upon the position of their lines of action relative to the moment centre. The values given in Eq. (10.25) apply only to Fig. 10.21(a) and could change for different moment centres and/or differently positioned shear loads.

EXAMPLE 10.8

Determine the shear flow distribution in the walls of the thin-walled closed section beam shown in Fig. 10.22, the wall thickness, t, is constant throughout.

Since the z axis is an axis of symmetry, $I_{zy} = 0$, and since $S_z = 0$, Eq. (10.24) reduces to

$$q_s = -(S_y/I_z)\int_0^s ty \, ds + q_{s,0}$$

where

$$I_z = (\pi tr^3/2) + 2 \times 2rt \times r^2 + [t(2r)^3/12] = 6.24tr^3$$

We now "cut" the beam section at 1. Any point may be chosen for the "cut" but the amount of computation will be reduced if a point is chosen which coincides with the axis of symmetry. Then

$$q_{b,12} = -(S_y/I_z)\int_0^\theta tr \sin\theta \, r d\theta$$

which gives

$$q_{b,12} = 0.16(S_y/r)[\cos\theta]_0^\theta$$

so that

$$q_{b,12} = 0.16(S_y/r)(\cos\theta - 1) \tag{i}$$

When $\theta = \pi/2$, $q_{b,2} = -0.16(S_y/r)$. The shear flow in the wall 23 is then

$$q_{b,23} = -(S_y/I_z)\int_0^{s_1} tr \, ds_1 - 0.16(S_y/r)$$

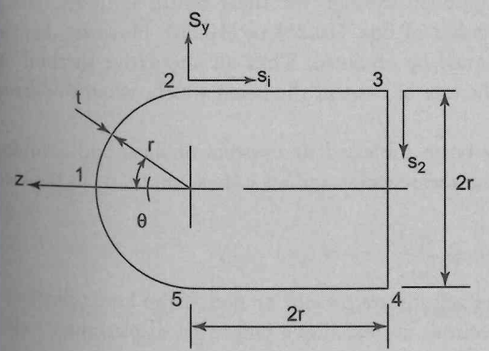

FIGURE 10.22
Beam section of Ex. 10.8.

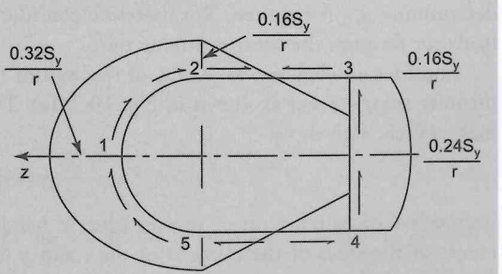

FIGURE 10.23
Shear flow distribution in beam of Ex. 10.8.

so that

$$q_{b,23} = -0.16(S_y/r^2)(s_1 + r) \qquad \text{(ii)}$$

and when $s_1 = 2r$, $q_{b,3} = -0.48(S_y/r)$. Then, in the wall 34

$$q_{b,34} = -0.16(S_y/tr^3)\int_0^{S_2} t(r - s_2)\mathrm{d}s_2 - 0.48(S_y/r)$$

so that

$$q_{b,34} = -0.16(S_y/r)(rs_2 - 0.5\,s_2^2 + 3r^2) \qquad \text{(iii)}$$

The remaining distribution follows from symmetry. Now taking moments about O and using Eq. (10.26)

$$0 = 2\left[\int_0^{\pi/2} q_{b,12}\,r^2\,\mathrm{d}\theta + \int_0^{2r} q_{b,23}\,r\,\mathrm{d}s_1 + \int_0^{r} q_{b,34}\,2r\,\mathrm{d}s_2\right] + 2[4r^2 + (\pi r^2/2)]q_{s,0} \qquad \text{(iv)}$$

Substituting in Eq. (iv) for $q_{b,12}$ etc from Eqs (i), (ii) and (iii) gives

$$q_{s,0} = 0.32S_y/r$$

Adding $q_{s,0}$ to the q_b distributions of Eqs (i), (ii) and (iii) gives

$$q_{12} = 0.16(S_y/r^3)(r^2\cos\theta + r^2)$$
$$q_{23} = 0.16(S_y/r^3)(r^2 - rs_1)$$
$$q_{34} = 0.16(S_y/r^3)(0.5s_2^2 - rs_2 - r^2)$$

Note that q_{23} changes sign at $s_1 = r$. The shear flow distribution in the lower half of the section follows from symmetry and the complete distribution is shown in Fig. 10.23.

Shear centre

A complication arises in the determination of the position of the shear centre of a closed section beam since the line of action of the arbitrary shear load (applied through the shear centre as in Ex. 10.7) must be known before $q_{s,0}$ can be determined from either of Eqs. (10.25) or (10.26). However, before the position of the shear centre can be found, $q_{s,0}$ must be obtained. Thus an alternative method of determining $q_{s,0}$ is required. We therefore consider the rate of twist of the beam which, when the shear loads act through the shear centre, is zero.

Consider an element, $\delta s \times \delta x$, of the wall of the beam subjected to a system of shear and complementary shear stresses as shown in Fig. 10.24(a). These shear stresses induce a shear strain, γ, in the element which is given by

$$\gamma = \phi_1 + \phi_2$$

irrespective of whether direct stresses (due to bending action) are present or not. If the linear displacements of the sides of the element in the s and x directions are δv_t (i.e. a tangential displacement) and δw, respectively, then as both δs and δx become infinitely small

$$\gamma = \frac{\partial w}{\partial s} + \frac{\partial v_t}{\partial x} \qquad (10.27)$$

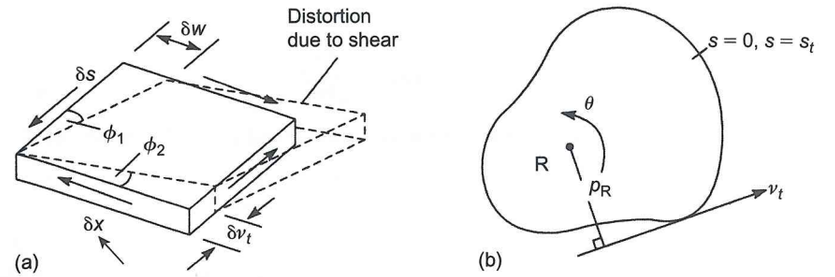

FIGURE 10.24
Rate of twist in a thin-walled closed section beam.

Suppose now that the beam section is given a small angle of twist, θ, about its centre of twist, R. If we assume that the shape of the cross section of the beam is unchanged by this rotation (i.e. it moves as a rigid body), then from Fig. 10.24(b) it can be seen that the tangential displacement, v_t, of a point in the wall of the beam section is given by

$$v_t = p_R\theta$$

Hence

$$\frac{\partial v_t}{\partial x} = p_R\frac{\partial \theta}{\partial x}$$

Since we are assuming that the section rotates as a rigid body, it follows that θ is a function of x only so that the above equation may be written

$$\frac{\partial v_t}{\partial x} = p_R\frac{\mathrm{d}\theta}{\mathrm{d}x}$$

Substituting for $\partial v_t/\partial x$ in Eq. (10.27) we have

$$\gamma = \frac{\partial w}{\partial s} + p_R\frac{\mathrm{d}\theta}{\mathrm{d}x}$$

Now

$$\gamma = \frac{\tau}{G} = \frac{q_s}{Gt}$$

Thus

$$\frac{q_s}{Gt} = \frac{\partial w}{\partial s} + p_R\frac{\mathrm{d}\theta}{\mathrm{d}x}$$

Integrating both sides of this equation completely round the cross section of the beam, i.e. from $s = 0$ to $s = s_t$ (see Fig. 10.24(b))

$$\oint \frac{q_s}{Gt}\mathrm{d}s = \oint \frac{\partial w}{\partial s}\mathrm{d}s + \frac{\mathrm{d}\theta}{\mathrm{d}x}\oint p_R\,\mathrm{d}s$$

which gives

$$\oint \frac{q_s}{Gt}\,\mathrm{d}s = [w]_{s=0}^{s=s_t} + \frac{\mathrm{d}\theta}{\mathrm{d}x}2A$$

The axial displacement, w, must have the same value at $s = 0$ and $s = s_t$. Therefore the above expression reduces to

$$\frac{\mathrm{d}\theta}{\mathrm{d}x} = \frac{1}{2A}\oint \frac{q_s}{Gt}\,\mathrm{d}s \tag{10.28}$$

For shear loads applied through the shear centre, $\mathrm{d}\theta/\mathrm{d}x = 0$ so that

$$0 = \oint \frac{q_s}{Gt}\,\mathrm{d}s$$

which may be written

$$0 = \oint \frac{1}{Gt}(q_\mathrm{b} + q_{s,0})\mathrm{d}s$$

Hence

$$q_{s,0} = -\frac{\oint (q_\mathrm{b}/Gt)\mathrm{d}s}{\oint \mathrm{d}s/Gt} \tag{10.29}$$

If G is constant then Eq. (10.29) simplifies to

$$q_{s,0} = -\frac{\oint (q_\mathrm{b}/t)\mathrm{d}s}{\oint \mathrm{d}s/t} \tag{10.30}$$

EXAMPLE 10.9

A thin-walled, closed section beam has the singly symmetrical, trapezoidal cross section shown in Fig. 10.25. Calculate the distance of the shear centre from the wall AD. The shear modulus G is constant throughout the section.

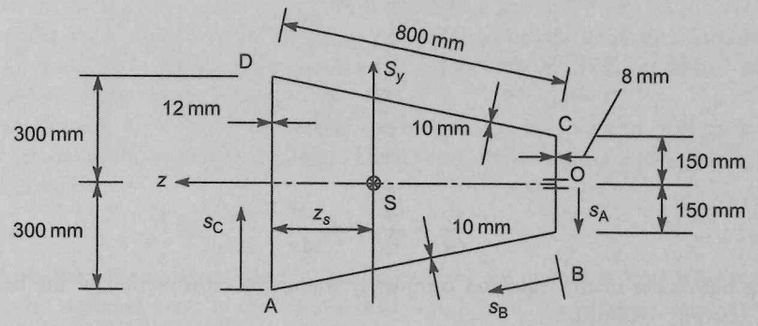

FIGURE 10.25
Closed section beam of Ex. 10.9.

The shear centre lies on the horizontal axis of symmetry so that it is only necessary to apply a shear load S_y through S to determine z_S. Furthermore the axis of symmetry coincides with the centroidal reference axis Gz so that $I_{zy} = 0$. Equation (10.24) therefore simplifies to

$$q_s = -\frac{S_y}{I_z}\int_0^s ty\,\mathrm{d}s + q_{s,0} \tag{i}$$

Note that in Eq. (i) only the second moment of area about the z axis and coordinates of points referred to the z axis are required so that it is unnecessary to calculate the position of the centroid on the z axis. It will not, in general, and in this case in particular, coincide with S.

The second moment of area of the section about the z axis is given by

$$I_z = \frac{12\times 600^3}{12} + \frac{8\times 300^3}{12} + 2\left[\int_0^{800} 10\left(150 + \frac{150}{800}s\right)^2 \mathrm{d}s\right]$$

from which $I_z = 1074\times 10^6\ \mathrm{mm}^4$. Alternatively, the second moment of area of each inclined wall about an axis through its own centroid may be found using the method described in Section 9.6 and then transferred to the z axis by the parallel axes theorem.

We now obtain the q_b shear flow distribution by 'cutting' the beam section at the mid-point O of the wall CB. Thus, since $y = -s_\mathrm{A}$ we have

$$q_{\mathrm{b,OB}} = \frac{S_y}{I_z}\int_0^{s_A} 8s_\mathrm{A}\,\mathrm{d}s_\mathrm{A}$$

which gives

$$q_{\mathrm{b,OB}} = \frac{S_y}{I_z}4s_\mathrm{A}^2 \tag{ii}$$

Thus

$$q_{\mathrm{b,B}} = \frac{S_y}{I_z}\times 9\times 10^4$$

For the wall BA where $y = -150 - 150s_\mathrm{B}/800$

$$q_{\mathrm{b,BA}} = \frac{S_y}{I_z}\left[\int_0^{s_B} 10\left(150 + \frac{150}{800}s_\mathrm{B}\right)\mathrm{d}s_\mathrm{B} + 9\times 10^4\right]$$

from which

$$q_{\mathrm{b,BA}} = \frac{S_y}{I_z}\left(1500s_\mathrm{B} + \frac{15}{16}s_\mathrm{B}^2 + 9\times 10^4\right) \tag{iii}$$

Then

$$q_{\mathrm{b,A}} = \frac{S_y}{I_z}\times 189\times 10^4$$

In the wall AD, $y = -300 + s_C$ so that

$$q_{b,AD} = \frac{S_y}{I_z}\left[\int_0^{s_C} 12(300 - s_C)ds_C + 189 \times 10^4\right]$$

which gives

$$q_{b,AD} = \frac{S_y}{I_z}(3600s_C - 6s_C^2 + 189 \times 10^4) \qquad \text{(iv)}$$

The remainder of the q_b distribution follows from symmetry.

The shear load S_y is applied through the shear centre of the section so that we must use Eq. (10.30) to determine $q_{s,0}$. Now

$$\oint \frac{ds}{t} = \frac{600}{12} + \frac{2 \times 800}{10} + \frac{300}{8} = 247.5$$

Therefore

$$q_{s,0} = -\frac{2}{247.5}\left(\int_0^{150} \frac{q_{b,OB}}{8} ds_A + \int_0^{800} \frac{q_{b,BA}}{10} ds_B + \int_0^{300} \frac{q_{b,AD}}{12} ds_C\right) \qquad \text{(v)}$$

Substituting for $q_{b,OB}$, $q_{b,BA}$ and $q_{b,AD}$ in Eq. (v) from Eqs (ii), (iii) and (iv), respectively, we obtain

$$q_{s,0} = -\frac{2S_y}{247.5I_z}\left[\int_0^{150} \frac{s_A^2}{2} ds_A + \int_0^{800} \left(150s_B + \frac{15}{160}s_B^2 + 9 \times 10^3\right) ds_B + \int_0^{300} \left(300s_C - \frac{1}{2}s_C^2 + \frac{189 \times 10^4}{12}\right) ds_C\right]$$

from which

$$q_{s,0} = -\frac{S_y}{I_z} \times 1.04 \times 10^6$$

Taking moments about the mid-point of the wall AD we have

$$-S_y z_S = 2\left(\int_0^{150} 786q_{OB}\, ds_A + \int_0^{800} 294q_{BA}\, ds_B\right) \qquad \text{(vi)}$$

Noting that $q_{OB} = q_{b,OB} + q_{s,0}$ and $q_{BA} = q_{b,BA} + q_{s,0}$ we rewrite Eq. (vi) as

$$S_y z_S = \frac{2S_y}{I_z}\left[\int_0^{150} 786(+4ds_A^2 - 1.4 \times 10^6)ds_A + \int_0^{800} 294(+1500s_B + \frac{15}{16}s_B^2 - 0.95 \times 10^6)ds_B\right] \qquad \text{(vii)}$$

Integrating Eq. (vii) and eliminating S_y gives

$$z_s = 282 \text{ mm}.$$

PROBLEMS

P.10.1 A cantilever has the inverted T-section shown in Fig. P.10.1. It carries a vertical shear load of 4 kN in a downward direction. Determine the distribution of vertical shear stress in its cross-section.

Ans. In web: $\tau = 0.004(44^2 - y^2)\text{N/mm}^2$, in flange: $\tau = 0.004(26^2 - y^2)\text{N/mm}^2$

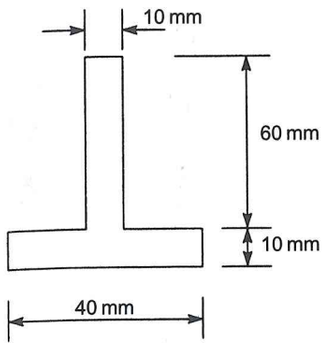

FIGURE P.10.1

P.10.2 An I-section beam having the cross-sectional dimensions shown in Fig. P.10.2 carries a vertical shear load of 80 kN. Calculate and sketch the distribution of vertical shear stress across the beam section and determine the percentage of the total shear load carried by the web.

Ans. τ (base of flanges) = 1.1 N/mm^2, τ (ends of web) = 11.1 N/mm^2, τ (neutral axis) = 15.77 N/mm^2, 95.9%.

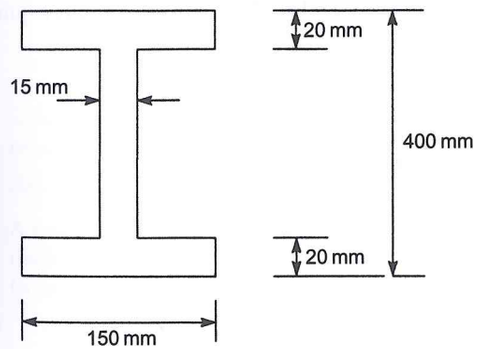

FIGURE P.10.2

P.10.3 A doubly symmetrical I-section beam is reinforced by a flat plate attached to the upper flange as shown in Fig. P.10.3. If the resulting compound beam is subjected to a vertical shear load of 200 kN, determine the distribution of shear stress in the portion of the cross section that extends from the top of the plate to the neutral axis. Calculate also the shear force per unit

length of beam resisted by the shear connection between the plate and the flange of the I-section beam.

Ans. τ (top of plate) = 0
τ (bottom of plate) = 0.68 N/mm^2
τ (top of flange) = 1.36 N/mm^2
τ (bottom of flange) = 1.78 N/mm^2
τ (top of web) = 14.22 N/mm^2
τ (neutral axis) = 15.15 N/mm^2
Shear force per unit length = 272 kN/m.

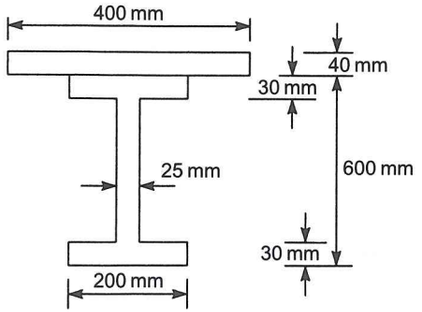

FIGURE P.10.3

P.10.4 A timber beam has a rectangular cross section, 150 mm wide by 300 mm deep, and is simply supported over a span of 4 m. The beam is subjected to a two-point loading at the quarter span points. If the beam fails in shear when the total of the two concentrated loads is 180 kN, determine the maximum shear stress at failure.

Ans. 3 N/mm^2.

P.10.5 A steel box girder is simply supported over a span of 5 m and is to be constructed by bolting flat plates to the flanges of two channel sections as shown in Fig. P.10.5. If the girder is required to

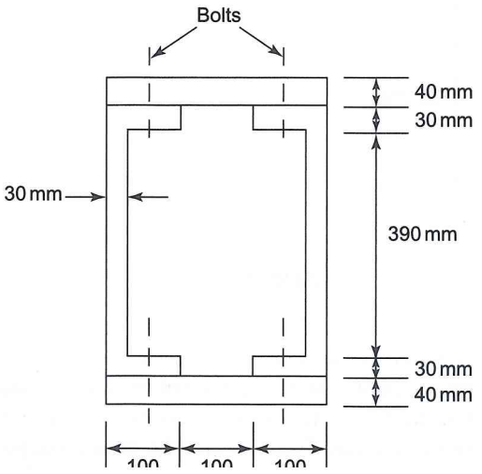

support a load of 500 kN at its mid-span calculate the number of bolts required/metre length of the beam. Take the allowable load/bolt as 150 kN and make full allowance for the self-weight of the plates and channel sections; the density of the steel is 77 kN/m^3.

Ans. 1 bolt/metre in each channel section flange.

P.10.6 If the maximum allowable shear stress in the box girder of P.10.5 is 100 N/mm^2 and the maximum allowable direct stress due to bending is 200 N/mm^2 determine the maximum concentrated mid-span load the box girder can carry and state which is the limiting case.

Ans. 1359 kN. Bending is the limiting case."

P.10.7 A beam has the singly symmetrical thin-walled cross section shown in Fig. P.10.7. Each wall of the section is flat and has the same length, a, and thickness, t. Determine the shear flow distribution round the section due to a vertical shear load, S_y, applied through the shear centre and find the distance of the shear centre from the point C.

Ans. $q_{AB} = -3S_y(2as_A - s_A^2/2)/16a^3 \sin\alpha$
$q_{BC} = -3S_y(3/2 + s_B/a - s_B^2/2a^2)/16a \sin\alpha$
S.C. is $5a \cos\alpha/8$ from C.

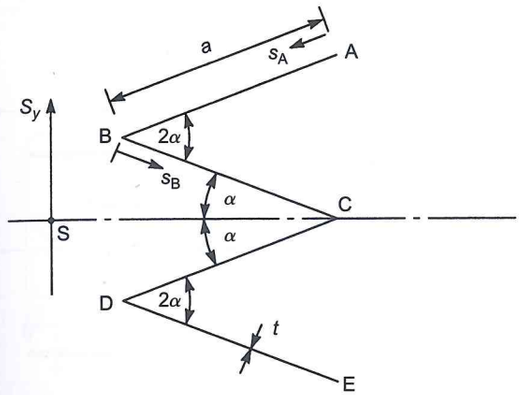

FIGURE P.10.7

P.10.8 Calculate the shear flow distribution in the thin-walled open section shown in Fig. P.10.8 produced by a vertical shear load, S_y, acting through its shear centre.

Ans. $q_\theta = (S_y/\pi r)(\cos\theta - 1)$.

P.10.9 A beam has the singly symmetrical, thin-walled cross section shown in Fig. P.10.9. The thickness t of the walls is constant throughout. Show that the distance of the shear centre from the web is given by

$$z_S = d\frac{\rho^2 \sin\alpha \cos\alpha}{1 + 6\rho + 2\rho^3 \sin^2\alpha} \quad \text{where } \rho = d/b$$

P.10.10 Determine the position of the shear centre of the thin-walled open section shown in Fig. P.10.10. The thickness t is constant.

Ans. $\pi r/3$ from the junction of the two semi-circular portions.

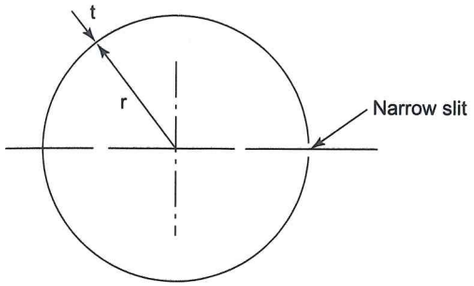

FIGURE P.10.8

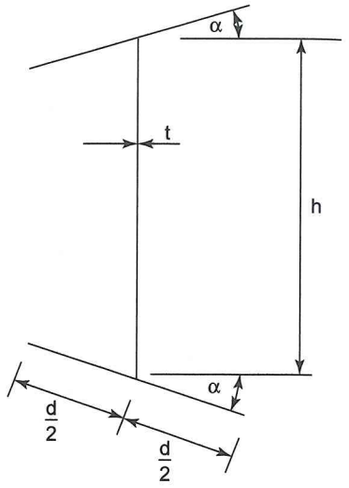

FIGURE P.10.9

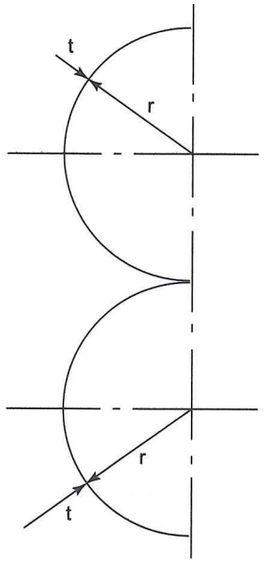

FIGURE P.10.10

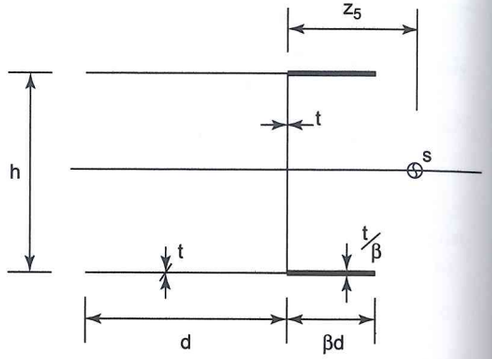

FIGURE P.10.11

P.10.11 Figure P.10.11 shows the cross section of a thin-walled, singly symmetrical I-section beam. Show that the distance z_S of the shear centre from the vertical is given by

$$\frac{z_S}{d} = \frac{3\rho(1-\beta)}{(1+12\rho)} \quad \text{where } \rho = d/h$$

P.10.12 Find the position of the shear centre of the thin-walled beam section shown in Fig. P.10.12.

Ans. $1.2r$ on the axis of symmetry to the left of the section.

P.10.13 Determine the horizontal distance from O of the shear centre of the thin-walled beam section shown in Fig. P.10.13. Note that the position of the centroid of area, G, is given.

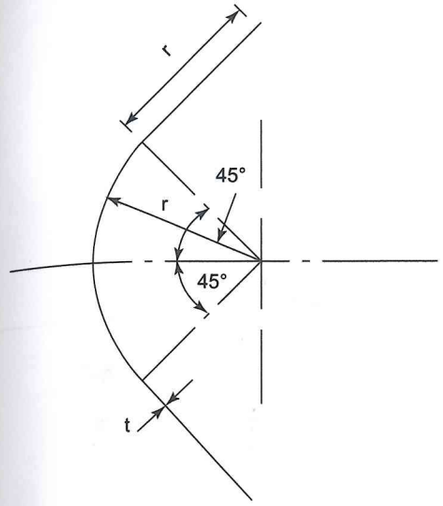

FIGURE P.10.12

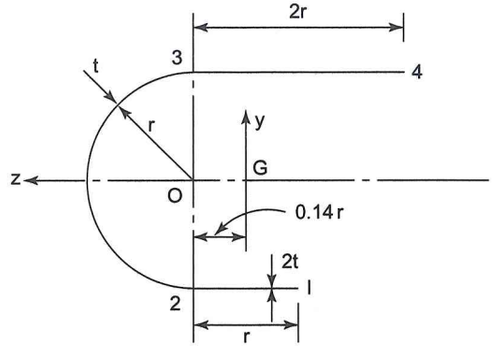

FIGURE P.10.13

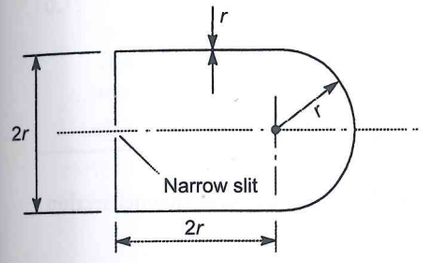

FIGURE P.10.14

P.10.14 Define the term 'shear centre' of a thin-walled open section and determine the position of the shear centre of the thin-walled open section shown in Fig. P.10.14.

Ans. $2.66r$ from centre of semicircular wall.

P.10.15 Determine the position of the shear centre of the cold-formed, thin-walled section shown in Fig. P.10.15. The thickness of the section is constant throughout.

Ans. 87.5 mm above centre of semicircular wall.

P.10.16 The thin-walled channel section shown in Fig. P.10.16 has flanges that decrease linearly in thickness from $2t_0$ at the tip to t_0 at their junction with the web. The web has a constant thickness t_0. Determine the distribution of shear flow round the section due to a shear load S_y applied through the shear centre S. Determine also the position of the shear centre.

Ans.

$$q_{AB} = -S_y t_0 h(s_A - s_A^2/4d)/I_z, \quad q_{BC} = -S_y t_0(hs_B - s_B^2 + 3hd/2)/2I_z,$$

where $I_x = t_0h^2(h+9d)/12$; $5d^2/(h+9d)$ from mid-point of web.